SELECTIVE AND EFFICIENT OXIDATION OF ALCOHOLS TO ALDEHYDES IN PRESENCE OF VISIBLE-LIGHT-DRIVEN PHOTOCATALYSTS: A GREEN ORGANIC SYNTHESIS APPROACH

BY

RAMI BAHAELDIN ABDELRAHMAN ELSAYED

A Thesis Presented to the
DEANSHIP OF GRADUATE STUDIES

KING FAHD UNIVERSITY OF PETROLEUM & MINERALS

DHAHRAN, SAUDI ARABIA

In Partial Fulfillment of the
Requirements for the Degree of

MASTER OF SCIENCE

In

CHEMISTRY

MAY 2014

KING FAHD UNIVERSITY OF PETROLEUM & MINERALS

DHAHRAN- 31261, SAUDI ARABIA

DEANSHIP OF GRADUATE STUDIES

This thesis, written by **RAMI BAHAELDIN ABDELRAHMAN ELSAYED** under the direction his thesis advisor and approved by his thesis committee, has been presented and accepted by the Dean of Graduate Studies, in partial fulfillment of the requirements for the degree of **MASTER OF SCIENCE IN CHEMISTRY.**

Dr. KHALID ALHOOSHANI
(Advisor)

Dr. ABDULLAH J. AL-HAMDAN
Department Chairman

Dr. MOHAMMAD QAMAR
(Member)

Dr. Salam A. Zummo
Dean of Graduate Studies

Dr. BASHEER CHANBASHA
(Member)

25/5/14
Date

DEDICATION

With all of my love I dedicate this thesis to my mother, for her endless support in each step of the way, love, prayers and motivation. My late father, whose words of inspiration and encouragement in pursuit of excellence, still linger on. A special feeling of gratitude to my loving uncle and sister for their unconditional support with my studies, love, encouragement and push for tenacity. My wonderful family and friends for believing in me and who have supported me throughout the process.

ACKNOWLEDGMENTS

All thank Almighty Allah for giving me the strength, courage and determination, as well as guidance in conducting this research study, despite all difficulties. My extreme grateful to the Chemistry Department and King Fahd University of Petroleum & Minerals for offering me this opportunity to complete my graduate studies.

Finally, the culmination of a journey that started with a single step and gradually developed into one mighty task! My joy and sense of fulfillment would not be complete without making mention of everyone who offered help and support, in one way or another, during the entire period of this MS.c study. The brevity of this acknowledgement does not in any way downplay the support I have received from anyone mentioned, or not mentioned, herein. Firstly, I wish to thank my committee members who were more than generous with their expertise and precious time. A special thanks to Dr. Khalid Alhooshani, my committee chairman for his countless hours of reflecting, reading, encouraging, and most of all patience throughout the entire process. Also, I would like to thank the other committee members, Dr. Qamar Mohammad, and Dr. Basheer Chanbasha. Through, their vast experience in this field of study, they have offered invaluable and constructive advice, help, support, motivation and guidance to make this MS.c study come to fruition. My deep thanks to all of the faculty members and staff in the chemistry department at KFUPM. I acknowledge the support provided by King Abdulaziz City for Science and Technology (KACST) through the Science & Technology Unit at King Fahd University of Petroleum & Minerals (KFUPM) for funding this work through project No. 10-NAN1387-04 as part of the National Science, Technology and Innovation Plan. The support of Center of Excellence in Nanotechnology is gratefully acknowledged.

TABLE OF CONTENTS

LIST OF TABLES

LIST OF FIGURES

LIST OF ABBREVIATIONS

BA	:	Benzylalcohol
4-MBA	:	4-methoxy benzylalcohol
4-NBA	:	4-nitro benzylalcohol
CA	:	Cinnamyl alcohol
FESEM	:	Field Emission Scanning Electron Microscope
HAAD-TEM	:	High-angle annular dark-field Transmission Electron Microscope
XRD	:	X-ray Diffractometer
BET	:	Brauner-Emmet-Teller
DRS	:	Diffuse Reflectance Spectrophotometer
EDS	:	Energy Dispersive X-ray Spectroscopy
FT-IR	:	Fourier transform infrared spectroscopy
CB	:	Conduction band
VB	:	Valence band
UV	:	Ultraviolet
GC-MS	:	Gas chromatography mass spectrometry
HP	:	Home prepared

ABSTRACT (ENGLISH)

Full Name : Rami Bahaeldin Abdelrahman Elsayed

Thesis Title : Selective and efficient oxidation of alcohols to aldehydes in presence of visible-light-driven photocatalysts: A green organic synthesis approach

Major Field : Chemistry

Date of Degree : May 2014

Achieving alcohols to aldehydes conversion in an energy efficient and environmentally benign way still remains a challenge. In this work, we describe highly efficient, chemoselective and quantitative conversion of alcohols (e.g., Benzylalcohol, 4-methoxybenzyl alcohol cinnamyl alcohol and 4-nitrobenzyl alcohol) to corresponding aldehydes using synthesized and characterized visible-light photocatalysts, i.e., silver orthophosphate (Ag_3PO_4) and platinum-modified nanoporous hierarchical bismuth tungstate spheres (Pt/Bi_2WO_6) in water under simulated sunlight at ambient conditions. Dependency of alcohol oxidation on substrate concentration, photocatalyst amount and metal loading was studied. The experimental results indicates that chemoselective (>99%), quantitative (>99%) and efficient conversion (>90%) of alcohols to the corresponding aldehydes were achieved using Ag_3PO_4, likewise, highly efficient, chemoselective (>99%) and quantitative (>99%) conversion were achieved using Pt/Bi_2WO_6. No overoxidation of the formed aldehyde was observed during the photooxidation process until comprehensive alcohol oxidation was attained. Pt/Bi_2WO_6 showed substantial oxidation under dark and course of conversion was different than that of under light. The effect of various radical scavengers was investigated and the rate determining step was elucidated. It has been envisaged that the reduction site of semiconductor photocatalysts plays more decisive role in determining the chemoselectivity as alcohol preferably get oxidized over that of water.

ABSTRACT (ARABIC)

ملخص الرسالة

الاسم الكامل : رامي بهاء الدين عبد الرحمن السيد

عنوان الرسالة : أكسدة الكحوليات إلى الالدهيدات المقابلة بكفاءة وانتقائية عاليه باستخدام حافزات ضوئية ـ ضوء مرئي: عملية تصنيع مسالمة بيئيا

التخصص : كيمياء

تاريخ الدرجة العلمية : مايو 2014

تمثل عملية تحويل الكحول إلى الالدهيدات المقابلة بطريقة سليمة بيئيا وغير مكلفه اقتصاديا تحديا حتى هذه اللحظة. في هذا البحث تم تحضير حافزين ضوئيين (ضوء مرئي)؛ فوسفات الفضة (Ag_3PO_4) و تنجسات البزموث المحورة والمطعمة بجزيئات نانومترية من البلاتين (Ag_3PO_4), وتم التحقق من بنيتهما التركيبية ومن ثم استخدما في عملية تحويل بعض المركبات الكحولية مثل (الكحول البنزيلي, 4- ميثوكسي الكحول البنزيلي, كحول السنميل و 4- نايترو الكحول البنزيلي) إلى الالدهيدات المقابلة بكفاءة عاليه و انتقائية كيميائية وكميا وذلك في وجود الماء, أشعة ضوء شمس (محاكة) تحت الظروف الاعتيادية. تم دراسة تأثير كلا من: تركيز المواد المتفاعلة, كمية الحافز الضوئي ونسبة الفلز المستخدم في التطعيم. عمليا تم الحصول على انتقائية كيمائيه > 99%, تحول كمي > 99% وكفاه تحويل > 90%باستخدام Ag_3PO_4, في المقابل تم الحصول على انتقائية كيمائيه > 99%, تحول كمي >99% وكفاه تحويل > 99% باستخدام Pt/Bi_2WO_6. لم يتم ملاحظه أي عملية أكسده للالدهيدات المتكونة خلال التفاعل حتى اكتمال تحول كل الكحوليات. وقد اظهر Pt/Bi_2WO_6 مقدرته الفعالة على أكسدة الكحوليات في عدم وجود الضوء, حيث أن التفاعل يسلك مسارا مختلفا عن ذلك في حالة وجود الضوء. تم استنتاج الخطوة المحددة للتفاعل عن طريق دراسة تأثير مختلف مثبطات الجذور الحرة. من هذه الدراسة نخلص إلى أن المواقع الاختزالية لأشباه موصلات الحافزات الضوئية تلعب دورا حاسما في تحديد الانتقائية الكيميائية حيث تفضل أكسدة الكحوليات عن الماء.

CHAPTER 1

INTRODUCTION

1.1 Alcohols to aldehydes conversion

Utilization of photocatalytic process for the synthesis of fine chemicals via an environmentally benign pathway is envisioned [1]. Light is one of the indispensable ideal reagents for a green chemical synthesis; unlike many ordinary reagents, light produces no waste, non-toxic, and can be generated from many renewable sources. Thus, transition metal photocatalysis is representing an auspicious pathway towards the development of industrial processes in an environmentally friendly fashion [2]. Attempts have been made to achieve numerous functional group transformations, such as amine to imine [3–5], nitro to azo [6], aniline to azobenzene [7], hexane to hexanone and hexanol [8], and alcohols to corresponding aldehydes [9–14]. Selective, efficient and complete oxidation of alcohols into corresponding carbonyl compounds, such as aldehydes, ketones, etc., is of paramount significance for fine chemical industries because carbonyl compounds are being used in food, beverage, and pharmaceutical industries as well as a raw material in chemical industries [15,16]. To achieve the aforementioned conversions, the use of stoichiometric inorganic reagents, such as $KMnO_4$, K_2CrO_4 etc., is predominant in industries. Although such reagents offer high activity and selectivity, accumulation of waste products arising from the use of these inorganic reagents poses threat to the

environment. Intensive effort, therefore, has been carried out in past years to develop 'green oxidation processes'. Although there are active heterogeneous metal catalysts being developed for the aerobic oxidation of various alcohols, the reactions are carried out in harmful organic solvents and/or under vigorous conditions [17–19]. On the contrary, semiconductor-mediated photocatalytic process in context of selective oxidation is still in its infancy as new photocatalysts are being explored to achieve oxidation of alcohols in a green fashion.

1.1.1 Conventional oxidation methods

One of the most fundamental synthesis of fine chemicals and intermediates in industrial synthetic chemistry is selective oxidation, because the corresponding carbonyl compounds serve as important and versatile intermediates for the synthesis of fine chemicals, especially the oxidation of alcohols to aldehydes which is truly a very important laboratory and commercial procedure [20]. Stoichiometric oxygen donors oxidizing reagents such as permanganate and dichromate have been conventionally used in order to achieve this transformation [17]. Chromium trioxide CrO_3, Chromate CrO_4^{-2} and dichromate $Cr_2O_7^{-2}$ are examples of oxidation reagents containing Cr(VI) used under acidic and aqueous conditions. These reagents are very strong oxidizers and under these vigorous reaction conditions aldehydes are formed, however the aldehydes are further oxidized to carboxylic acids. In the presence of pyridine and methylene chloride (CH_2Cl_2) as solvent chromium trioxide is often used to form Collin's which is a toxic complex composed of two molecules of pyridine (CrO_3-pyridine$_2$) and one molecule of CrO_3. This reagent contains no water and due to this it can be used to

oxidize a primary alcohol to an aldehyde without further oxidation to a carboxylic acid. Although Cr (VI) reagents are excellent oxidizing reagents, but it's all toxic, harmful and very hazardous to deal with [21,22]. Another oxidizing reagent is permanganate ion (MnO_4^-, obtained from potassium permanganate [$KMnO_4$]). Primary alcohols can be oxidized using permanganate in basic solution to form potassium carboxylate salts and then carboxylic acid after the addition of a strong acid such as dilute HCl. $KMnO_4$ can react with carbon—carbon triple bonds (alkynes) or double (alkenes) so, it can not be used to oxidize an alcohol which contains a triple or double bond. Furthermore, $KMnO_4$ can not be used to oxidize secondary alcohols to ketones because many ketones react further with $KMnO_4$ [21]. These stoichiometries oxidants appear to have a serious drawbacks under these vigorous conditions that they have serious toxicity issues associated with them and the production of a large amount of wastes lead to production of large amounts of hazardous and toxic wastes due to the use of halogenated organic compounds as solvents [17–19]. Therefore, the development of selective, efficient and environmentally friendly catalysts for alcohol oxidation is a subject of a major interest. Thus, Several studies have been investigated for transition metal-based homogeneous systems such as rhenium, ruthenium, iron, tungsten, palladium, manganese, and copper. Moreover, Pt, Fe, Ru, Au and Pd nanoparticals supported on AC, poly-ethylene glycol, alumina, titania, silica, zeolite, hydroxyapatite, etc. have been studied as heterogeneous catalysts for the aerobic oxidation of alcohols (eq 1). However, the use of metal-catalyzed

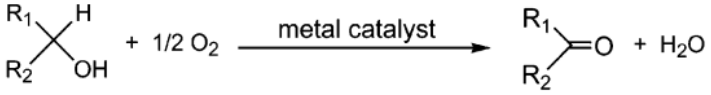

(1)

R_1, R_2= H, alkyl, aryl

aerobic processes often require a large amount of the catalyst, an excess of bases or ligands and high oxygen pressures. Moreover, the difficulties in recovering the expensive catalyst metals and ligands from the reaction mixture limit the use of homogeneous metal catalysts on an industrial scale [23].

1.1.2 Photocatalytic oxidation method

The degradation process of harmful molecules using heterogeneous photocatalysis was successfully applied Since 1970 on the basis of the generally known statement that this process is quite unselective oxidation especially if it's performed in water. Commercial specimens of anatase/rutile mixed phases or Anatase (such as Degussa P25) are commonly used in the degradation processes. Recent studies have, however highlighted that various reactions in the field of organic syntheses can be performed using photocatalysis as a major role. One of these reactions is the partial oxidation of -CH_2OH group to –CHO, which is an important key to the production of many organic products [9]. The need for an environmentally friendly oxidation process is today of primary importance where the sun as a green and free energy source can be used. Photocatalysis is an indispensable oxidation method, especially when used with organic-free solvents. One of the main goals in organic syntheses is the selective oxidation of hydroxyl groups. Thus, environmentally harmful conditions, which involve organic solvents at high pressure and temperature, and also stoichiometric oxygen donors (such as chromate and permanganate), which produce large amounts of dangerous waste, are unfavorable [12]. Utilization of heterogeneous semiconductor-mediated photocatalytic process for oxidation of alcohols seems propitious owing to its environmentally friendly and

renewable attributes. Yet, photocatalytic process in context of selective oxidation is still in its infancy as new photocatalysts are being explored to achieve oxidation of alcohols in a green fashion [24–27]. The fundamentals of semiconductor-mediated photocatalytic process have been well documented in the literature by a multitude of authors [28–30]. Briefly, by providing energy equal to or greater than the band gap of semiconductor photocatalyst, an electron may be promoted from the valence band to the conduction band (e^{-}cb) leaving behind an electron vacancy or "hole" in the valence band (h^{+}vb). If the charge separation is maintained, the electron and hole may migrate to the catalyst surface where they participate in redox reactions with absorbed species. Specially, h^{+}vb may oxidize surface-bound H_2O or OH^{-} to produce hydroxyl radical ($OH^{\bullet}$), and e^{-}cb can reduce oxygen to generate superoxide radical anion ($O_2^{-\bullet}$) fig 1.1. These radical species are extremely reactive and make the photocatalytic process somewhat non-selective. Due to its non-selective attributes, most of the previous studies involving photocatalysis focused on environmental cleanup, H_2 production, and CO_2 reduction, etc.. [28,31,32]. Recently, the perspectives of photocatalytic oxidation process for the synthesis of fine chemicals such as, alcohols to aldehydes in energy efficient and environmentally benign pathway have been envisaged and numerous photocatalysts are being explored [33–36].

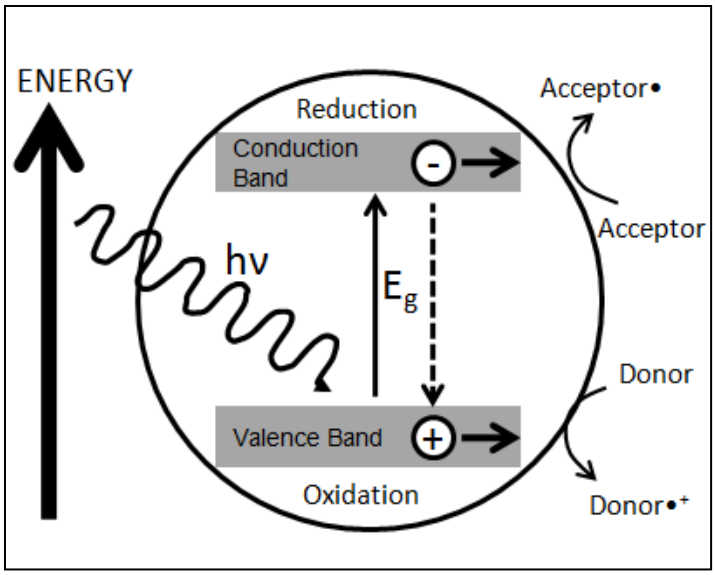

Figure 1.1 Schematic representation of the photocatalytic process, reproduced from [37].

1.2 Band gap and radicals formation

Due to the electronic structure of Semiconductors (e.g. ZnO, ZnS, CdS, $FezO_3$, TiO_2, etc..) they can act as sensitizers for light-reduced redox processes, which is characterized by band gap: a band of energy in the region between the conduction bands (CB) And valence bands (VB). The competition between the process of removing the electrons from the surface of the semiconductor and the recombination process of the electron/vacancy pair determines the efficiency of photocatalysis [28,38]. The recombination process can take place in the case of unsuitable electron and hole scavengers where the stored energy is dissipated within a few nanoseconds. But if the electron or hole is trapped by a suitable scavenger or surface defect state the recombination is inhibited and redox reactions may occur. The VB holes are powerful oxidants (+1.0 to +3.5 V vs NHE

depending on the semiconductor and pH), while the CB electrons are good reductants (+0.5 to -1.5 V vs NHE) [28]. The band gap of various semiconductor materials is shown in fig 1.2.

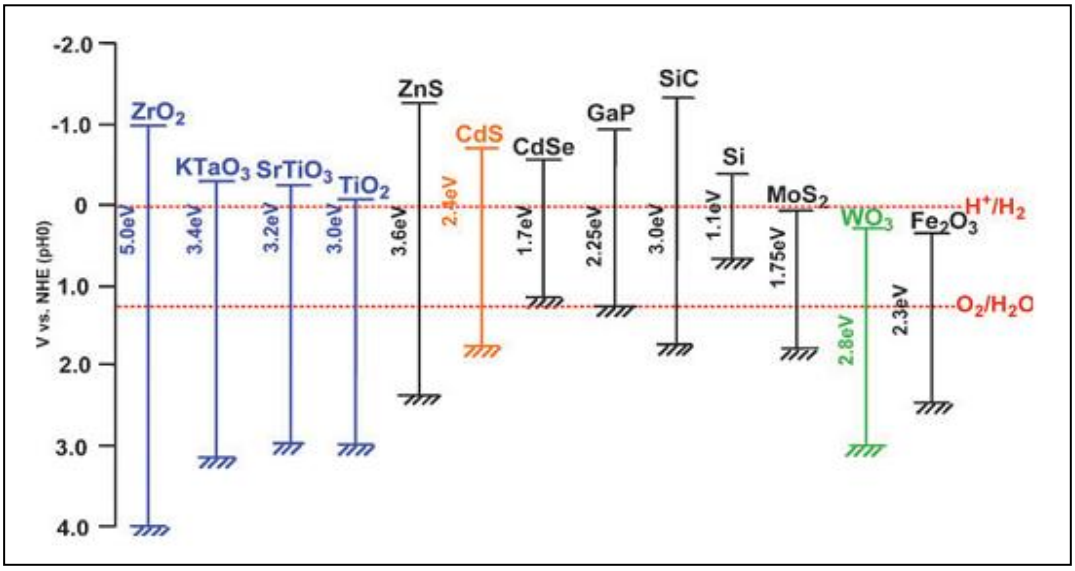

Figure 1.2 Band levels of various semiconductor materials, reproduced from [57].

Irradiation of semiconductor, such as nitrogen-doped TiO_2, carbon-doped TiO_2, GaP, GaAs, CdS, or CdSe, can form electrons with a high reduction potential and irradiation of semiconductor, such as metal-doped TiO_2, WO_3, or Fe_2O_3, can generate holes with high oxidation. Thus, the challenge could be addressed by designing or selecting photocatalysts with appropriate band edges from both types to generate a system with holes having a high oxidation potential or/and electrons having a high reduction potential as needed. As mentioned before the non-selective nature of photocatalysis could be attributed to the formation of extremely reactive and short-lived radicals such as $OH^{\bullet}$, $O_2^{-\bullet}$, $HO_2^{\bullet}$ etc. Possible radicals formation in the case of water oxidation on the surface of photocatalysts is shown in subsequent reactions below [39].

$$photocatalyst \xrightarrow{irradiation} e^- + h^+$$

$$H_2O + h^+ \longrightarrow {}^{\bullet}OH + H^+$$

$$O_2 + e^- \longrightarrow {}^{\bullet}O_2^- \xrightarrow{H^+} HO_2^{\bullet}$$

$$2HO_2^{\bullet} \longrightarrow O_2 + H_2O_2 \xrightarrow{{}^{\bullet}O_2^-} {}^{\bullet}OH + OH^- + O_2$$

Development of photocatalysts that can selectively drive the oxidation of alcohols in water under mild conditions remains an attractive challenge. One of the intrinsic prerequisites of the photocatalysts for high selectivity and conversion appears to be a combination of high oxidation potential of valence band holes and low reduction potential of conduction band electrons. Recently, silver orthophosphate (Ag_3PO_4) is reported to have exceptional before-mentioned electronic attributes and high photocatalytic activity fig 1.3 [40,41]. Bi_2WO_6 was also reported as a highly efficient visible-light-driven photocatalyst, stable, non-toxic and have an appropriate band gap. In addition, Pt deposition onto the surface of Bi_2WO_6 inhibit the electron-hole pair recombination, which remains more ubiquitous in absence of oxidant [42]. Therefore Silver based (Ag_3PO_4) and Bismuth based (Pt-Bi_2WO_6) catalysts are chosen to study the photoxidation of some selected alcohol such as, benzyl alcohol (BA), 4-methoxy benzyl alcohol (4-MBA) and cinnamyl alcohol (CA) to corresponding aldehydes in water at room temperature under simulated sunlight excitation which is an energy efficient and environmentally benign process.

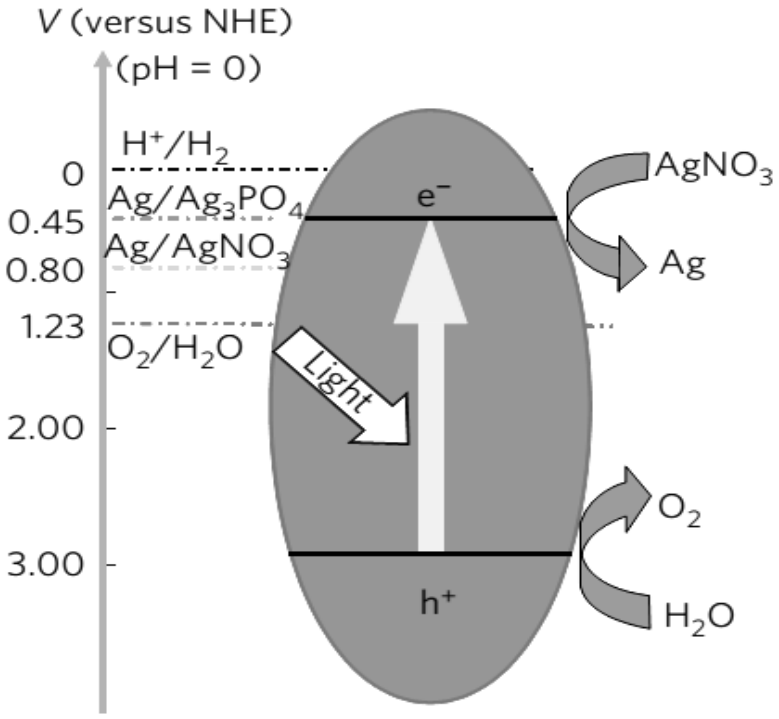

Figure 1.3 Schematic drawing of redox potentials of Ag_3PO_4, reproduced from [40].

1.3 Objectives of the study

The main objective of this study is to develop and synthesize Silver (Ag) based and Bismuth (Bi) based catalysts for photocatalytic oxidation of alcohols to corresponding aldehydes. This will be achieved by the following specific objectives:

i. Synthesis of silver orthophosphate (Ag_3PO_4) by a simple ion-exchange method.

ii. Synthesis of bismuth tungstate (Bi_2WO_6) by a hydrothermal method followed by photodeposition method for Pt deposition on the surface of Bi_2WO_6.

iii. Optimization of the synthesis conditions for both of the catalysts.

iv. Characterization of both catalysts using different analysis techniques, such as field emission scanning electron microscope (FESEM), transmission electron microscope (TEM), X-ray diffractometer (XRD), Raman spectroscopy, Brauner-Emmet-Teller (BET) surface area measurement, diffuse reflectance UV-visible spectrophotometer (DRS), energy dispersive X-ray spectroscopy (EDS), Fourier transform infrared spectroscopy (FT-IR) and thermogravimetric analysis (TGA).

v. Performance evaluation of the photocatalytic activity of both catalysts towards the oxidation of some selected alcohols, such as benzyl alcohol (BA), 4-methoxy benzyl alcohol (4-MBA), cinnamyl alcohol (CA) and 4-nitro benzylalcohol (4-NBA) to the corresponding aldehyde.

vi. Studying different experimental parameters to enhance the photocatalytic activity of the catalysts, such as alcohol concentration, catalyst amount, reaction time, O_2 and N_2 bubbling and the effect of electron withdrawing or/and electron donating groups.

vii. Studying the conversion efficiency in water at room temperature under simulated sunlight excitation using gas chromatography mass spectrometer (GC-MS).

viii. Investigate the selectivity of the prepared catalysts towards alcohols oxidation to the corresponding aldehydes.

ix. Assessment of the conversion yield of the photocatalytic reaction.

CHAPTER 2

LITERATURE REVIEW

Ever since the discovery of light-activated water splitting on a TiO_2 electrode (the so-called Honda effect) [43], photocatalytic processes have been widely investigated owing to their renewable attributes. Most of the earlier studies involving photocatalysis focused on environmental cleanup, H_2 production, and CO_2 reduction etc. [28,31,32]. Recently, the utilization of photocatalytic process for the synthesis of fine chemicals via an environmentally benign pathway has been explored [1,2]. Many literatures reported for alcohol oxidation into corresponding carbonyl compounds, such as aldehydes, ketones, etc.., using different type of ultraviolet-light active photocatalysts, Visible-light-active photocatalysts and other photocatalysts.

2.1 Ultraviolet-light active photocatalysts

Many works have been conducted by many researchers for the oxidation of different alcohols to the corresponding carbonyl compounds using ultraviolet-light active photocatalyst. Palmisano et al. investigated the photocatalytic oxidation of 4-methoxybenzyl alcohol to p-anisaldehyde in aqueous suspensions using home-prepared and commercial titanium dioxide (TiO_2) catalysts. The preparation of nanostructured TiO_2 samples was carried out by boiling aqueous solutions of titanium tetrachloride ($TiCl_4$), under mild conditions, for different times. The highest yield obtained for the

conversion of 4-methoxybenzyl alcohol to p-anisaldehyde was (41.5 %) with conversions of (65 %) using home-prepared titanium dioxide catalyst compared to the commercial TiO_2 samples which give a maximum yield of only (10.8 %). The main oxidation product was found to be carbon dioxide. Other by-products formed were traces of aliphatic products and 4-methoxybenzoic acid [14]. Another approach done by Augugliaro et al. for the oxidation of benzyl alcohol (BA) and 4-methoxybenzyl alcohol (4-MBA) using home-prepared aqueous suspensions of TiO_2 and commercial TiO_2 catalysts. CO_2 and corresponding aromatic aldehydes were the main oxidation products for both alcohols. The selectivity of the home-prepared catalysts towards the aldehyde production was up to 28% and 50% conversion for benzyl alcohol and for 4-methoxybenzyl alcohol was 41% and 65% conversion, which is about four times higher than the commercial TiO_2.Using small amounts of an aliphatic alcohol such as ethanol, methanol, tert-butanol or 2-propanol found to be efficient for enhancing the selectivity of aldehyde formation up to 1.5 times but decreases the overall oxidation rate of aromatic alcohols [44].

Augugliaro et al. investigated the photocatalytic oxidation of 4-MBA and BA but this time with another rutile TiO_2 prepared from $TiCl_4$ at low temperature. An improvement in the selectivity towards the formation of aromatic aldehydes was observed, 60 and 38 % for 4-MBA and BA, respectively table 2.1. CO_2 reported to be the only byproduct formed. Aldehyde and acid were detected besides some hydroxylated aromatic compounds [45].

Table 2.1 Selectivity towards aldehyde formation of many HP Rutile TiO_4 and commercial catalysts

Catalyst	HP298	HP333	HP333D	HP673	HP973	Merch	Sigma-Aldrich
Selectivity BA [%mol]	12.1	38.2	33.5	12.2	9.9	7.9	9.2
Selectivity 4-MBA [%mol]	-	60.0	56.2	50.1	40.0	15.9	20.9

The same group of researchers (Augugliaro et al.) performed a photocatalytic oxidation of 4-MBA using home-prepared anatase, rutile, and brookite TiO_2 to study the selectivity towards the formation of 4-methoxy benzaldehyde in organic-free water suspensions in the presence of a UV lamp. The obtained photoreactivity resulted from the HP and commercial catalysts were summarized in table 2.2 [46].

Table 2.2 Photoreactivity results of HP and commercial catalysts

Catalyst	**HPA[a]**	**HPA[a]**	**HPR[b]**	**HPR[b]**	**HPB[c]**	**HPB[c]**	**SA[d]**	**Merck[e]**
SSA/m2 g-1	235	235	107	107	82	82	2.5	10
Particle size/ nm	28	28	50	50	95	95	240	170
Selectivity [%mol]	31	39	58	62	39	50	21	16

BET (SSA) specific surface areas of catalysts, [a]Home-prepared anatase, [b]Home-prepared rutile, [c]Home-prepared brookite, [d]Sigma-Aldrich rutile. [e]Anatase.

Another work done by Raffaele et al. to oxidize benzylalcohol to benzaldehyde using TiO_2/Cu(II) photocatalyst under acidic conditions, in aqueous solution irradiated by UV

lamp. With respect to the initial concentration of benzylalcohol the highest yield obtained in this work was 35% of benzaldehyde. Partial conversion of benzaldehyde to benzoic acid has been observed. Some by-products, such as 4-hydroxy-benzaldehyde, 2-hydroxy-benzaldehyde, 4-hydroxy-benzylalcohol and 2-hydroxy-benzylalcohol, has been detected and this formation of by-products was Attributed to the formation of active $OH^{\bullet}$ radicals. During the process Cu(II) was totally reduced to copper(0). The reduced copper(0) was easily reoxidized to Cu(II) in the presence of oxygen, in the dark [47].

Daijiro et al. tried to perform a photocatalytic selective oxidation of alcohols to aldehydes using a new system where TiO_2 was coated with WO_3 as an electron acceptor site to enhance the selectivity and inhibit the recombination of electrons to the valence band. WO_3/TiO was irradiated with a light source ($\lambda > 350$ nm) with O_2 in water. The highest catalytic activity for the loaded WO_3 on the catalyst (TiO_2) was 8 wt %, which gave much better selectivity (60%) than the previously reported systems. This high activity of this catalyst was attributed to transfer of TiO_2 electron's from the conduction band to the surface of WO_3 which leads to charge separation and inhibit the recombination of the electrons therefore, increasing the oxidation efficiency of the catalyst. The high aldehyde selectivity is due to the coating by WO_3 where, the availability of TiO_2 becomes less so, the adsorption of the formed aldehydes on the surface of TiO_2 will be suppressed and no further reaction of aldehydes will occur fig 2.1 [48].

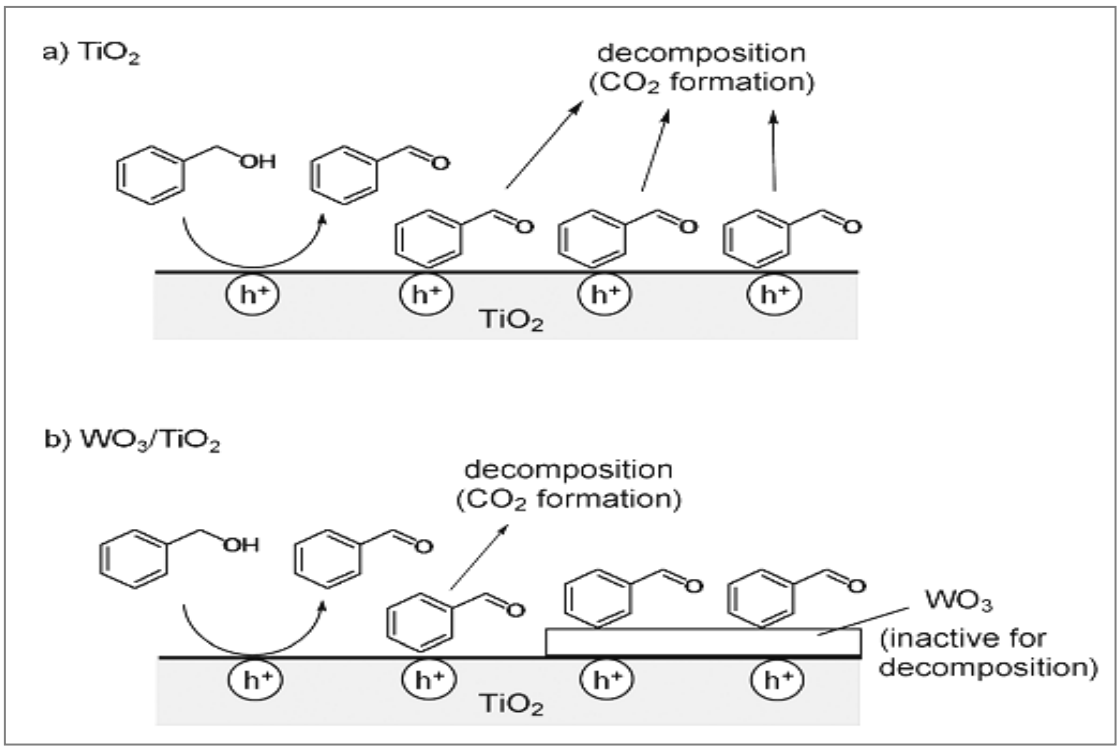

Figure 2.1 Reactions on surfaces of a) TiO_2 and b) WO_3/TiO_2, reproduced from [48].

A highly selective photocatalyst for the oxidation of benzylalcohol was reported by Wei et al. using modified TiO_2 by transition metal clusters under UV irradiation in presence of molecular oxygen. According to the metal type, preparation method, metal loading and reaction conditions different photocatalytic performance were observed. The highest photocatalytic oxidation activity towards benzylalcohol to the corresponding carbonyl compounds obtained by Ir/TiO_2 system (92% selectivity and 8.9% conversion). Loading of iridium on the surface of TiO_2 can inhibit the recombination of electrons to the photogenerated holes which increase the photocatalytic activity and also helps to activate the molecular oxygen to increase the selectivity in the photocatalytic oxidation reactions. Oxidation of the formed aldehyde to CO_2 was avoided under solvent-free conditions and this is due to the suppression of $OH^{\bullet}$ formation, but the formation of benzoic acid and subsequent esterification couldn't be avoided which is a common problem for the oxidation of primary alcohols. A mechanism for the oxidation process are shown in fig 2.2 [35].

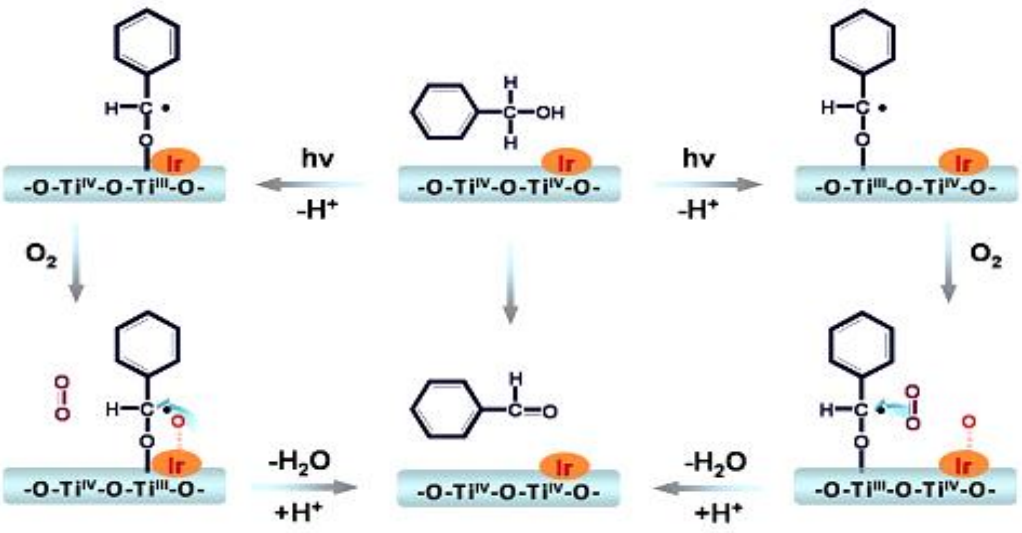

Figure 2.2 Mechanism for the oxidation process of benzylalcohol to benzaldehyde, reproduced from [35].

Last but not least in using UV active photocatalyst, Shinya et al. conducted a series of reaction using TiO_2 loaded with Nb_2O_5 between (0-5 mol%) for the photooxidation of some alcohols such as, 3-pentanol, cyclohexanol, 1-pentanol, and 2-pentanol. When the amount of Nb_2O_5 increased the formation of O_3^- Significantly decreased and this was investigated by ESR. It was found that loading over 4 mol% of Nb_2O_5 will completely disappear the formation of O_3^-, which will increase the selectivity of the catalyst but at the same time it will decrease the photocatalytic activity. The highest selectivity towards the partial oxidation products was 97% with 3 mol% of Nb_2O_5 loading. At the conversion level of 20% with 3 mol% of Nb_2O_5 loading the selectivity obtained was 85% under atmospheric oxygen, 0.1g catalyst and 10 ml alcohol without the usage of solvent. A schematic draw for the photooxidation of alcohols over TiO_2/ Nb_2O_5 are shown in fig 2.3 [33].

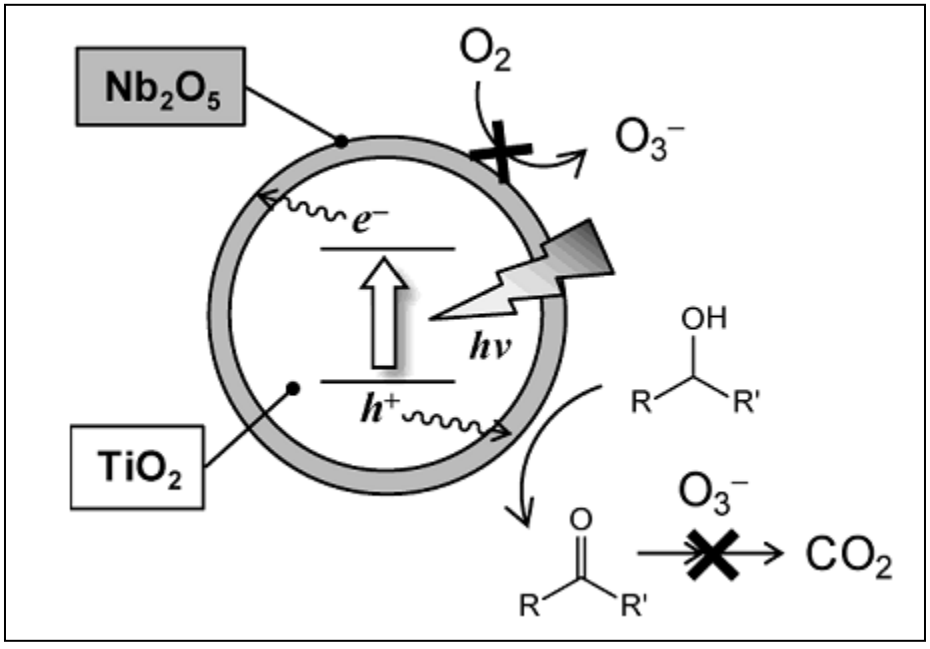

Figure 2.3 Photooxidation of alcohols over TiO_2/ Nb_2O_5, reproduced from [33].

2.2 Visible-light-active photocatalysts

Using UV light for the irradiation of catalyst is the most commonly used in the photocatalytic experiments specially for TiO_2. The first report for the selective photooxidation of alcohols (4-tertiary-butylbenzyl alcohol, 4-(trifluoromethyl) benzyl alcohol, 4-methoxybenzyl alcohol, 4-methylbenzyl alcohol, 4-chlorobenzyl alcohol, and 4-nitrobenzyl alcohol) into corresponding aldehyde under visible light irradiation using TiO_2 has been done by Shinya et al. A high selectivity and conversion yield were obtained >99% under atmospheric O_2 using organic solvent (Acetonitrile), and this prevents the formation of radicals which are responsible for the non-selective oxidation process. They demonstrated this high percent by the adsorption of alcohols on the surface of the TiO_2 to form a surface complex, involving OH groups, that leads to the absorption of visible light and resulting in a high conversion and selectivity [49].

Zhang et al. conducted a series of reactions using cadmiumsulfide nanocomposites assembled on two-dimensional graphene Scaffold (CdS-GR) under visible-light irradiation for selective photooxidation of alcohols into corresponding aldehydes. They evaluated the photocatalytic activity of the catalyst with different weight addition ratios of GR (blank-CdS, CdS 1% GR, CdS 5% GR, CdS 10% GR, and CdS 30% GR). The reactions were carried out in different solvents for 4 h irradiation. The photocatalytic activity is shown in fig 2.4. It was found that the optimal performance obtained for the photooxidation of alcohols was by (CdS 5% GR), with ~ 45% conversion, ~ 45% yield and >99% selectivity, using trifluorotoluene as a solvent. The enhancement in the

photocatalytic activity and selectivity is attributed to two reasons, first the fabrication of the catalyst with GR which is a highly conductive and inhibit the recombination of the excited electrons, second the usage of organic solvent (trifluorotoluene) prevents the formation of radicals which are in charge of the non-selective photooxidation process [24].

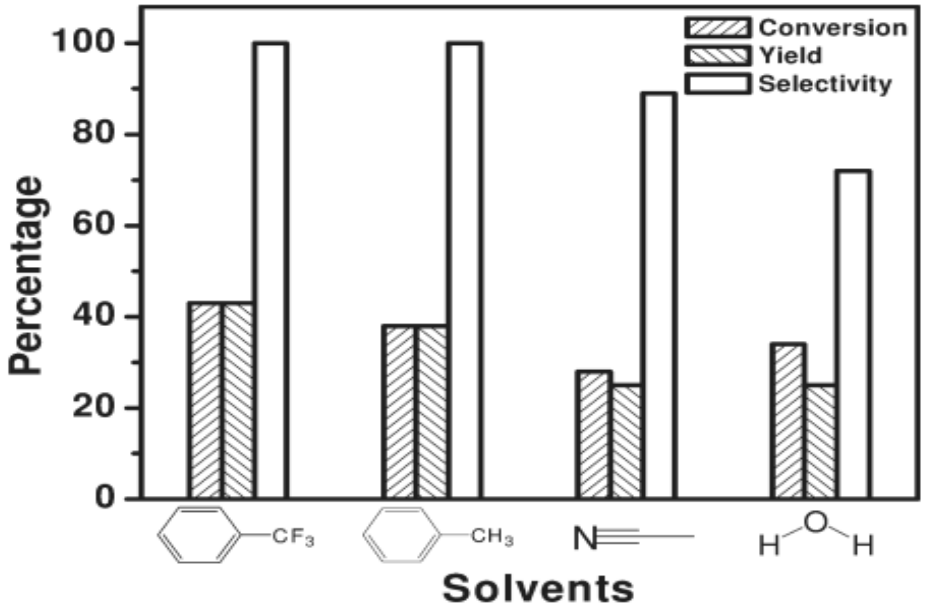

Figure 2.4 Photocatalytic activity of (CdS 5% GR) in different solvents, reproduced from [24].

Further enhancement for a selective oxidation of alcohols to aldehydes using visible light irradiation has been done by the same group of researchers (Zhang et al.) using CdS 5% GR decorated by TiO_2 nanoparticles to form a ternary CdS-GR-TiO_2 hybrid. The enhancement of the photocatalytic activity attributed to the introduction of TiO_2 which Accelerates the interfacial charge-transfer rate, prolongs the lifetime of photogenerated electron−hole pairs and enlarge the surface area. The highest photocatalytic performance in both conversion and yield found to be for CdS-5% GR-10% TiO_2 nanocomposite [25]. Another approach has been done by Atsuhiro et al. where they tried to use cerium (IV) oxide (CeO_2) loaded with gold (Au) nanoparticals, prepared by the photodeposition method, for the photocatalytic oxidation of aromatic alcohols to the corresponding aldehydes under irradiation of green light, in an aqueous solution in the presence of O_2. 1 wt% of Au was chosen to evaluate the photocatalytic performance where the surface of CeO_2 is fully saturated. Benzylalcohol was examined for the photooxidation process, it was found that benzylalcohol was consumed after 20 h of irradiation to form only benzaldehyde without any detection of CO_2. A high selectivity and conversion of benzylalcohol were obtained >99% for both. Only (33 μmol) from alcohols was used, Au/CeO_2: 50 mg, water: 5 cm^3 and O_2 : 1 atm [26].

Zhang and co-workers investigated the role of O_2 in the selective photocatalytic oxidation of benzylalcohol to benzaldehyde and how selectivity depends on the position of valence band of semiconductors. A series of reactions have been employed for a different reported photocatalysts (g-C_3N_4, P25, $In(OH)_xS_y$, Bi_3O_4Br,Cu_2O, and BiOBr) having a different band gap to study the photooxidation process of benzylalcohol under

visible light and O_2 role. These photocatalysts classified as 5 types (I-V) according to the band gap of each catalyst fig 2.5. From the obtained results it was concluded that to have a selective photocatalyst for the oxidation of benzylalcohol to benzaldehyde under visible light irradiation the CB position of the catalyst must be more negative than the reduction potential of $O_2/^{\bullet}O_2^-$ (−0.33 V), the VB position must be must be laid between the reduction potentials of BA/BAD and BAD/oxidized BAD (1.98–2.50 V) and the energy of band gap must be just a little bit more than 2.31 eV.

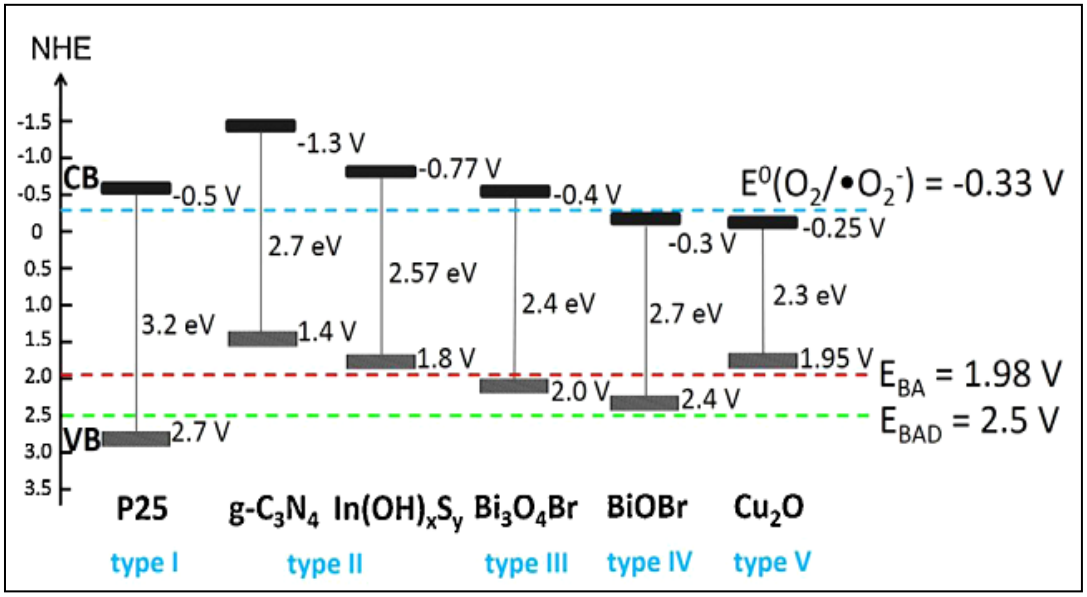

Figure 2.5 Catalysts energy band position, reproduced from [29].

Therefore, they used $Bi_{12}O_{17}C_{l2}$ (nanobelts) photocatalyst to confirm the aforementioned conclusion, where it has the three criteria for a selective photooxidation process of BA to BAD. It was found that the main role of O_2 is to trap the electrons generated by light to form $^{\bullet}O_2^-$. This process helps to inhibit the electrons recombination and it is not contributing in the benzylalcohol oxidation. The highest conversion and selectivity

obtained in presence of O_2, using acetonitrile as a solvent and under visible light irradiation for 8 hours and was 41% and >99% respectively [29].

2.3 Other Catalysts

There are a huge number of heterogeneous metal catalysts that can be used for the oxidation of alcohols to corresponding carbonyls, but as mentioned before that there are some drawbacks for using such kind of catalysts which limit the use of these catalysts on an industrial scale. Table 2.3 summarizes several studies using different type of catalyst for the oxidation of alcohols.

Table 2.3 Summary of different catalysts for alcohol oxidation.

Author	Catalyst	Conclusion	Reference
Xianqin et al.	Au/RGO	BA conversion 65% BAD selectivity 93%	[50]
Christopher et al.	meso-Al_2O_3	BA conversion 70% BAD selectivity 97%	[51]
Dan et al.	Au-Pd/TiO_2	BA conversion 70% BAD selectivity 91.6%	[52]
Eduardo et al.	Ru(PPP)/MB-H_2O_2	BA conversion >99% BAD selectivity >99%	[53]
Kohsuke et al.	PdHAP-0	BA conversion >99% Yield 99%	[20]
Hua-yin et al.	Mn_2O_3- NP	BA conversion 65% Yield 65%	[54]
Hui et al.	Au/CuO	BA conversion 58.5% BAD selectivity 98.2%	[55]
Ankush et al.	$CpMo(CO)_3(C{\equiv}CPh)$	BA conversion 86% BAD selectivity 92%	[56]
Kazuya	Pt–TiO_2	BA conversion 99% BAD selectivity >99%	[57]

CHAPTER 3

RESEARCH METHODOLOGY

3.1 Chemicals and materials

Most of the chemicals were purchased from Sigma Aldrich with a purity > 99.99% (e.g., benzyl alcohol (BA), 4-methoxy benzylalcohol (4-MBA), cinnamyl alcohol (CA), 4-nitro benzylalcohol (4-NBA), Benzaldehyde, 4-methoxy benzaldehyde, Cinnamaldehyde, 4-nitro benzaldehyde and Platinum hexachloroplatinate H_2PtCl_6). Other chemicals and materials have been used are as follow: Disodium Hydrogen Phosphate heptahydrate ($Na_2HPO_4.7H_2O$), crystalline/ACS certified, fisher chemicalSilver, nitrate ($AgNO_3$), >99.0%, Sigma Aldrich, pluronic F127, Sigma Aldrich, Bismuth nitrate pentahydrate $Bi(NO_3)_3.5H_2O$, 99.99%, Aldrich, Sodium tungstate dihydrate ($Na_2WO_4.2H_2O$), >99%, Sigma Aldrich and Terephthalic acid, 98%, Aldrich. 150 ml size reactor was used with 230 W tungsten-halogen lamp (OSRAM) which emits <2% UV light. Also O_2 and N_2 cylinders were used with a purity of 99.9999%.

3.2 Synthesis of Ag_3PO_4

Ag_3PO_4 was prepared following the synthesis procedure documented in the literature [40]. In a typical synthesis, required amount of $Na_2HPO_4.7H_2O$ (0.27 g, 0.001 mol) was

dissolved in double distilled water (50 mL) followed by addition of $AgNO_3$ (0.34 g, 0.002 mol). A bright yellow precipitate was immediately formed and resulting suspension was kept under stirring for 2 h for a complete reaction. The product was collected by centrifugation, washed several times with water and ethanol and was dried at 90 ^{o}C for overnight.

3.3 Synthesis of nanoporous hierarchical Bi_2WO_6

In a typical synthesis, 0.5 g Pluronic F127 was completely dissolved in 20 ml water acidified with nitric acid (pH ~1). Bismuth nitrate (0.08 M) was added and the solution was stirred until a clear solution was obtained. On the other hand, an aqueous solution of sodium tungstate $Na_2WO_4.{}_2H_2O$ (0.04 M, 20 ml water) was prepared separately. Solution of sodium tungstate was added drop wise to the mixture of bismuth nitrate with vigorous stirring at room temperature. As a result, a white colloidal solution was obtained which was further kept under stirring for 2 h. Then, the solution was transferred into a 125 ml Teflon vessel and heated at 170 °C for 20 h under autogenous pressure. After cooling, the product was collected, thoroughly washed with water and ethanol to remove any residual surfactant and dried at 110 °C under vacuum overnight.

3.4 Synthesis of (Pt/Bi_2WO_6)

The deposition of platinum onto the surface of the Bi_2WO_6 was performed using a photo-deposition method in a similar immersion well photochemical reactor fig 3.1. Briefly, 130

ml of water was added to the reaction vessel and the required amounts of metal salt (H_2PtCl_6) and Bi_2WO_6 were added. The suspension was stirred and purged with high purity argon gas for at least 1h to remove the dissolved oxygen. Methanol (10 vol%) was added as an electron donor. Irradiation was carried out using a 230 W tungsten-halogen lamp (OSRAM) for 6 h. After irradiation, the Pt loaded catalyst was washed with water and ethanol and separated through centrifugation and dried at 110 °C under vacuum overnight.

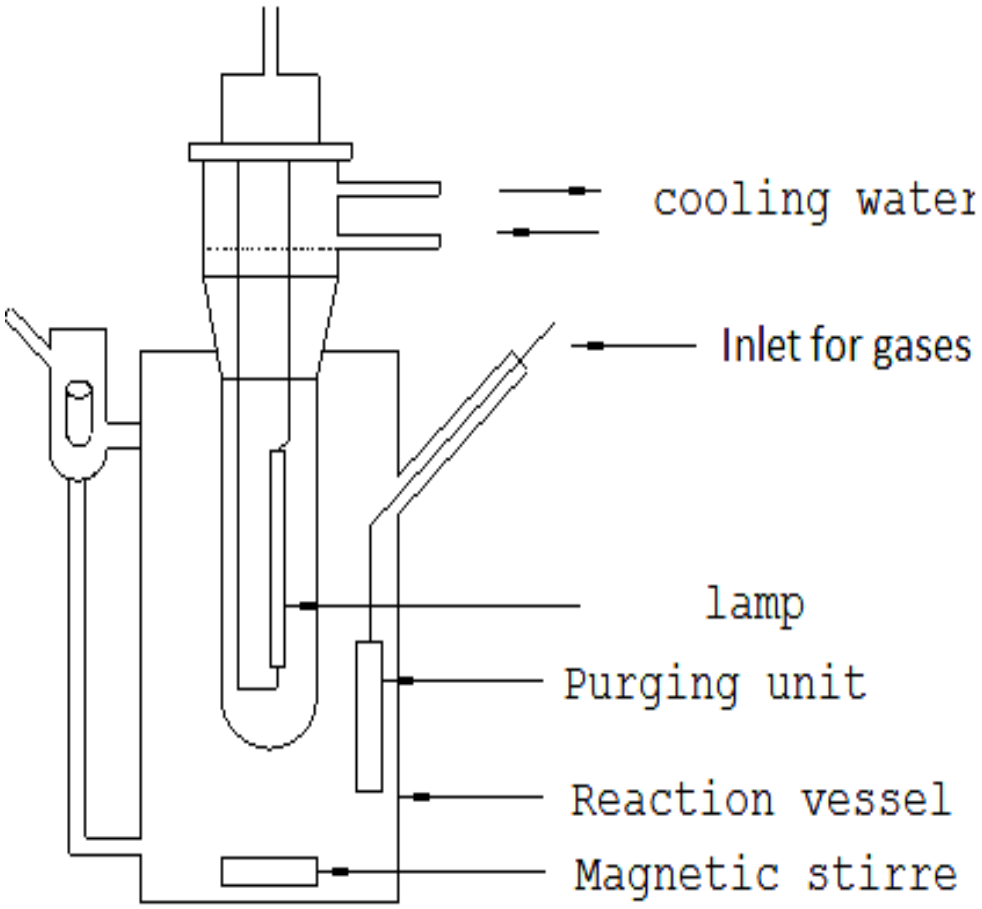

Figure 3.1 Schematic draw of photo-reactor.

3.5 Characterization

The prepared catalysts were characterized by different techniques such as, field emission scanning electron microscope (FESEM), transmission electron microscope (TEM), X-ray diffractometer (XRD), Raman spectroscopy, Brauner-Emmet-Teller (BET) surface area measurement, diffuse reflectance UV-visible spectrophotometer (DRS), energy dispersive X-ray spectroscopy (EDS) and Fourier transform infrared spectroscopy (FT-IR).

3.5.1 Field Emission Scanning Electron Microscope (FESEM)

Field emission scanning electron microscope (TESCAN LYRA 3 FEG) was used to investigate the surface topography of the catalysts.

3.5.2 Transmission Electron Microscope (TEM)

High-angle annular dark-field transmission electron microscope (HAAD-TEM), FEI Company, was used to create a magnified detailed images for the catalysts also to have an information on the internal structure of the samples.

3.5.3 X-ray Diffractometer (XRD)

XRD, (Shimadzu XRD Model 6000, Japan), is an excellent analytical technique used for phase identification of a crystalline material.

3.5.4 Raman spectroscopy

Raman, iHR320 Horiba Spectrometer with CCD was used to observe vibrational, rotational, and other low-frequency modes in the catalysts which provides a fingerprint by which the molecule can be identified.

3.5.5 Brauner-Emmet-Teller (BET) surface area measurement

BET analysis (Micromeritics, USA) was used to provide precise-specific surface area, pore area, pore volume and pore size of the tested catalysts.

3.5.6 Diffuse Reflectance UV-visible Spectrophotometer (DRS)

Diffuse Reflectance Spectroscopy (DRS), JASCO V670 was used to measure the characteristic reflectance spectrum produced as light passed through the catalysts which contains information about the optical properties and structure of the catalysts being measured.

3.5.7 Energy Dispersive X-ray Spectroscopy (EDS)

EDS (Oxford Instrument-England and X-Max detector) was used for the elemental analysis or chemical characterization of the samples.

3.5.8 Fourier transform infrared spectroscopy (FT-IR)

FT-IR (Nicolet 6700 spectrometer-Thermo electron, USA) was used to identify chemical bonds in the catalysts by producing an infrared absorption spectrum. The recorded spectra

is a distinctive molecular fingerprint that can be used to screen and scan samples for many different components and also for detecting functional groups in the samples.

3.6 Photocatalytic experiments

The photocatalytic activity for the oxidation of alcohols was evaluated using immersion well photochemical reactor made of Pyrex glass equipped with a magnetic stirring bar, a water circulating jacket and with openings for supply of gases. A detailed schematic of photocatalytic reactor is delineated in fig 3.2. For irradiation experiment, 130 ml solution was taken into the photo-reactor and required amount of photocatalyst was added and the solution was stirred for at least 15 min in the dark. The zero time reading was obtained from the solution withdrawn before the light was turned on. Irradiations were carried out using a 230 W tungsten-halogen lamp (OSRAM) which emits <2% UV light, a radiation spectrum emulating sunlight. The temperature was controlled and kept at room temperature by circulating cold water through the outer jacket of the reactor. Samples (3 ml) were collected before and at regular intervals during the irradiation and the catalyst was removed by filtration.

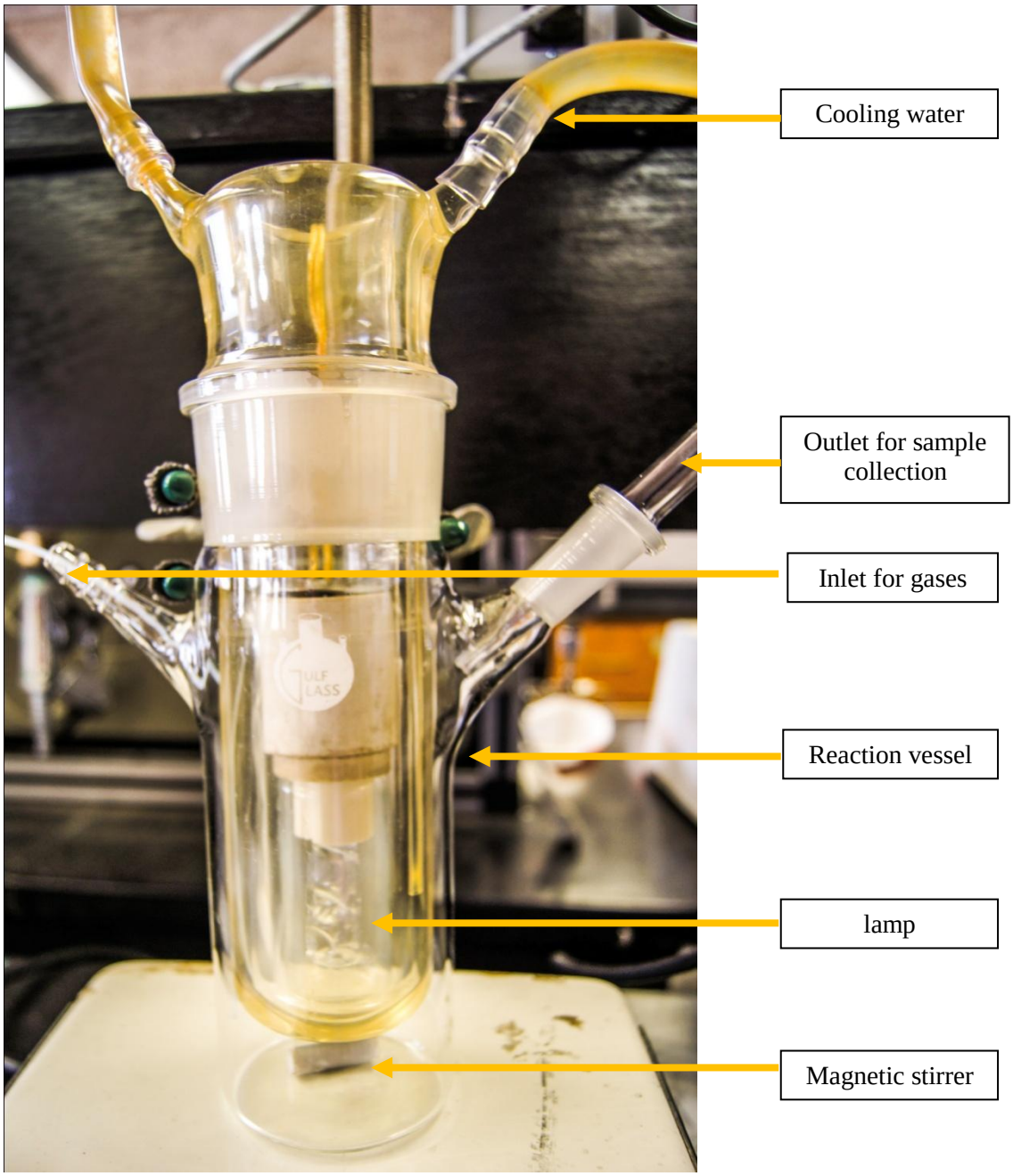

Figure 3.2 photo-reactor set up.

3.7 GC-MS analysis

All the irradiated solutions were extracted by 3 ml of chloroform in three portions, 1 ml each, for maximum extraction. Analysis of the extracted samples was carried out by gas chromatography mass spectrometer (Agilent Technologies fig 3.3) using capillary column (5% phenyl methyl siloxan, 30 m × 320 µm × 0.25 µm). Selected ion monitoring mode (SIM) was used for routine analysis. Programing of the GC oven temperature was as follows: it was set to reach 40 ^{0}C in 1 min, then 10 ^{0}C/min to reach 200 ^{0}C. Injection volume was 100 nl with split ratio 2:1. The calibration curves were obtained by injecting standards solutions of reactants and products, such as benzyl alcohol, benzaldehyde, 4-methoxy benzyl alcohol, and 4-methoxy benzaldehyde and so on. The concentrations of alcohols and aldehydes were determined from the peak areas. Percent (%) conversion and selectivity was calculated using below formulae;

$$\text{Selectivity} = \frac{Cp}{(C\text{r}_0 - Cr)} \times 100\%$$

$$\%\,\text{Conversion} = \frac{(Cr_0 - Cr)}{C\text{r}_0} \times 100\%$$

Cr_0 = the initial concentration of the reactant, Cr = the concentration of the reactant during the reaction, Cp = the concentration of the product during the reaction.

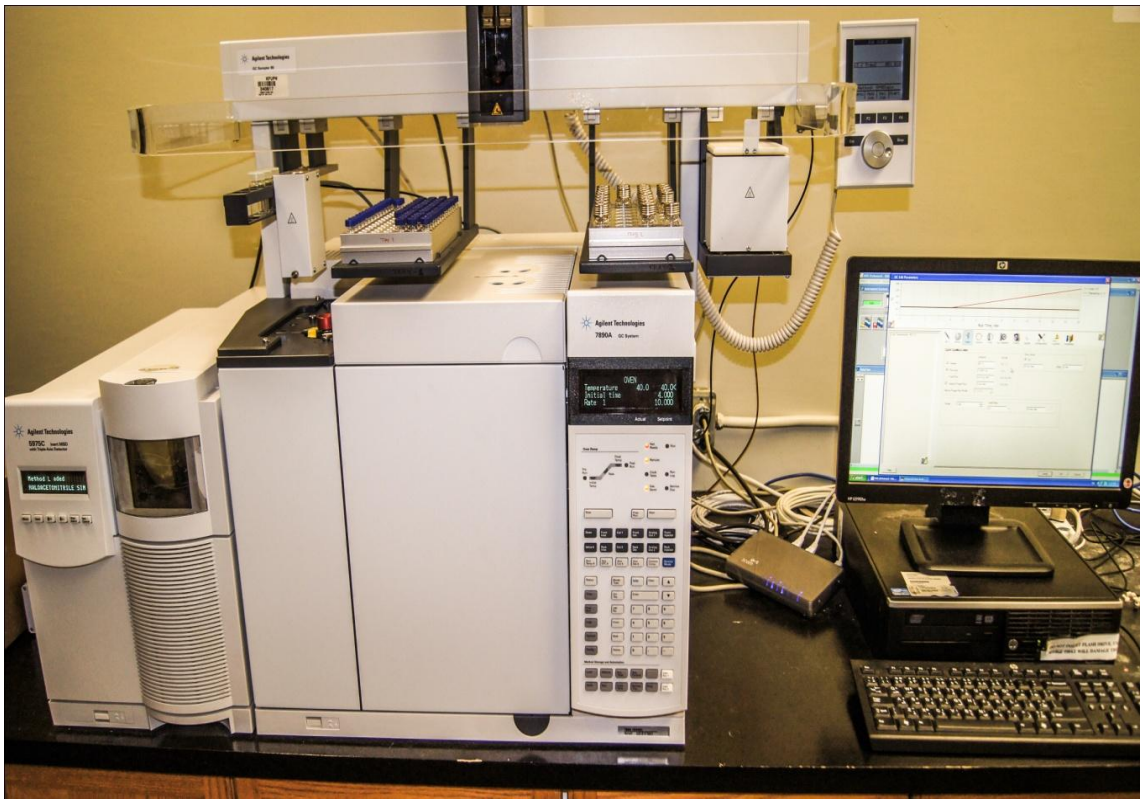

Figure 3.3 Gas chromatography mass spectrometer (Agilent Technologies).

3.8 Photoluminescence studies

3.8.1 Ag_3PO_4 Photoluminescence study

A 100 mL of the 5×10^{-4} M terephthalic acid aqueous solution with concentration of 2×10^{-3} M NaOH was taken into the photo-reactor. Reactions were carried out both in the absence or presence of 1×10^{-3} M BA. Required amount of Ag_3PO_4 was added and resulting suspension was kept under stirring for 15 min under dark. Then, the lamp was turned on and samples were collected, after every 2 mins, and filtered to remove catalyst particles. Photoluminescence analysis of irradiated solutions was performed on a fluorescence spectrophotometer (Horiba, FluoroLog®-3) using an excitation wavelength of 308 nm.

3.8.2 Pt/Bi_2WO_6 Photoluminescence study

A 120 mL of the 5×10^{-4} M terephthalic acid aqueous solution with concentration of 2×10^{-3} M NaOH was taken into the photo-reactor. Reactions were carried out both in the absence or presence of 1×10^{-3} M 4-MBA. Required amount of Pt/Bi_2WO_6 was added and resulting suspension was kept under stirring for 15 min under dark. Then, the lamp was turned on and samples were collected and filtered to remove catalyst particles. Photoluminescence analysis of irradiated solutions was performed on a fluorescence spectrophotometer (Horiba, FluoroLog®-3) using an excitation wavelength of 308 nm.

CHAPTER 4

RESULTS AND DISCUSSION FOR Ag_3PO_4 PHOTOCATALYST

4.1 Characterization

4.1.1 Field emission scanning electron microscope

To investigate the surface topography of the catalyst analysis was performed using (FESEM) field emission scanning electron microscope, (TESCAN LYRA 3 FEG). The particle agglomerates have sharp-faceted features of fractured surfaces and fall in the range of ~ 0.5 to 2 μm. Fig 4.1 shows scanning microscopic image of Ag_3PO_4.

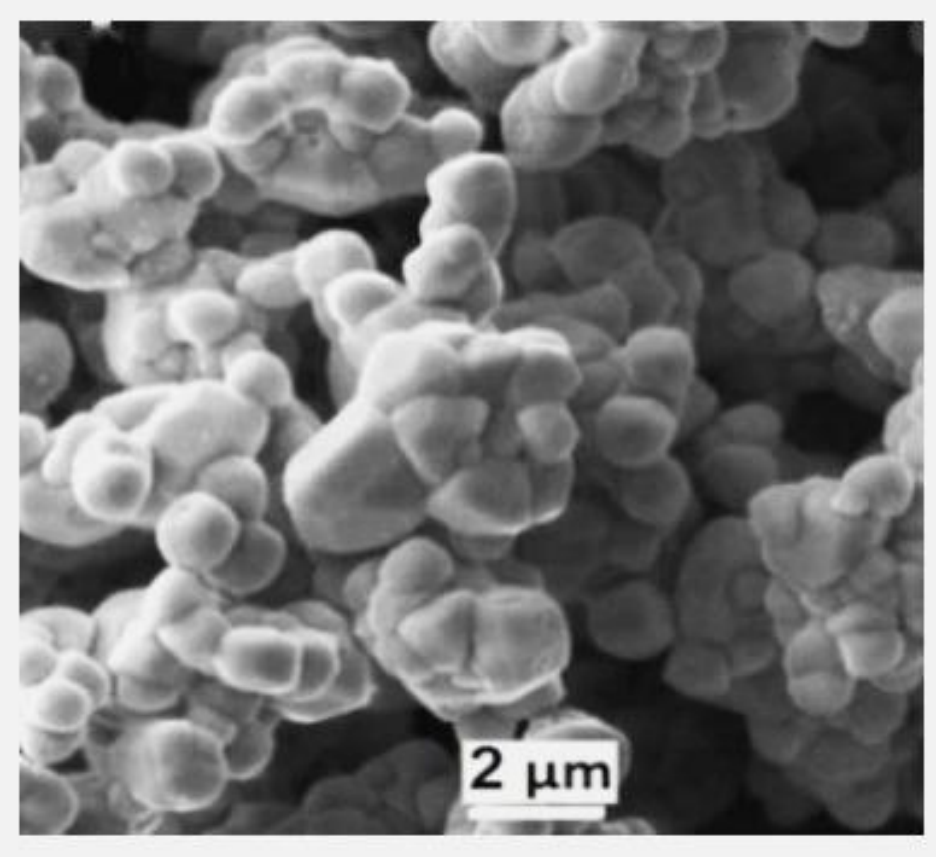

Figure 4.1 Field emission scanning electron microscopic image.

4.1.2 X-ray Diffractometer

X-ray diffraction analysis was employed using Shimadzu XRD Model 6000, Japan. The XRD analysis revealed the formation of a single phase crystalline material and the peaks could be indexed as those belonging to Ag_3PO_4 in BCC structure (JCPDS no.: 6-505); sharpness of the peaks is representative of a polycrystalline material. Fig 4.2 shows the XRD pattern of Ag_3PO_4.

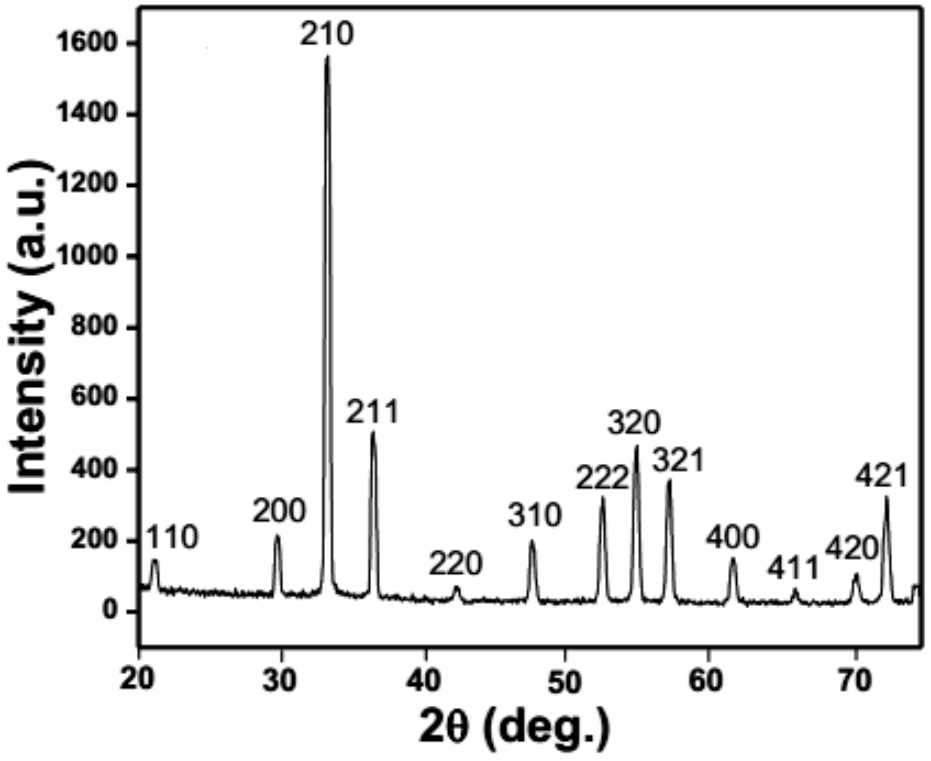

Figure 4.2 Powder XRD patterns of Ag_3PO_4.

4.1.3 Diffuse Reflectance UV-visible Spectrophotometer

Optical properties were examined by diffuse reflectance spectroscopy (DRS), JASCO V670. Which evinced that Ag_3PO_4 is capable of absorbing light with wavelength shorter than 530 nm (capable to absorb visible light). Direct and indirect band gaps were measured to be 2.42 and 2.34 eV, respectively. Fig 4.3 (a) & (b) show diffuse reflectance spectrum of Ag_3PO_4.

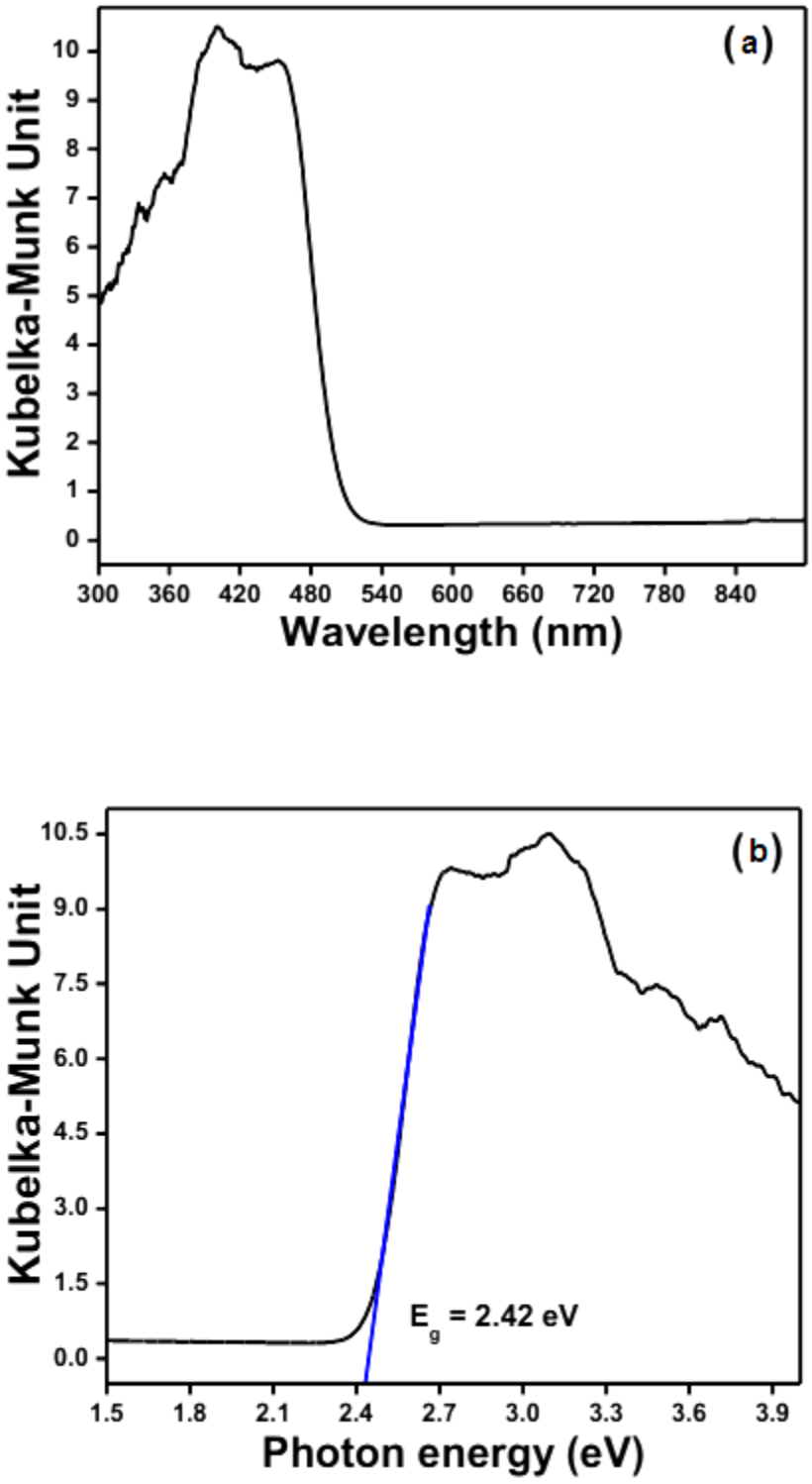

Figure 4.3 (a) & (b) Diffuse reflectance spectrum of Ag_3PO_4.

4.2 Activity and selectivity evaluation of Ag_3PO_4

To evaluate the activity and selectivity of Ag_3PO_4, the oxidation reactions were carried out in water at room temperature and ambient pressure using a light source that simulated sunlight. The conversion of BA to benzaldehyde was followed by GC-MS analysis and the complete course of evolution in BA and benzaldehyde concentration with irradiation time is presented in fig 4.4 (a-h). In addition, analysis of irradiated samples taken out at regular time interval was carried out by UPLC to substantiate the GC-MS analysis.

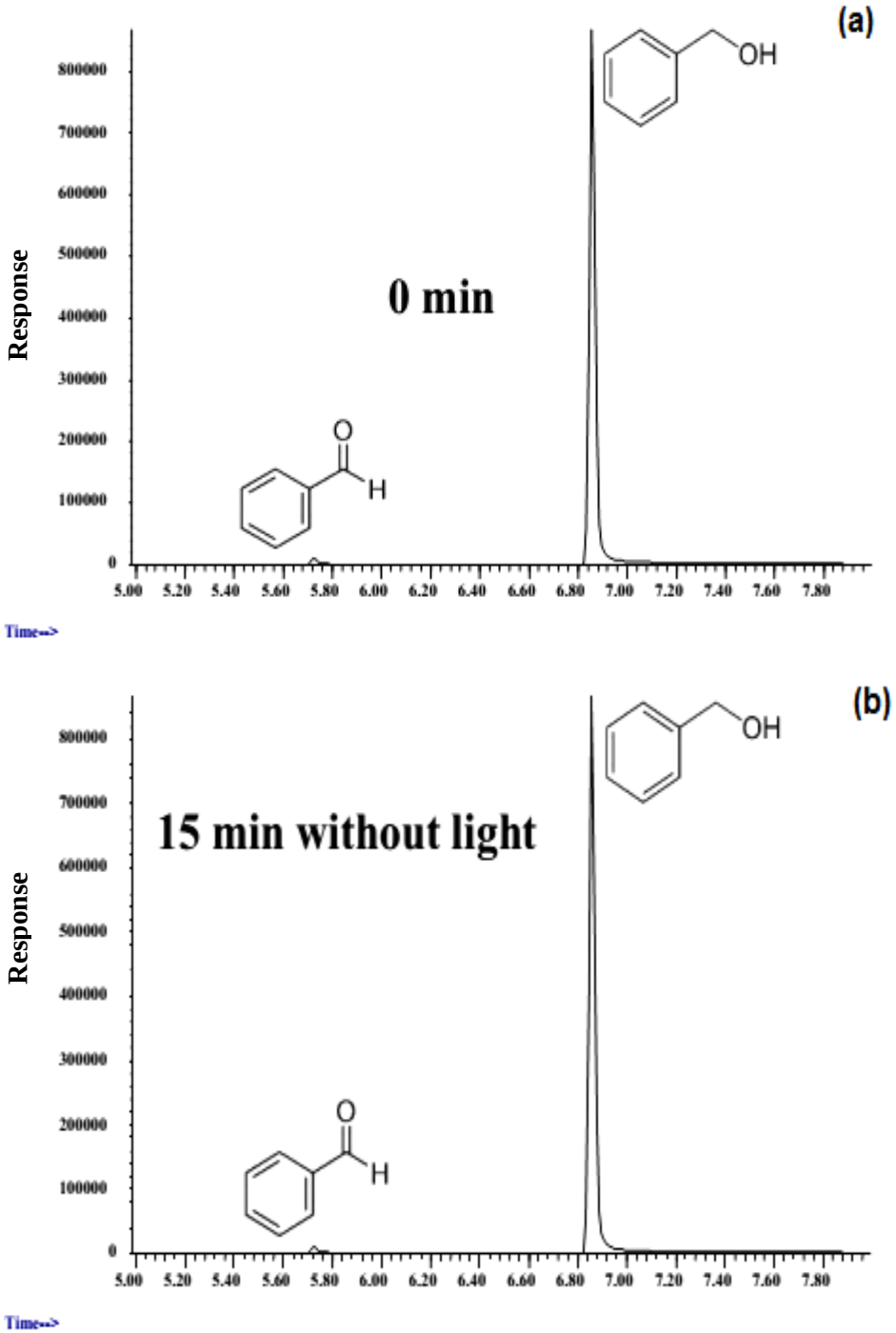

Figure 4.4 (a) & (b) Representative GC-MS chromatograms showing a time-dependant conversion of BA to benzaldehyde.

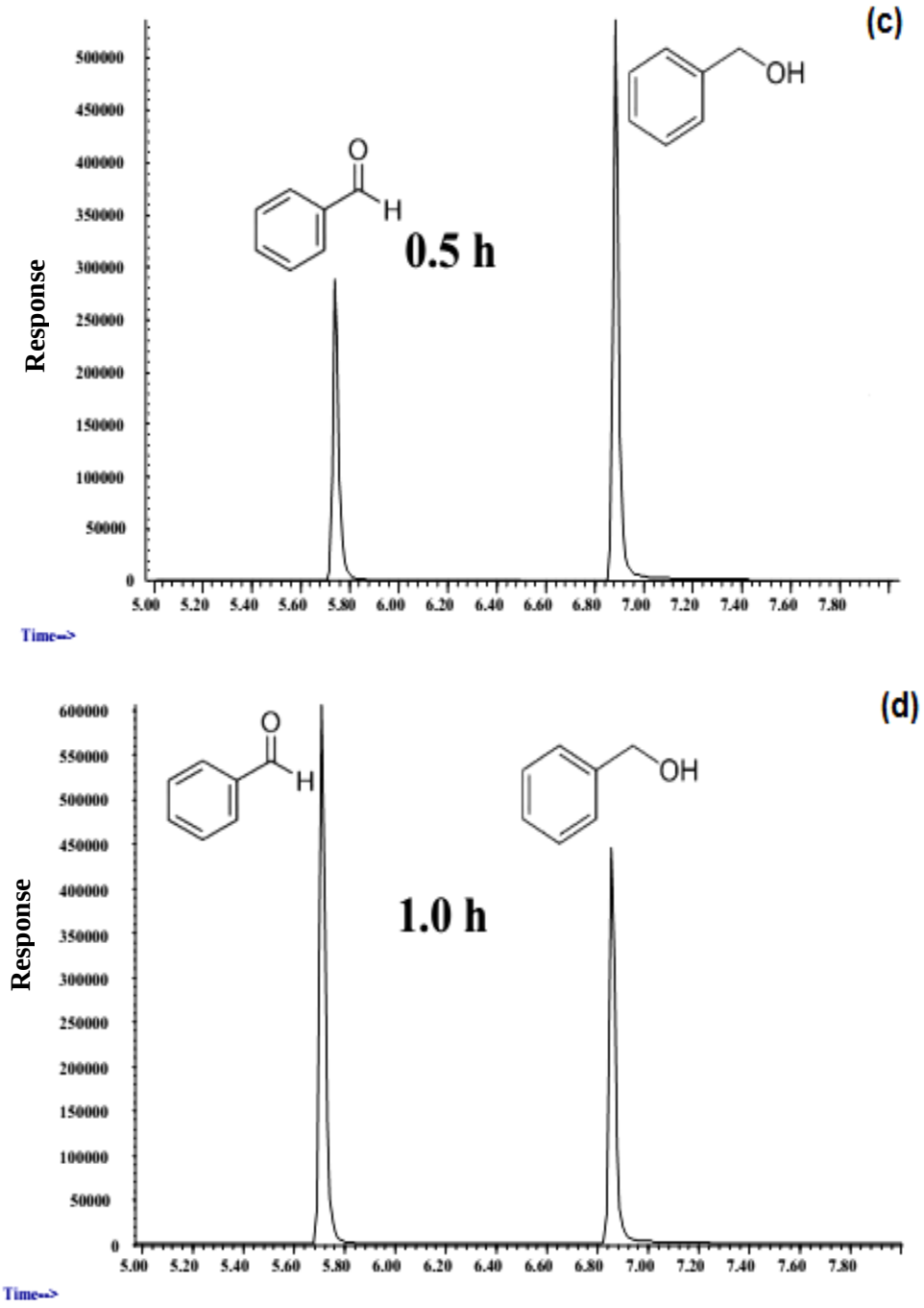

Figure 4.4 (c) & (d) Representative GC-MS chromatograms showing a time-dependant conversion of BA to benzaldehyde.

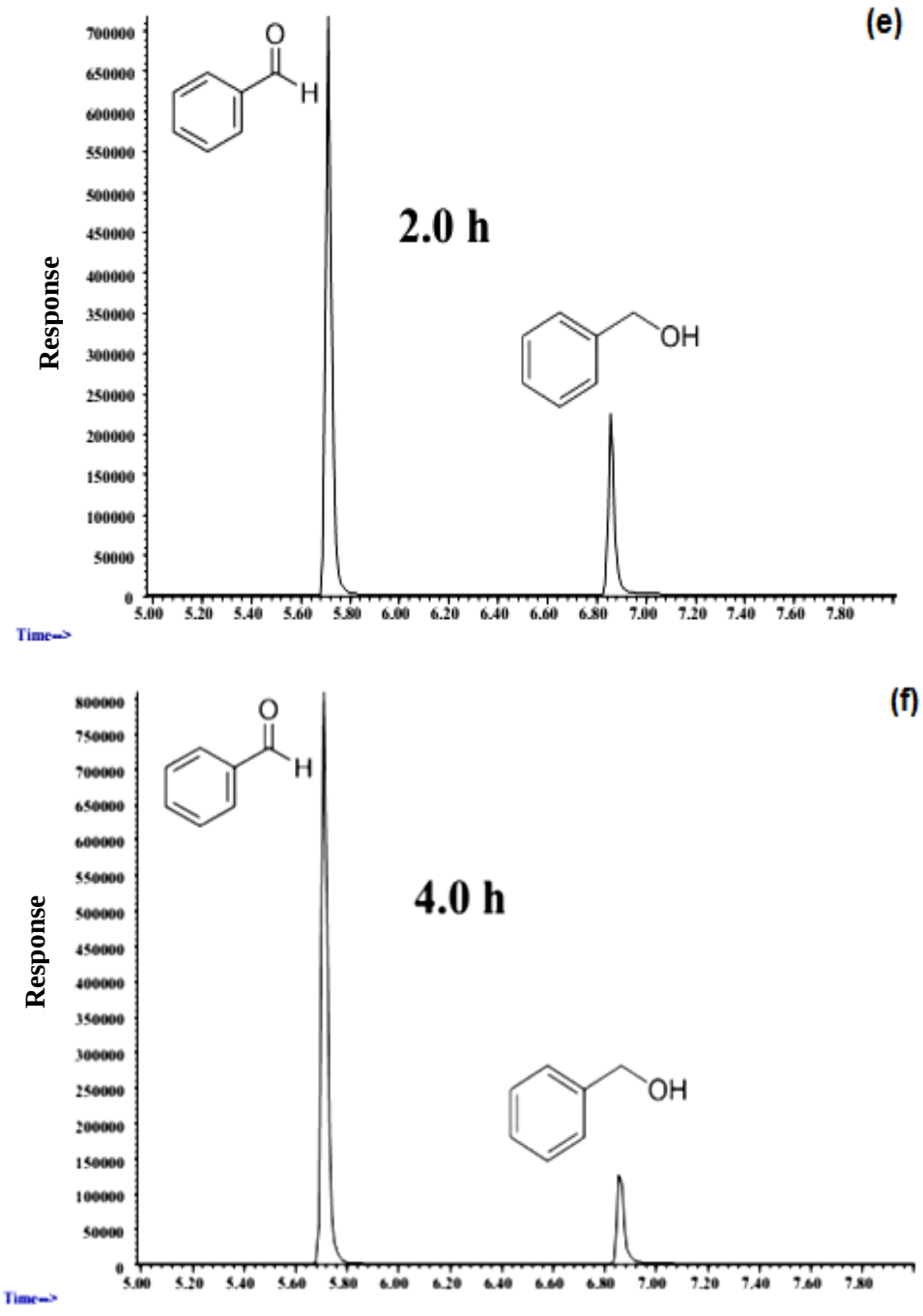

Figure 4.4 (e) & (f) Representative GC-MS chromatograms showing a time-dependant conversion of BA to benzaldehyde.

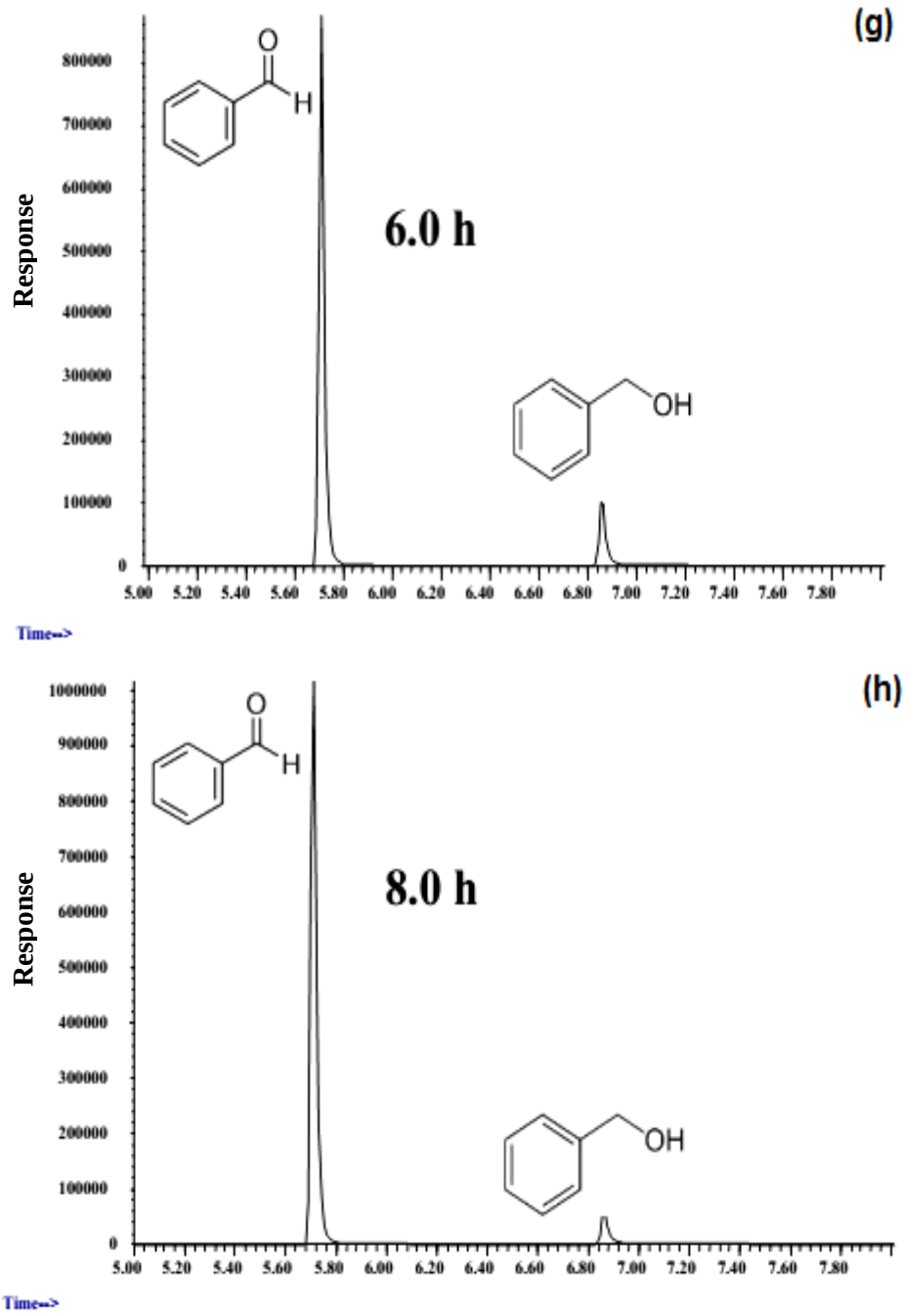

Figure 4.4 (g) & (h) Representative GC-MS chromatograms showing a time-dependant conversion of BA to benzaldehyde.

An exemplified time-dependant conversion of benzyl alcohol to benzaldehyde is shown in fig 4.5 As can be seen, ~90% of BA was converted to benzaldehyde with >99% yield after ~ 4 h of irradiation. A quantitative analysis of BA and benzaldehyde concentrations revealed the mole-to-mole conversion. Although one of the overriding limitations in achieving selective oxidation by photocatalytic process is the overoxidation of reactants or products during longer irradiation time, no change in aldehyde concentration occurred even after 8 h signifying that the Ag_3PO_4 was extremely selective for BA, but not for benzaldehyde oxidation.

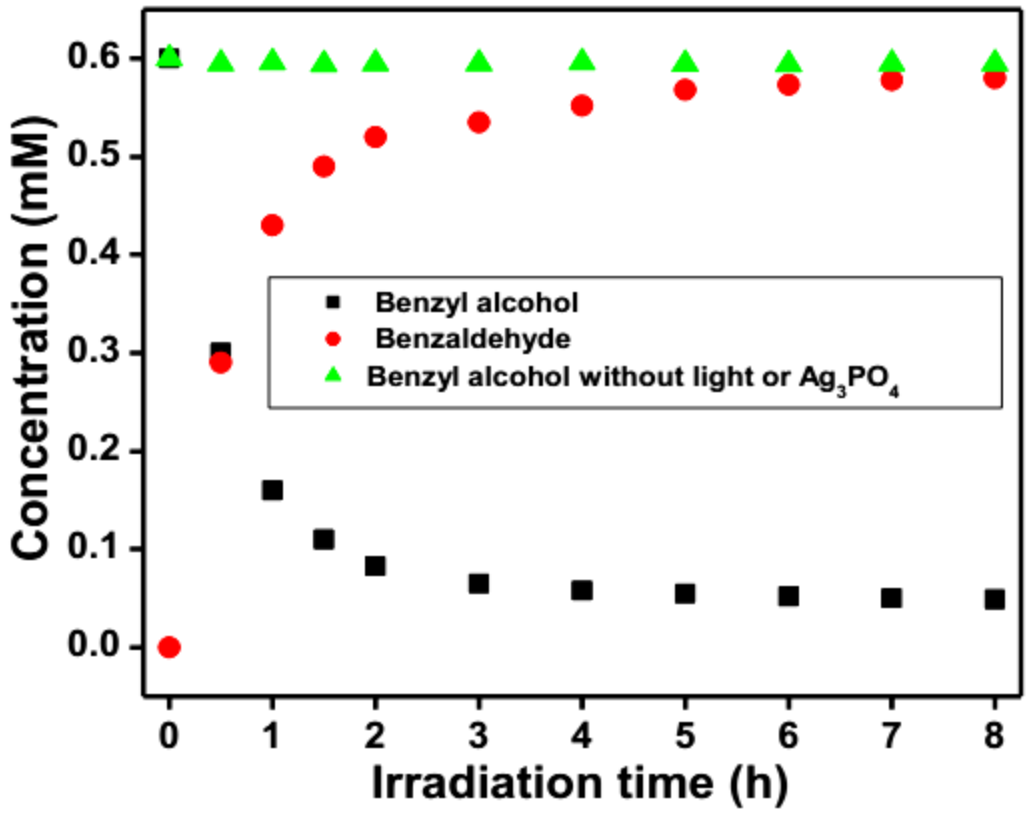

Figure 4.5 Change in the concentrations of benzyl alcohol and benzaldehyde upon irradiation with and without Ag_3PO_4. Experimental conditions: Ag_3PO_4 = 2 gL^{-1}, initial alcohol concentration = 0.6 mM, irradiation time = 8 h, volume (H_2O) = 130 ml.

In a recent study [48], the overoxidation or simultaneous oxidation of benzyl alcohol and benzaldehyde has been attributed to the complexation of benzaldehydes, unlike benzyl alcohol, with TiO_2 surface. Interestingly, the overoxidation was much averted when TiO_2 surface was substantially covered with the layers of WO_3, as WO_3 was found to be passive towards surface complexation with benzaldehyde. In this study, to investigate if there is any interaction between BA or benzaldehyde and Ag_3PO_4 surface, adsorption experiments were carried out by stirring the aqueous suspension of Ag_3PO_4 with BA or aldehyde or mixture of BA and benzaldehyde (1:1 volume ratio) under dark for 24 h. After experiment, the catalyst was separated by centrifugation and dried under vacuum, and the change in catalysts surface was followed by FTIR & Raman, while any change in alcohol or aldehyde concentration was analyzed by GC-MS. Presence of any trace of alcohol or aldehyde was not noticeable, as could be seen from FTIR spectrums illustrated in fig 4.6, Furthermore, GC-MS analysis did not indicate any apparent change in alcohol or aldehyde concentrations. The dearth of noticeable physisorption of BA or benzaldehyde onto the surface of Ag_3PO_4 explains, to certain extent, the suppression of aldehyde oxidation. Furthermore, controlled experiments, in the absence of catalyst or light, were also performed which did not show any change in alcohol concentration, indicating that both light and catalyst were required to trigger and sustain the oxidation.

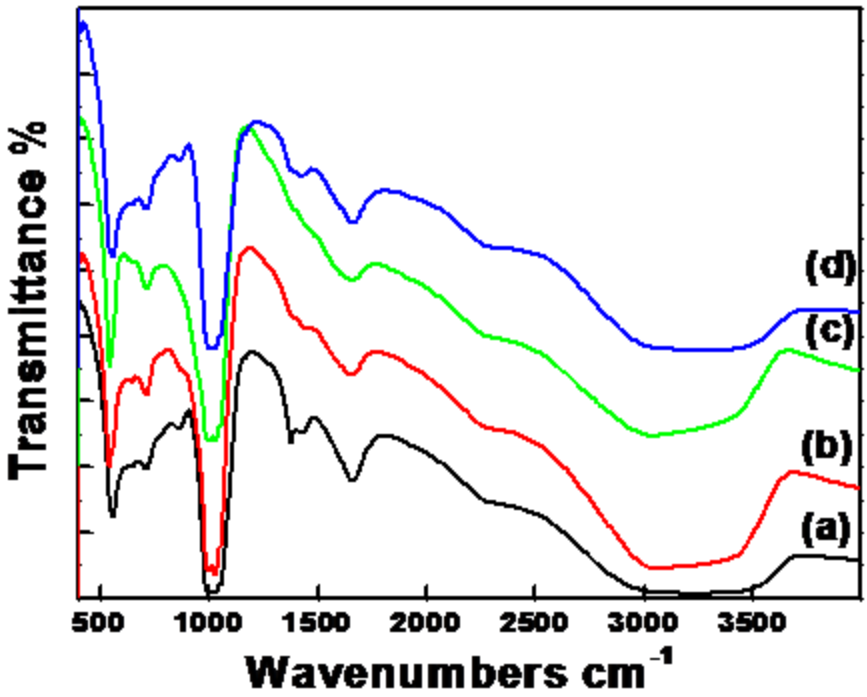

Figure 4.6 FTIR spectrums of Ag_3PO_4 analyzed after adsorption experiments; (a) pure Ag_3PO_4, (b) Ag_3PO_4 obtained after pure BA adsorption experiment, (c) Ag_3PO_4 obtained after pure benzaldehyde adsorption experiment, and (d) Ag_3PO_4 obtained after mixture of BA: benzaldehyde (1:1 volume ratio) adsorption experiment. Experimental conditions: Ag_3PO_4 = 2 gL^{-1}, substrate concentration = 0.6 mM, reaction time = 24 h, Volume (H_2O) = 130 ml.

4.3 Oxidation dependency on alcohol concentration and catalyst amount

From a mechanistic and application point of view, it is important to correlate the dependence of oxidation with the alcohol concentration and the catalyst loading. Hence, the conversion of BA with its concentrations and catalyst loading was studied and results are shown in fig 4.7 (a) & (b). As readily seen, the conversion increased monotonically with BA concentration up to 0.6 mM followed by a decrease at higher concentration. This could be due to the fact that up to 0.6 mM BA concentration, sufficient number of active sites is available on the photocatalyst surface which promote oxidation and hence lead to higher conversion. Decrease in percent conversion at 0.8 mm could be attributed to the existence of a finite number of active sites. Since highest conversion was observed at 0.6 mM concentration of BA, the effect of catalyst loading on percentage conversion was investigated at this optimal BA concentration, which showed a parabolic dependence-characteristic of heterogeneous catalytic process. This is expected; an increase in the amount of photocatalyst leads to more photon absorption. This in turn, leads to a higher degree of surface activation, thereby causing an increase in the degree of BA adsorption and, generating more holes in the valence band for oxidation. This triggers interfacial electron transfer from BA to the valence band holes, causing an increase in conversion.

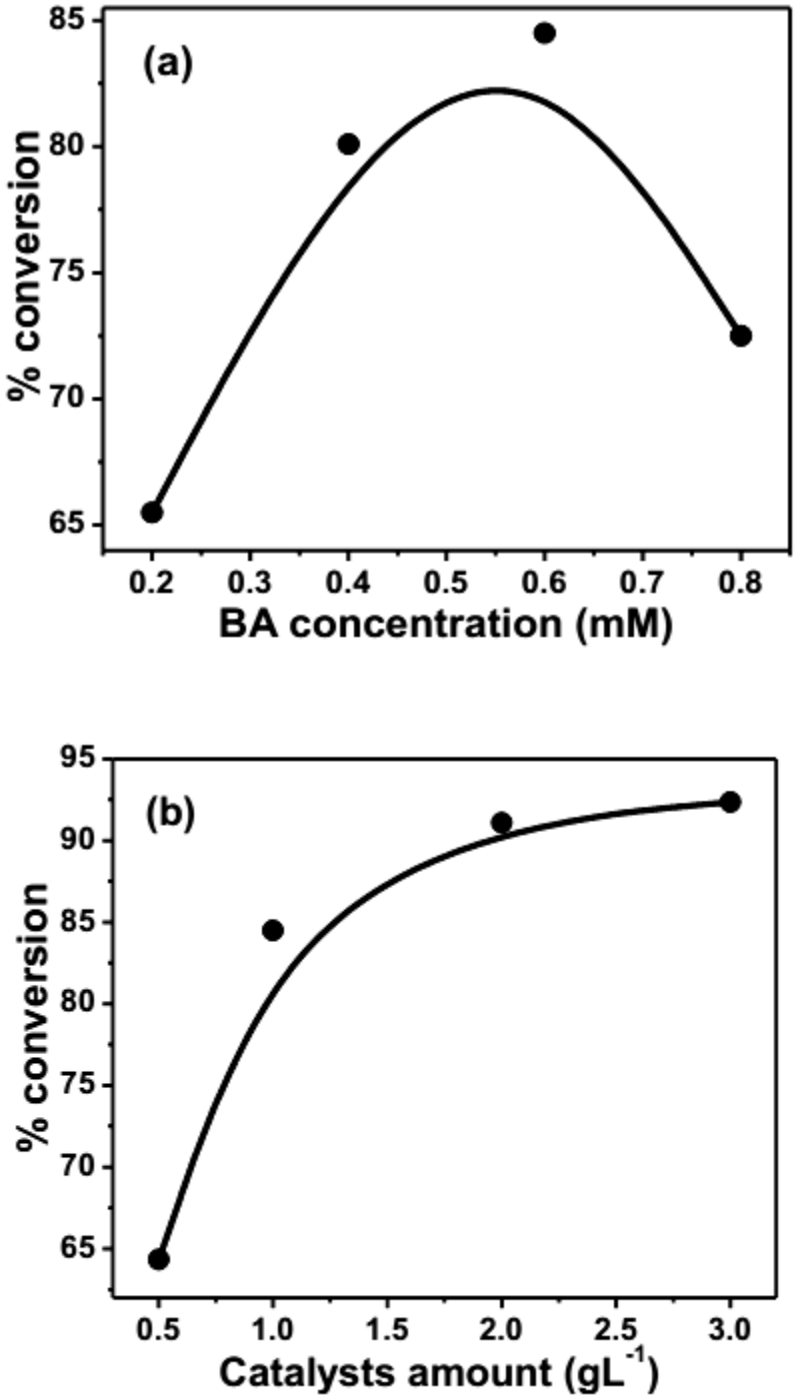

Figure 4.7 Dependence of BA oxidation on (a) BA concentration and (b) Ag_3PO_4 amount. Experimental conditions: irradiation time = 8 h, volume (H_2O) = 130 ml.

In order to assess the performance and selectivity of Ag_3PO_4 for other alcohols, oxidation of 4-MBA and cinnamyl alcohol was also studied, and the results are summarized in table 4.1.

Table 4.1 A comparative photocatalytic oxidation of benzylalcohol, 4-methoxy benzylalcohol and cinamyl alcohol to their corresponding aldehydes under identical experimental conditions. [a]

Substrate	Product	Conversion	Selectivity	Yield
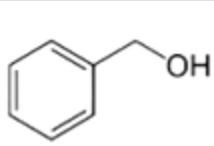	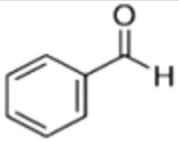	>85%	>99%	>99%
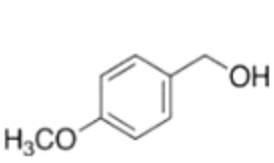	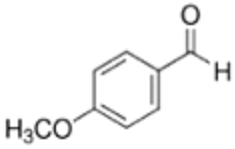	>85%	>99%	>99%
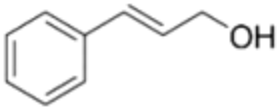	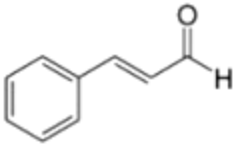	~90%	>90% (*)	>90%

[a] Ag_3PO_4 = 1 gL^{-1}, initial alcohol concentration = 0.6 mM, irradiation time = 8 h, volume (H_2O) = 130 mL, (*) traces of benzaldehyde and benzene acetaldehyde were form.

As was the case with BA, 4-MBA also underwent >85% oxidation forming anisaldehyde in yield and selectivity exceeding 99% (on mole-to-mole conversion basis). However, in the case of cinnamyl alcohol, although the conversion was ~90%, selectivity was partially lost as benzaldehyde and benzene acetaldehyde were also formed in addition to cinnamaldehyde, whose yield was still >90%. Time-dependant conversion of 4-methoxybenzyl alcohol into *p*-anisaldehyde and cinnamyl alcohol into cinnamaldehyde are shown in fig 4.8 (a) & (b).

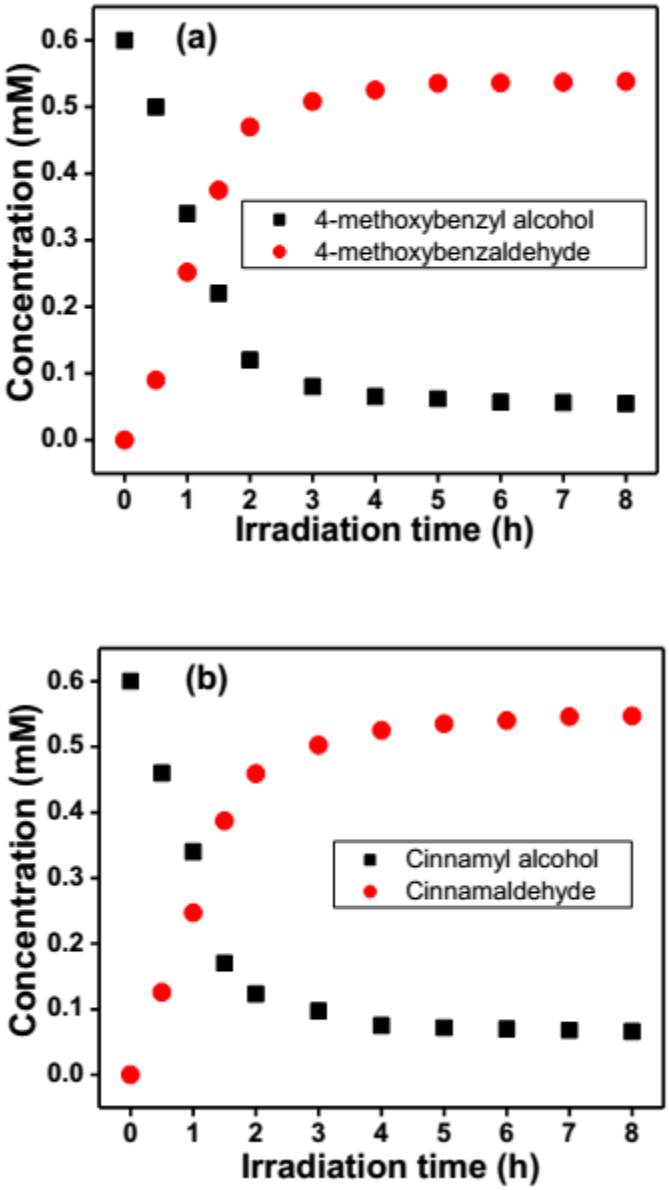

Figure 4.8 Conversion of (a) 4-methoxybenzyl alcohol into p-anisaldehyde and (b) cinnamyl alcohol into cinnamaldehyde with respect to irradiation time. Experimental conditions: Ag_3PO_4 = 2 gL^{-1}, alcohol concentration = 0.6 mm, Irradiation time = 8 h, Volume (H_2O) =130 ml.

4.4 Radicals formation and reaction mechanism

Unlike previous reports on the photocatalytic oxidation of alcohols, greater selectivity was observed in this study. Essentially, the non-selective nature of photocatalysis could be attributed to the formation of extremely reactive and short-lived radicals such as $OH^{\bullet}$, $O_2^{-\bullet}$, $HO_2^{\bullet}$ etc., O_2 is readily reduced to $O_2^{-\bullet}$ by excited conduction band electrons while the holes in the valence band can oxidize water, generating $OH^{\bullet}$ radicals. These radical species are extremely reactive, though short lived, and make the photocatalytic process somewhat non-selective. Particularly, O_2 may affect the overall photocatalytic oxidation in two ways; as an oxidant (electron acceptor) or direct incorporation of molecular oxygen to yield product. Hence, formation or the involvement of such radicals was examined in order to understand the operative mechanism responsible for the high selectivity. To determine the role of $O_2^{-\bullet}$, the oxidation of BA was carried out both in the absence and presence of molecular O_2, by bubbling N_2 or O_2 through photoreactor. Results showed that the conversion was independent of the ambient environment, indicating that O_2 seemingly did not play any role in the oxidation of BA. This could be attributed to the lower or more negative redox potential of $O_2/O_2^{-\bullet}$ (-0.16 eV, 1M vs. NHE at pH = 7) [48], than the electrode potential of $/Ag_3PO_4$ (+0.8 eV vs. NHE at pH = 7) [40]. Findings further suggested that the oxidation of alcohols via photocatalytic process essentially proceeds through the involvement of valence band holes, rather than direct incorporation of molecular oxygen. Based on these observations, a plausible mechanism involving 2 electrons and protons transfer process operative in the oxidation of alcohols to corresponding aldehydes is illustrated in fig 4.9. Furthermore, the path (A)

appears to be more likely as the formation of radical at the β-carbon may result in the delocalization of this electron in the adjacent benzene ring, imparting additional stability and rather slow oxidation of BA. It seemed plausible to postulate that the excited electrons were taken up by Ag^{+} ions of the Ag_3PO_4 because the standard redox potential of Ag(I) (Ag^{+}/Ag^{o} = +0.8 eV) is higher or more positive than the conduction band potential of Ag_3PO_4 which implies that the Ag^{+} is likely to be reduced to Ag^{o} by excited conduction band electrons. This assumption was corroborated by XRD analysis of irradiated/used Ag_3PO_4, which showed the presence of metallic silver in the sample.

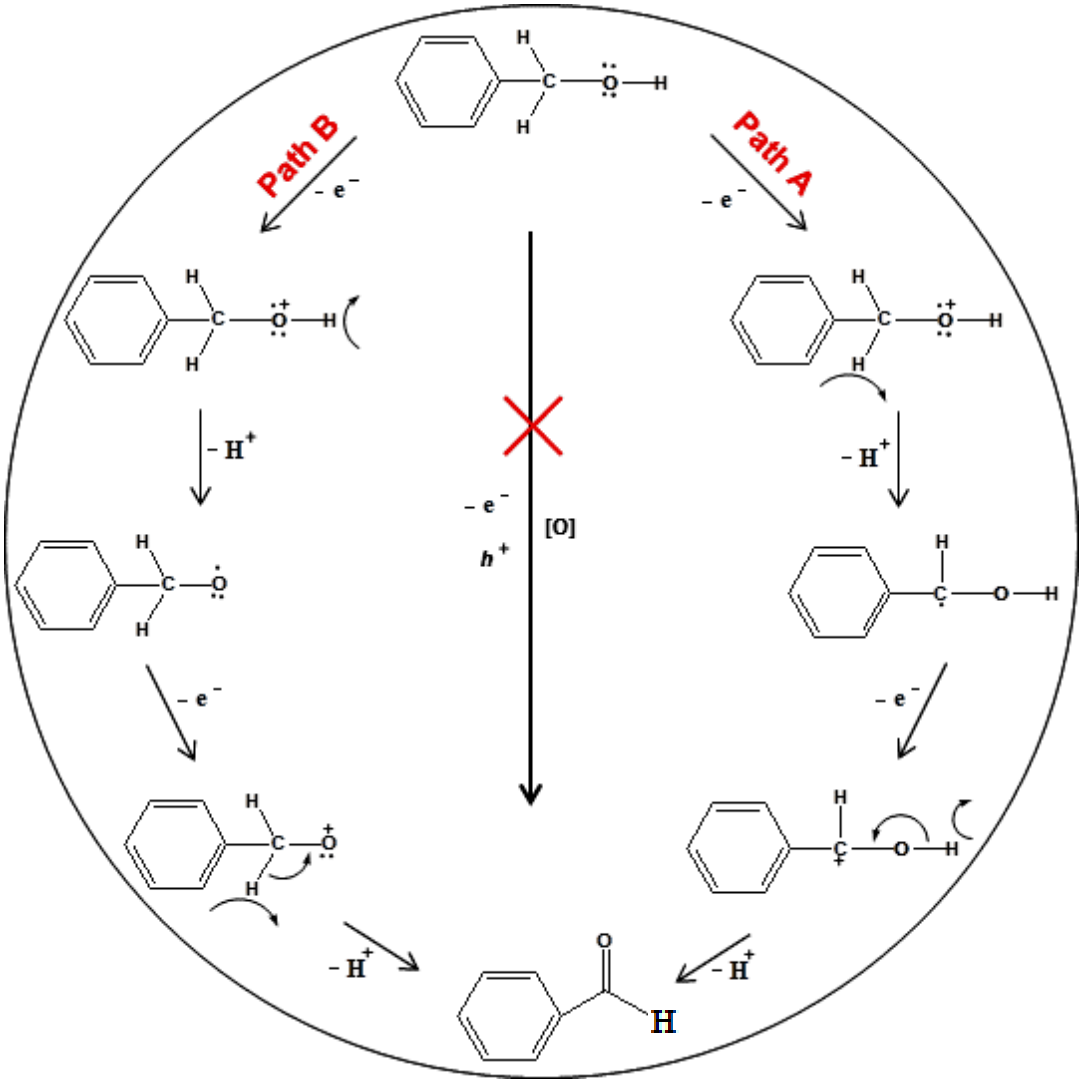

Figure 4.9 A proposed mechanism of photocatalytic oxidation of alcohol.

Additionally, the role of $OH^{\bullet}$ produced through water oxidation in the reaction media was investigated. Since terephthalic acid tends to trap $OH^{\bullet}$ radicals and gets transformed into fluorescent 2-hydroxyterephthalic [58], photocatalytic experiments were performed to monitor the generation of $OH^{\bullet}$ via employing terephthalic acid as a probe molecule both in the absence or presence of BA. The change in fluorescence intensity, which is a function of OH radicals, was monitored by photoluminescence. The time-dependant evolution of the fluorescence spectra for terephthalic or 2-hydroxyterephthalic acid in the absence or presence of BA is shown in fig 4.10. High intensity was observed when terephthalic acid was irradiated without BA, indicating generation of $OH^{\bullet}$ via oxidation of H_2O. However, in the presence of BA, the intensity was strongly suppressed revealing preferred oxidation of BA over that of water.

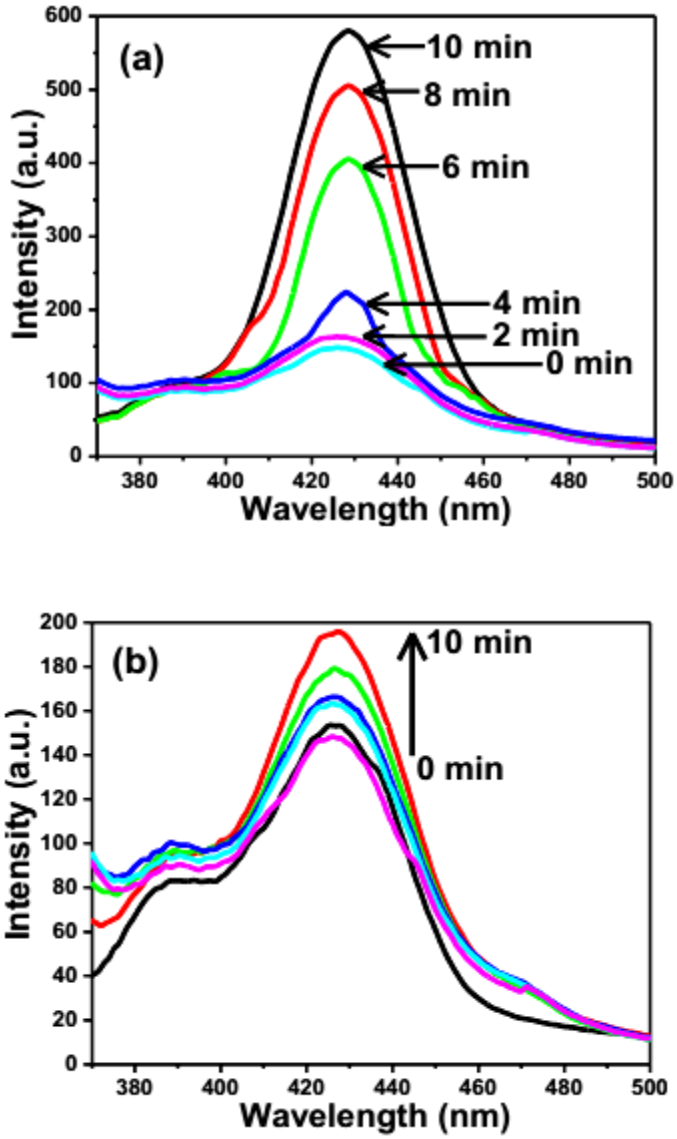

Figure 4.10 Change in fluorescence intensity of terephthalic acid with respect to irradiation time in aqueous suspensions of Ag_3PO_4 in (a) absence or (b) presence of BA.

The observed role of O_2, accompanied by Ag^+ to Ag^0 reduction and suppression of $OH^\bullet$ formation, corroborates the plausible mechanism depicted in fig 4.11 for the selective oxidation of alcohols in presence of Ag_3PO_4.

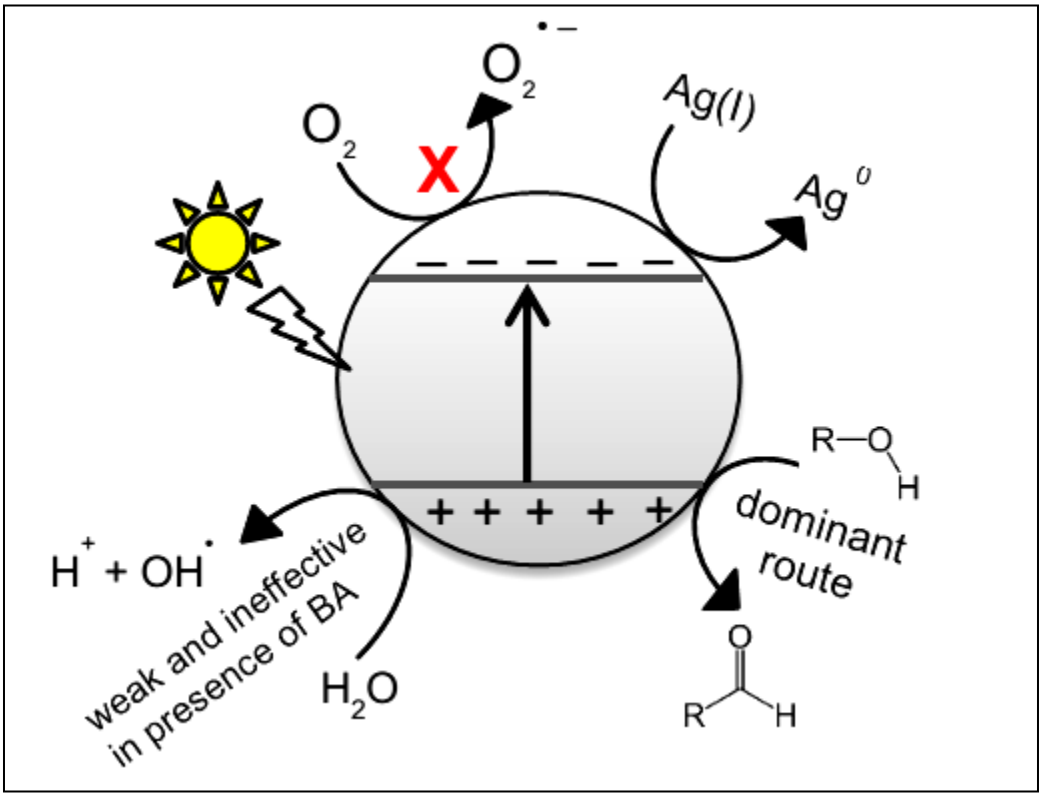

Figure 4.11 Schematic draw shows the involvement of $O_2^{-\bullet}$, $OH^\bullet$ and holes in the selective photocatalytic oxidation of alcohols. R = aryl group.

CHAPTER 5

RESULTS AND DISCUSSION FOR Pt/Bi_2WO_6 PHOTOCATALYST

5.1 Characterization

Structural details of Bi_2WO_6 or Pt/Bi_2WO_6 were investigated employing standard analytical techniques. Representative images showing the shape and morphology of sample are illustrated in Fig (5.1 – 5.3).

5.1.1 Field emission scanning electron microscope

SEM analysis was performed using field emission scanning electron microscope (TESCAN LYRA 3 FEG). Fig 5.1 (a) & (b) shows scanning microscopic images of Pt/Bi_2WO_6. Images confirmed the formation of self-assembled spheres with hierarchical architecture. The diameter and thickness of the spheres were measured to be 2–4 μm and <1 μm, respectively. High resolution images revealed that the hierarchical structure was consisting of rod-like crystallites, as illustrated in fig 5.1 (b).

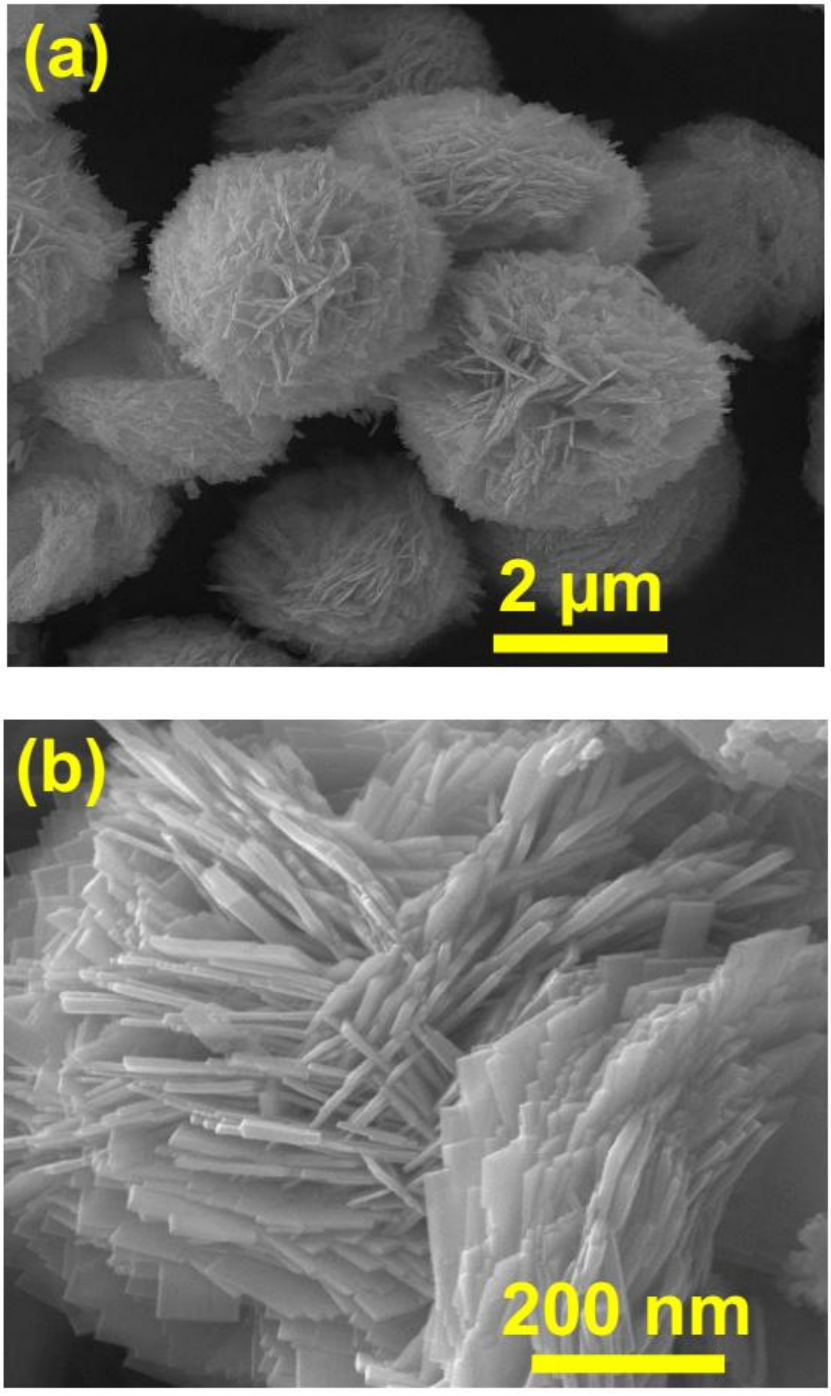

Figure 5.1 (a) & (b) Field emission scanning electron microscopic image.

5.1.2 Transmission Electron Microscope (TEM) and Brauner-Emmet-Teller (BET) surface area measurement

High-angle annular dark-field transmission electron microscope (HAAD-TEM), FEI Company and BET analysis (Micromeritics, USA) were used. Analysis of high resolution TEM images showed the presence of two types of porosity; mesoscopic porosity, fig 5.2 (a), and ordered porosity fig 5.2 (b). The pore size was measured to be >3 nm; it corroborated the observation of BET analysis which measured the pore size ~3.5 nm. BET surface area of Pt/Bi_2WO_6 was measured to be ~50.4 m^2g^{-1}. The shape of deposited Pt nanoparticles, fig 5.2 (c) was observed to spherical while the size was determined to be ~2 nm.

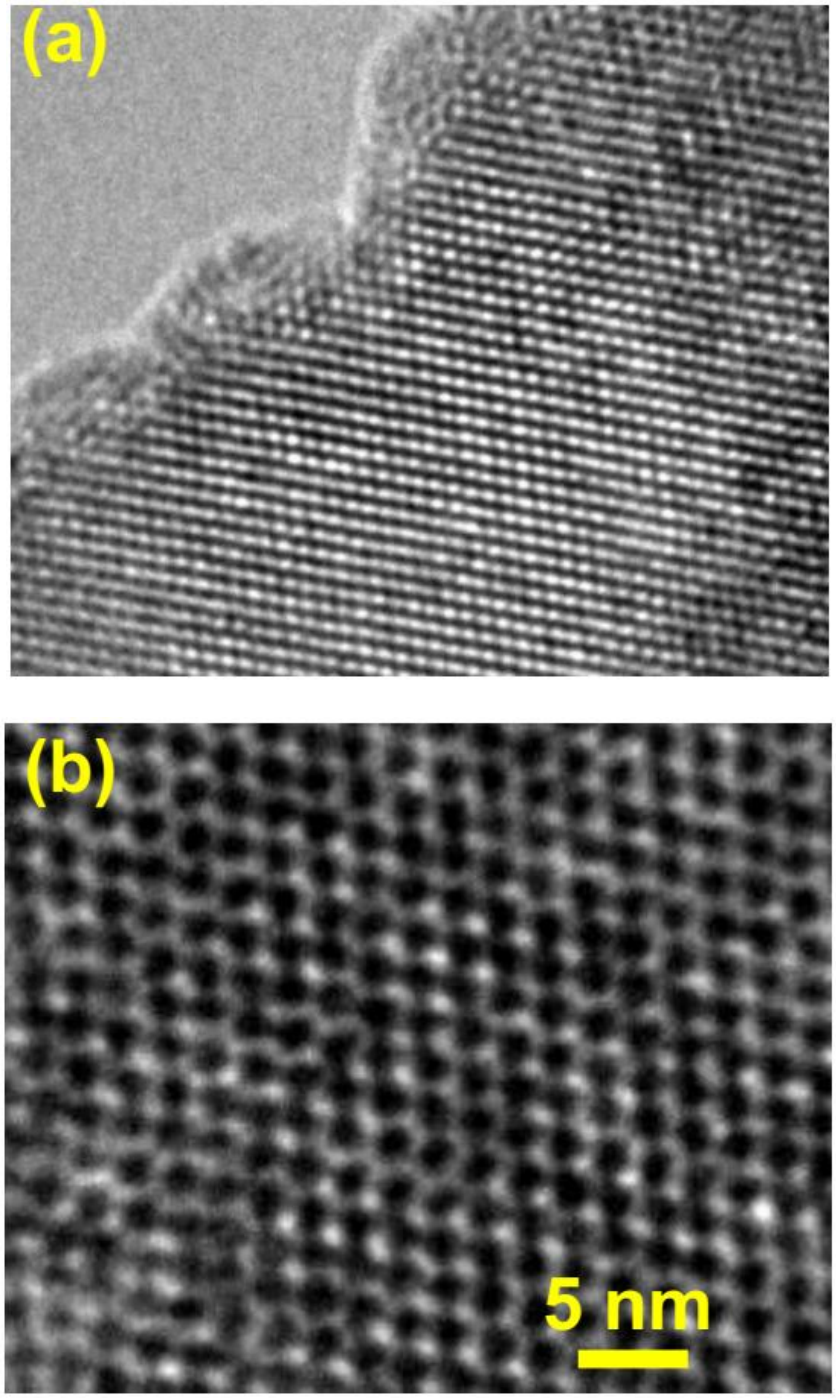

Figure 5.2 (a) & (b) High-angle annular dark-field Transmission Electron Microscopic image.

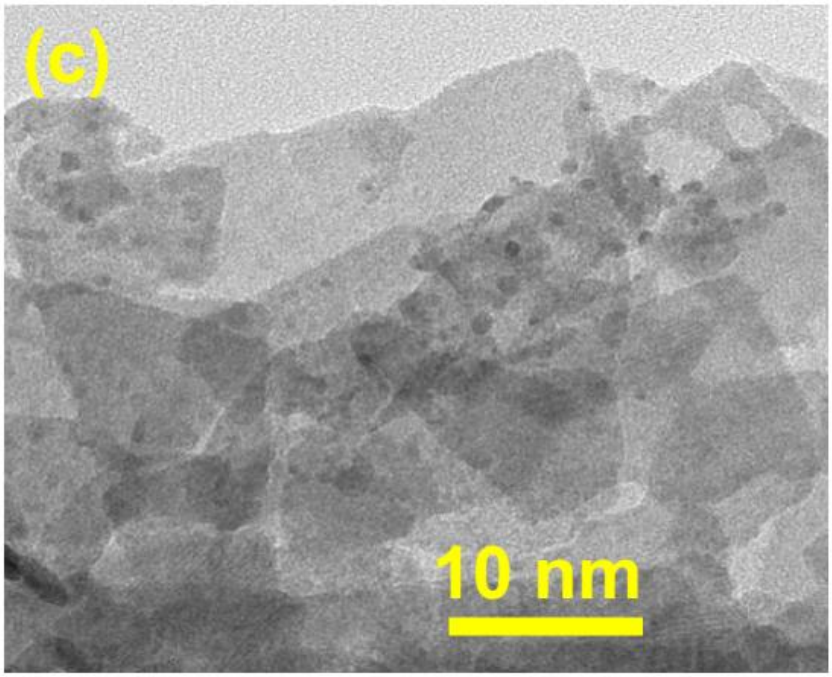

Figure 5.2 (c) High-angle annular dark-field Transmission Electron Microscopic image.

5.1.3 Energy Dispersive X-ray Spectroscopy (EDS)

Energy dispersive X-ray (Oxford Instrument-England and X-Max detector) was used for the elemental analysis of the catalyst. The EDS analysis of the catalyst confirms its chemical composition which consists of (PT, W, O, and Bi). Fig 5.3 shows the chemical characterization of Pt/Bi_2WO_6.

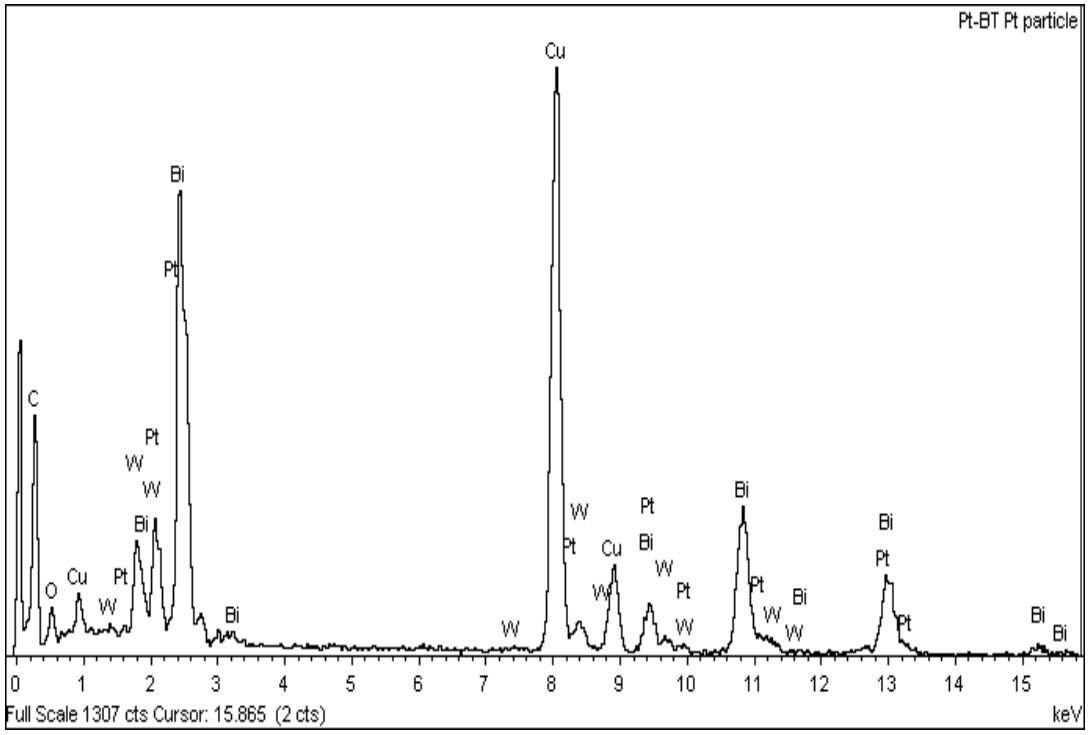

Figure 5.3 EDS spectrum of Pt/Bi_2WO_6.

5.1.4 X-ray Diffractometer (XRD)

X-ray diffractometer, (Shimadzu XRD Model 6000, Japan), was used for the phase identification of the catalyst. The crystalline nature of the sample was determined by XRD and the obtained diffraction patterns are presented in fig 5.4. Which confirmed a well crystalline russellite structure of bismuth tungstate (peaks positons & indexing).

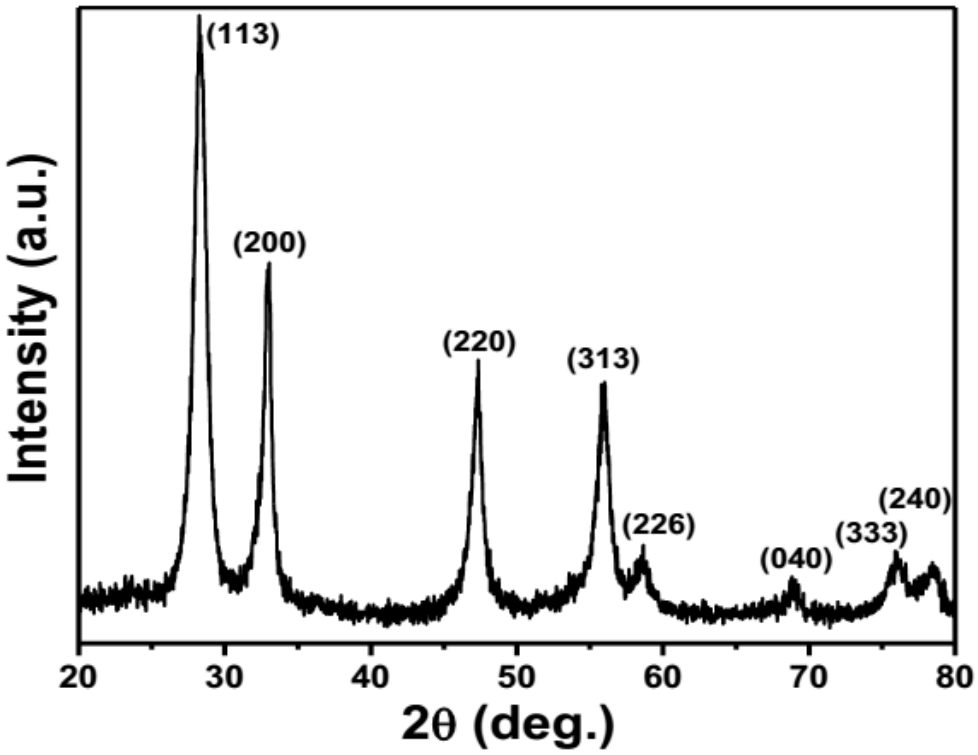

Figure 5.4 XRD of platinized nanoporous Bi_2WO_6.

5.2 Activity evaluation of Pt/Bi_2WO_6

The photocatalytic activity of Bi_2WO_6 synthesized at different temperature such as 130, 150, 170 and 190 °C was investigated. Since Bi_2WO_6 synthesized at 170 °C showed the best photocatalytic activity, all the Bi_2WO_6 samples were synthesized at this temperature. All the photocatalytic reactions were carried out in water at room temperature and ambient pressure under simulated sunlight. The openings of photoreactor were properly closed in order to preclude the escape of product(s) formed during reaction. The products formed during the photooxidation of alcohols were extracted and analyzed by GC-MS analysis, in addition to Ultra Performance Liquid Chromatography (UPLC) which substantiated the GC-MS observation. A representative time-dependent variation in concentrations of 4-MBA and anisaldehyde is presented in fig 5.5 (a). As can be apparently seen, upon irradiation concentration of 4-MBA decreased with time and after ~ 4h of irradiation >95% of 4-MBA was converted to *p*-anisaldehyde with >99% yield and >99% selectivity. A quantitative analysis of 4-MBA and anisaldehyde concentrations revealed the mole-to-mole conversion and trace formation of any other product was not noticeable throughout the course of the reaction. In order to follow the course of oxidation process after exhaustive alcohol oxidation, irradiation was prolonged and photocatalyst amount was increased (1.0 gL^{-1}). Fig 5.5 (b) shows the change in 4-MBA concentration under prolonged irradiation, while corresponding evolution in GC-MS spectra is delineated in fig 5.6 (a-h) Interestingly, after almost complete oxidation of 4-MBA, oxidation of *p*-anisaldehyde ensued.

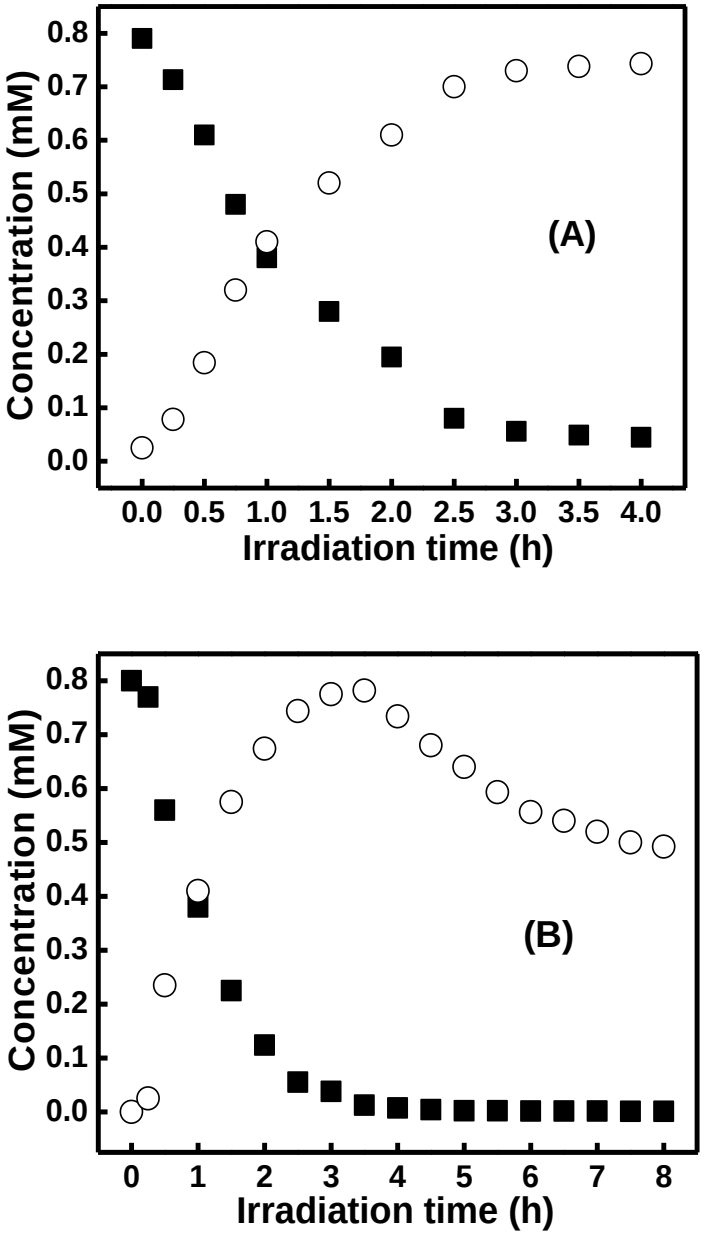

Figure 5.5 (a) & (b) Change in the concentrations of alcohols and aldehydes upon irradiation; (A & B) 4-MBA and p-anisaldehyde in the presence of Pt/Bi_2WO_6.
Experimental conditions: 4-MBA or 4-NBA concentration = 0.8 mM, $0.5\%Pt/Bi_2WO_6$ amount = 0.5 gL^{-1}, volume (H_2O) = 130 mL. Symbols: [●] 4-MBA or 4-NBA, [○] *p*-anisaldehyde or *p*-nitrobenzaldehyde.

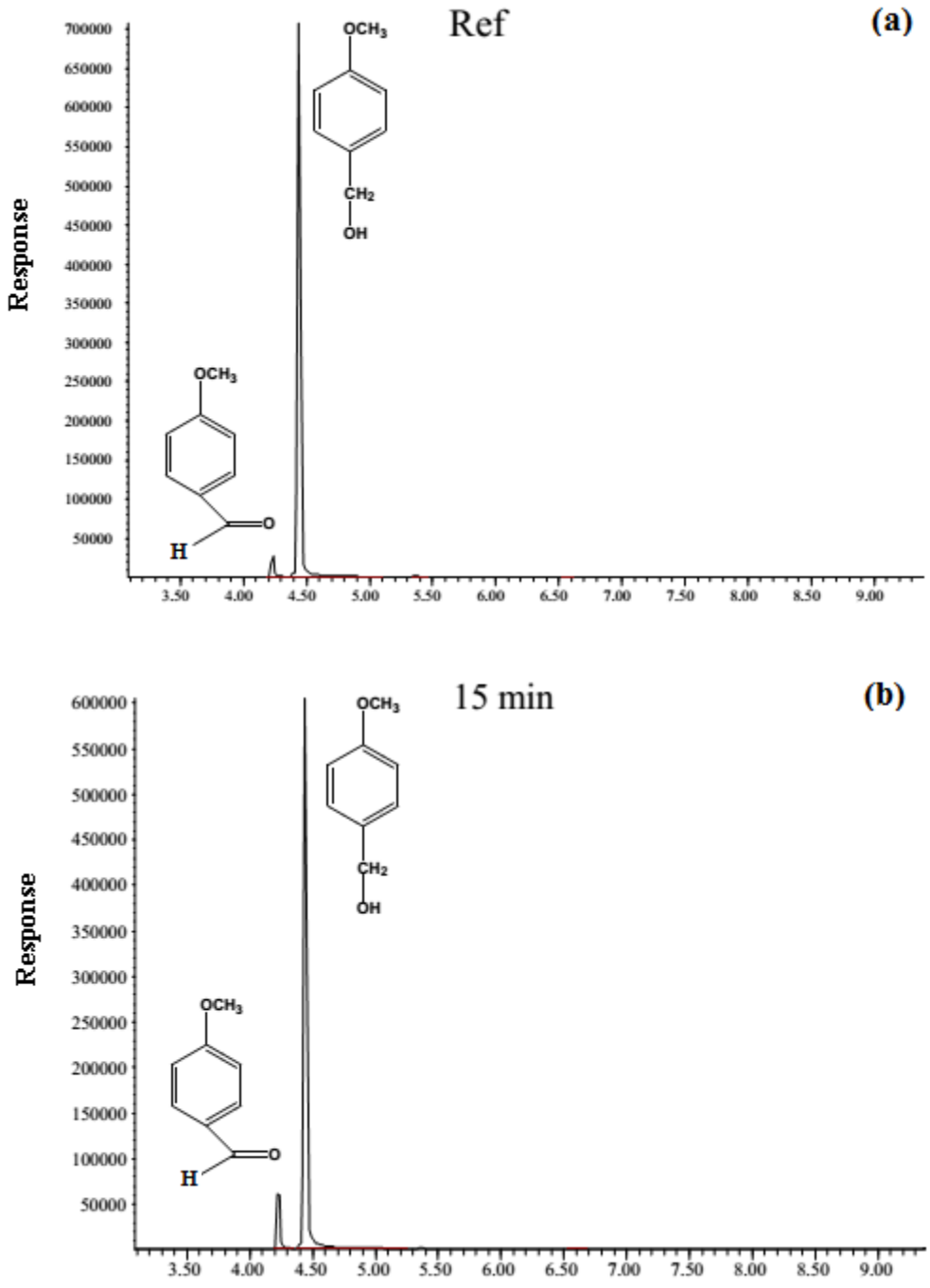

Figure 5.6 (a) & (b) Change in GC-MS chromatograms showing the time-dependant conversion of 4-MBA into p-anisaldehyde.

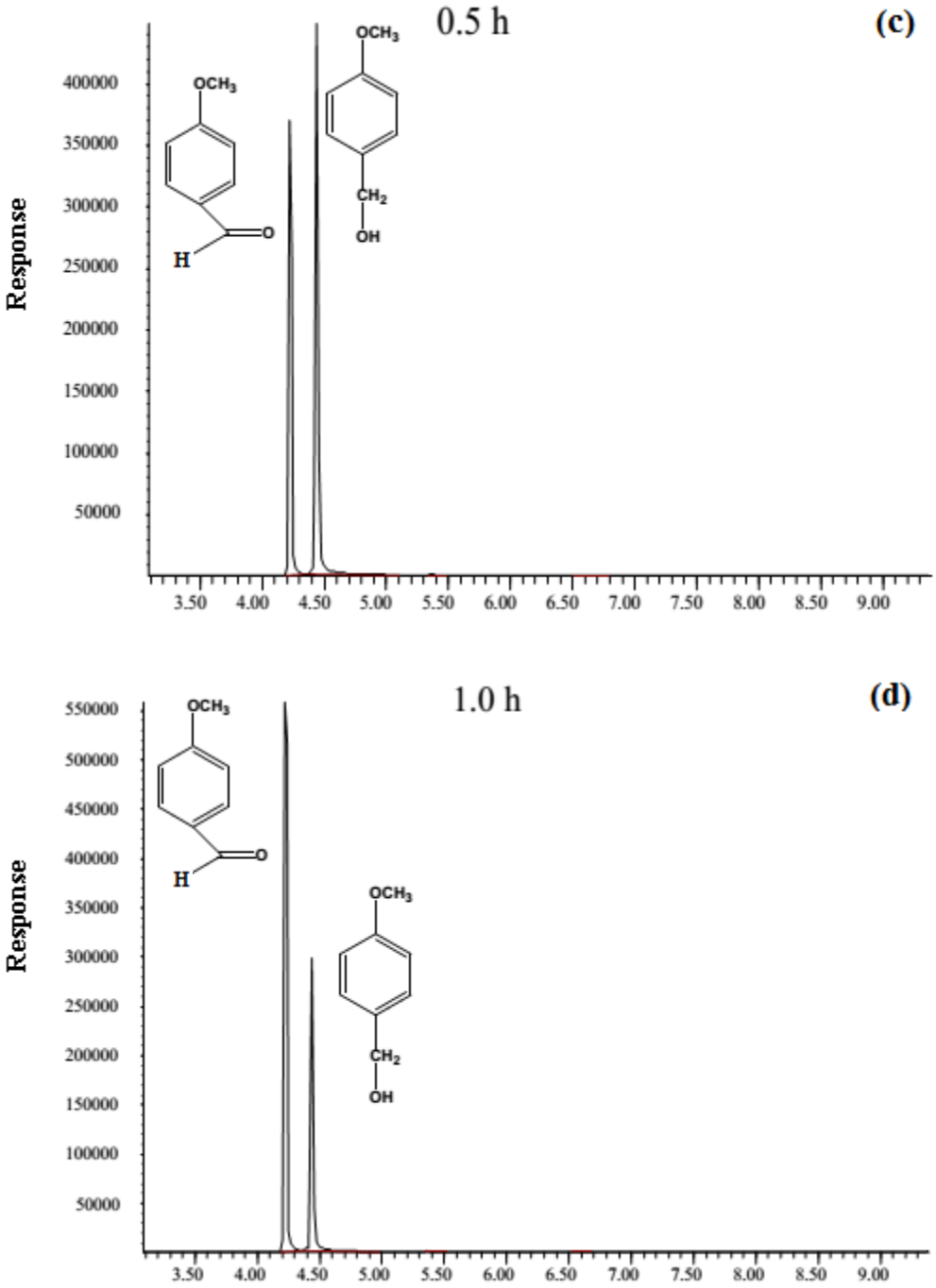

Figure 5.6 (c) & (d) Change in GC-MS chromatograms showing the time-dependant conversion of 4-MBA into p-anisaldehyde.

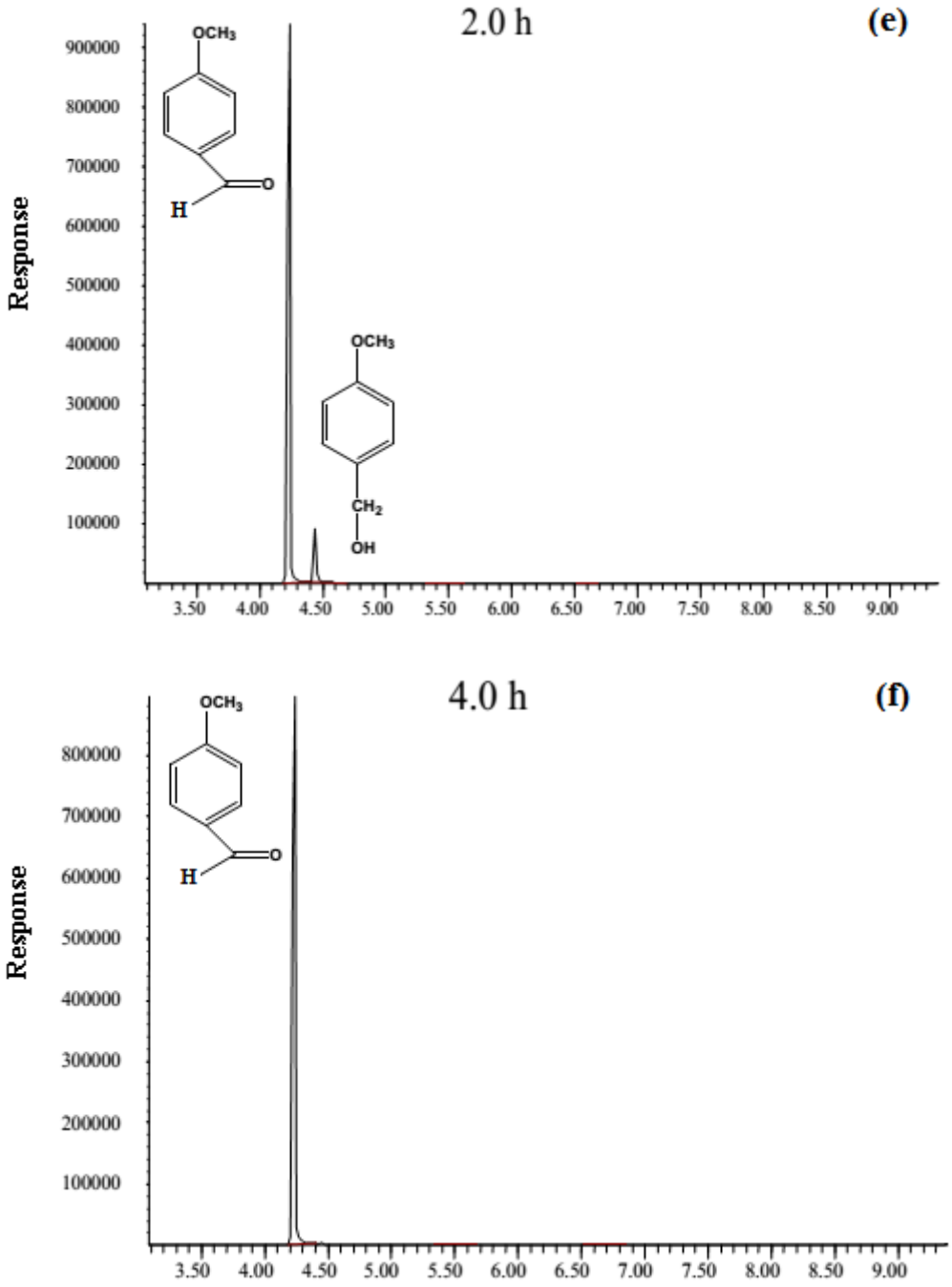

Figure 5.6 (e) & (f) Change in GC-MS chromatograms showing the time-dependant conversion of 4-MBA into p-anisaldehyde.

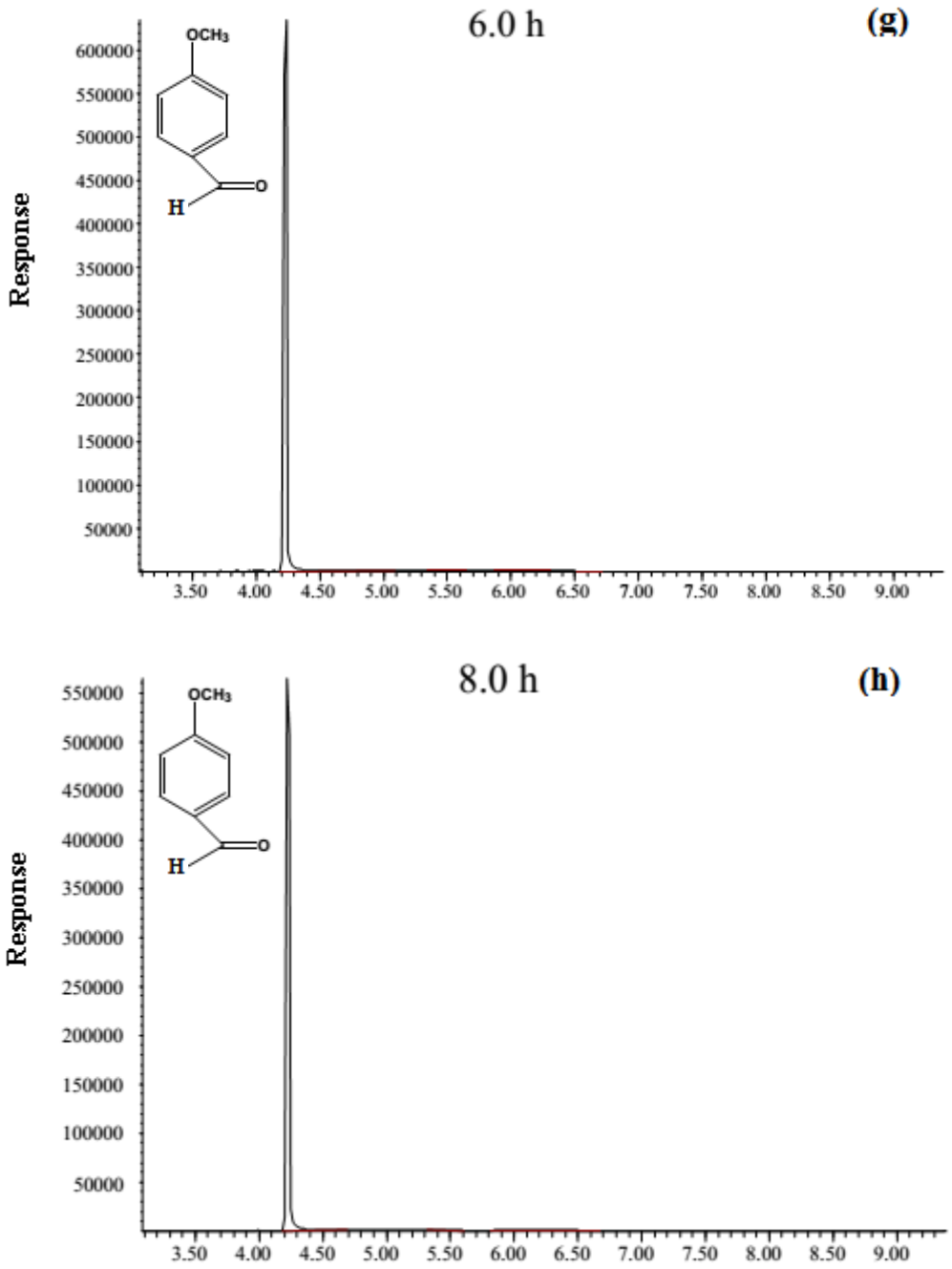

Figure 5.6 (g) & (h) Change in GC-MS chromatograms showing the time-dependant conversion of 4-MBA into p-anisaldehyde.

In addition to 4-MBA, conversion of 4-nitrobenzyl alcohol (4-NBA) was also studied to evaluate and verify the selectivity and efficiency of Pt/Bi_2WO_6 towards other alcohol. Furthermore, selection of 4-NBA would also shed light on the effect of electron withdrawing substituent on the oxidation process. Results are presented in fig 5.7 (a), which showed that 4-NBA underwent >85% oxidation forming 4-nitrobenzaldehyde with yield and selectivity exceeding 99% (on mole-to-mole conversion basis), though 4-NBA oxidized slower than that of 4-MBA. A slower oxidation of 4-NBA could be ascribed to the electron withdrawing attributes of nitro group which makes $–CH_2–OH$ electron deficient and thus somewhat resistant to oxidation. Oxidation of 4-MBA was also examined in the presence of pure Bi_2WO_6 and results, presented in fig 5.7 (b), indicated <45% conversion, though the selectivity was maintained.

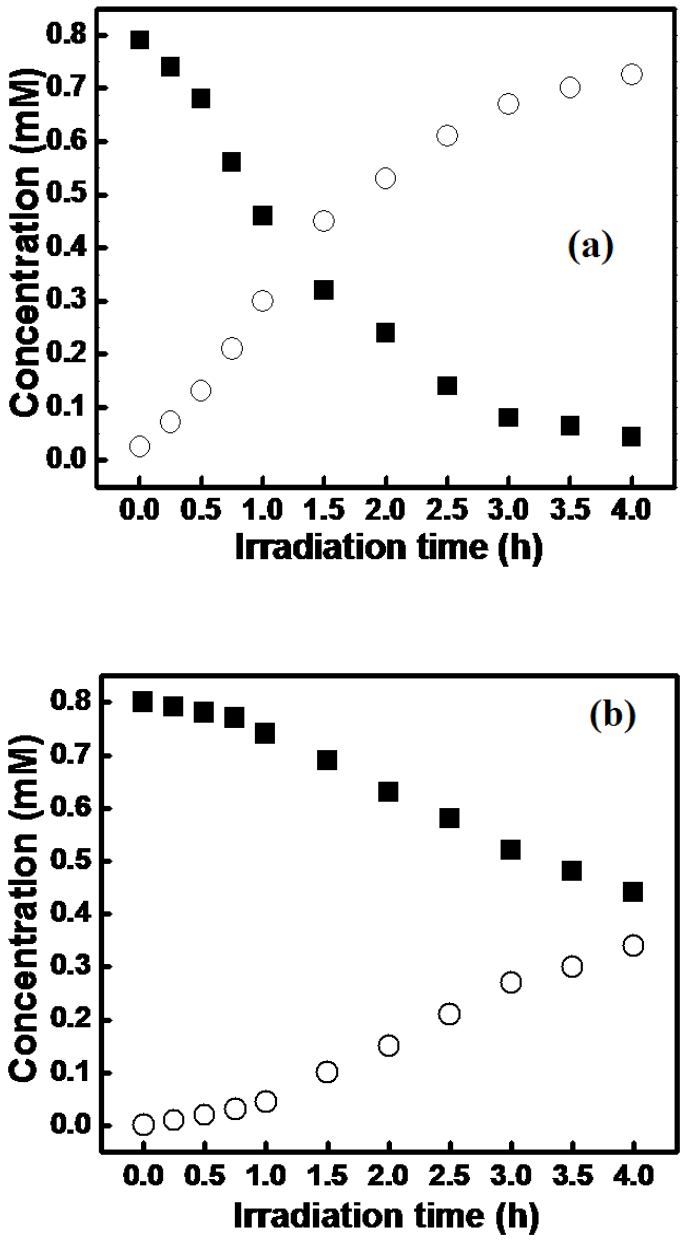

Figure 5.7 (a) & (b) Change in the concentrations of alcohols and aldehydes upon irradiation; (a) 4-NBA and *p*-nitrobenzaldehyde in the presence of Pt/Bi_2WO_6 and (b) 4-MBA and *p*-anisaldehyde in presence of pure Bi_2WO_6.
Experimental conditions: 4-MBA or 4-NBA concentration = 0.8 mM, $0.5\%Pt/Bi_2WO_6$ amount = 0.5 gL^{-1}, volume (H_2O) = 130 mL. Symbols: [●] 4-MBA or 4-NBA, [○] *p*-anisaldehyde or *p*-nitrobenzaldehyde.

Unlike previous studies in which one of the predominant constraints in achieving selective oxidation by photocatalytic process has been the overoxidation of reactants or products during longer irradiation time, this study presents peculiar example of complete oxidation of alcohol followed by aldehyde in presence of Pt/Bi_2WO_6. In a recent study [48], the overoxidation was correlated with the complexation of aldehydes, unlike alcohol which does not complex, with TiO_2 surface. When TiO_2 surface was substantially covered with the layers of WO_3, overoxidation was much averted because WO_3 was found to be inactive for aldehyde oxidation. In this study, to investigate if there is any interaction between *p*-anisaldehyde and Pt/Bi_2WO_6 surface, adsorption experiments were carried out and any change in catalysts surface was followed by FTIR while any change in aldehyde concentration was analyzed by GC-MS. FTIR spectrums, presented fig 5.8, showed identical patterns and presence of any trace of aldehyde was not noticeable. Furthermore, GC-MS analysis did not indicate any decrease in aldehyde concentrations. The dearth of noticeable physisorption of *p*-anisaldehyde onto the surface of Pt/Bi_2WO_6 explains, to certain extent, the suppression of aldehyde oxidation.

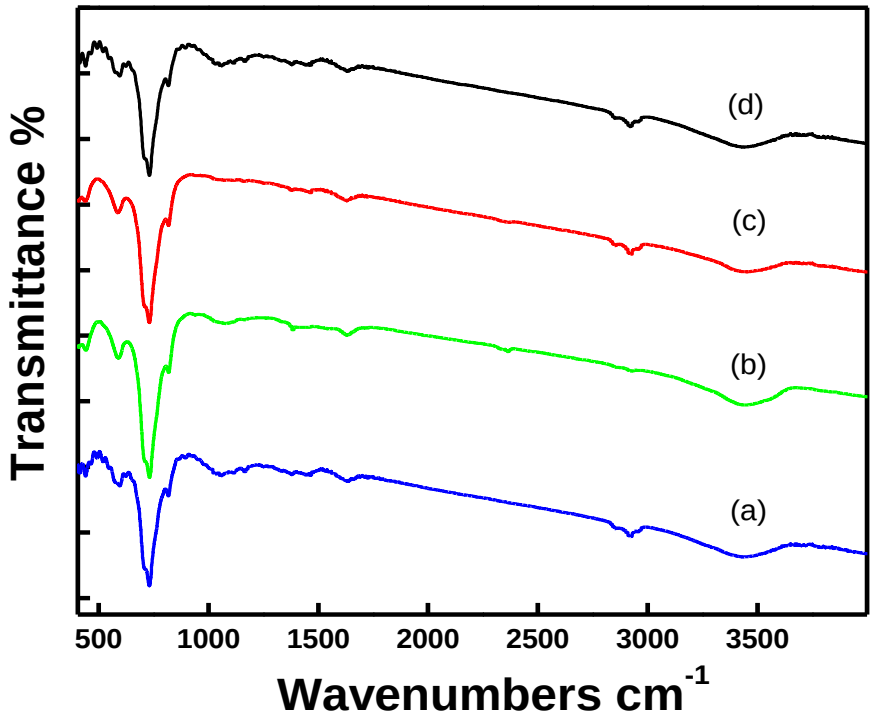

Figure 5.8 FTIR spectrums of Pt/Bi_2WO_6 analyzed after adsorption experiments of p-anisaldehyde; (a) 0 h, (b) 4 h (c) 8 h and (d) 12 h.

5.3 Oxidation dependency on alcohol concentration, catalyst amount and amount of deposited Pt

From a mechanistic and application standpoint, it is important to correlate the dependence of oxidation with the substrate concentration, the catalyst loading and the amount of deposited Pt. Therefore, the effect of such parameters was investigated and the results are illustrated in fig 5.9 (a-c). As readily seen, the oxidation increased monotonically with 4-MBA concentration up to 0.8 mM followed by a decrease at higher concentration. This could be due to the fact that up to 0.8 mM 4-MBA concentration, sufficient number of active sites is available on the photocatalyst surface which promote oxidation and hence lead to higher conversion. Decrease in percent conversion at 1.0 mM could be attributed to the existence of a finite number of active sites. Since highest conversion was observed at 0.8 mM concentration of 4-MBA, the effect of catalyst loading on percentage conversion was investigated at this optimal 4-MBA concentration. The obtained conversion trend showed a parabolic dependence, which is a characteristic of heterogeneous catalytic process. Besides the availability of more photocatalyst's surface, an increase in the amount of photocatalyst leads to more photon absorption, which in turn generates a higher amount of active surface or photo-excited holes in valence band for oxidation. This triggers interfacial electron transfer from 4-MBA to the valence band holes, causing an increase in conversion. Since Pt nanoparticles deposited onto the surface of Bi_2WO_6 significantly improved the photocatalytic activity, the amount of deposited Pt may play an important role in the optimization of the photocatalytic oxidation of 4-MBA

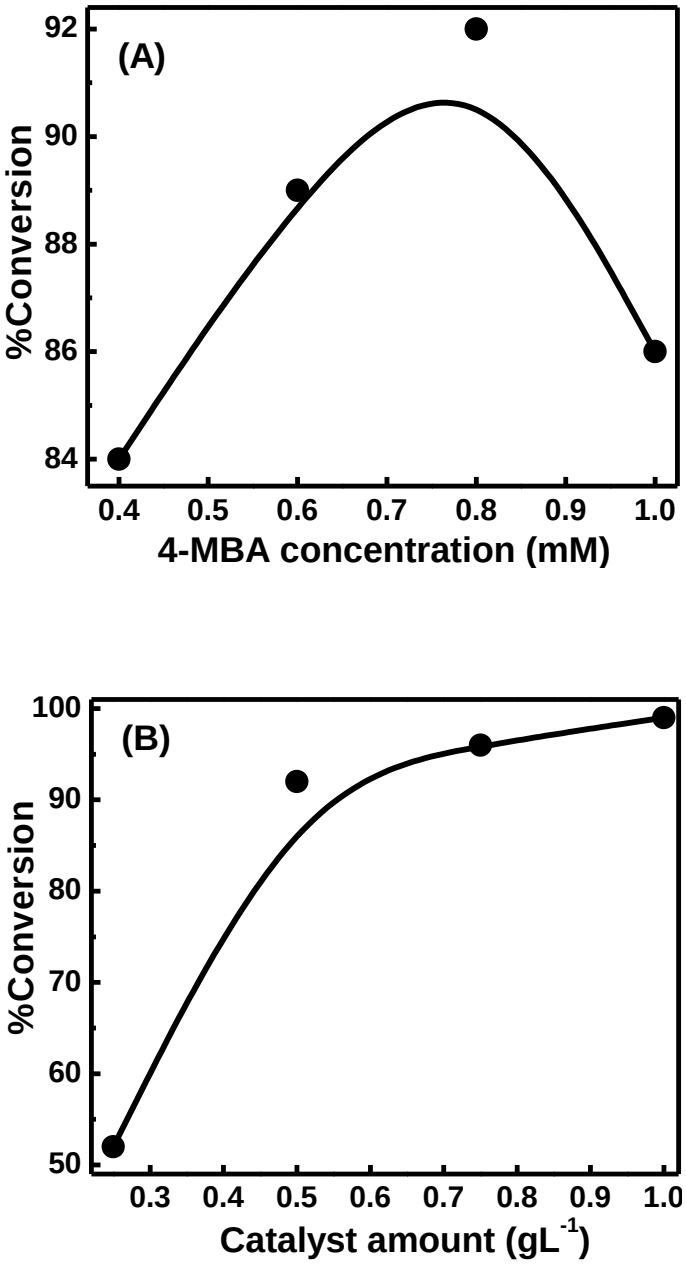

Figure 5.9 (a) & (b) Dependence of 4-MBA oxidation on (A) 4-MBA concentration and (B) Pt/Bi_2WO_6 amount. Pt amount deposited on Bi_2WO_6.
Experimental conditions: irradiation time = 4 h, 4-MBA concentration = 0.8 mM, $0.5\%Pt/Bi_2WO_6$ amount = 0.5 gL^{-1}, volume (H_2O) = 130 mL.

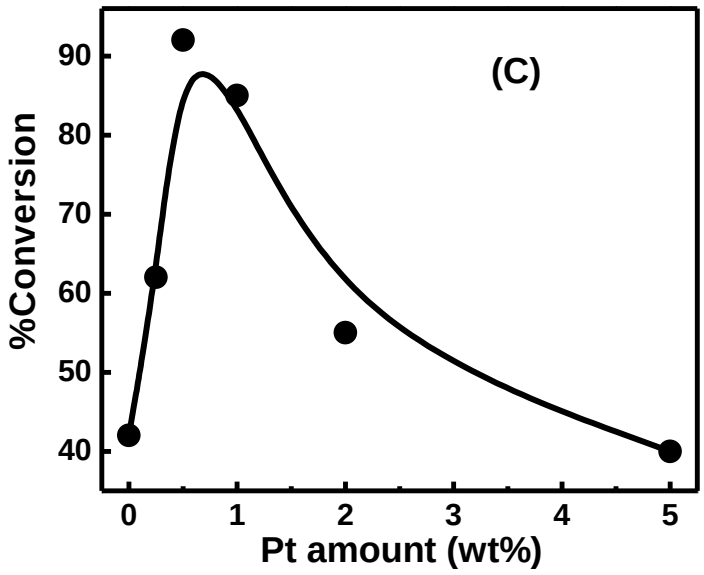

Figure 5.9 (c) Dependence of 4-MBA oxidation on Pt amount deposited on Bi_2WO_6.
Experimental conditions: irradiation time = 4 h, 4-MBA concentration = 0.8 mM, 0.5%Pt/Bi_2WO_6 amount = 0.5 gL^{-1}, volume (H_2O) = 130 ml.

Change in alcohol and aldehyde concentrations or % conversion with respect to Pt amounts (0.25, 0.5, 1.0, 2.0 and 5.0 wt%) is presented in fig 5.9 (c). As could be apparently seen, the highest conversion was obtained with 0.5 wt% Pt, followed by a decrease at higher Pt loadings. The improvement in oxidation in the presence of platinized bismuth tungstate may be attributed to the possible formation of a Schottky barrier between Pt and Bi_2WO_6. In general, the formation of a Schottky barrier between noble metals and semiconductor photocatalysts has been discussed previously by other authors [28, 59, 60]. At higher Pt loadings, decrease in the oxidation efficiency may be rationalized in terms of the fact that substantial coverage of photocatalyst's surface by Pt may take place which could potentially serve as a shield and prevent the incident photons from impinging on the Bi_2WO_6 surface, thereby decreasing the photocatalytic performance [61]. Under optimized experimental conditions, the reaction rate for the conversion of alcohol was calculated to be 0.2 mMh^{-1}, using 1 gL^{-1} photocatalyst amount, which is to the best of our knowledge the highest rate reported as yet under photocatalytic conditions.

5.4 Radicals formation and reaction mechanism

In most of the earlier documented studies relating to the photocatalytic oxidation, the selectivity was essentially maintained up to a certain degree of alcohol oxidation (ca. 60%) and the selectivity diminished as the reaction proceeded owing to the overoxidation of by-products, oxidation of aldehyde for instance. Interestingly, the selectivity towards *p*-anisaldehyde sustained with Pt/Bi_2WO_6 until exhaustive oxidation of 4-MBA took place followed by further oxidation of *p*-anisaldehyde. Substantially, the non-selective behavior of semiconductor-mediated photocatalytic process could be attributed to the formation of extremely reactive and short-lived radicals such as $OH^{\bullet}$, $O_2^{-\bullet}$, $HO_2^{\bullet}$ etc. The mechanism for the formation of such radicals has been extensively discussed in the literature by multitude of authors. Briefly, exciton (e^- and h^+ pair) could be generated in photocatalysts upon providing appropriate photonic energy (equal to or greater than the band gap). Excited conduction band electrons could readily reduce O_2 to $O_2^{-\bullet}$ while the holes in the valence band can oxidize water, generating $OH^{\bullet}$ radicals. As stated above, these radical species are very reactive, though short lived, and make the photocatalytic process non-selective. Hence, in order to determine and interpret the operative mechanism responsible for the high selectivity, the involvement of such radicals in the oxidation process was examined. Since terephthalic acid is an excellent trapping agent for $OH^{\bullet}$, gets transformed into fluorescent 2-hydroxyterephthalic [58], it was utilized as a probe molecule to monitor the formation of $OH^{\bullet}$ in the reaction media. The change in fluorescence intensity, which is a function of OH radicals, was monitored by photoluminescence. Formation of $OH^{\bullet}$ in the reaction media was followed both in the

absence and presence of 4-MBA and results are illustrated in fig 5.10. Significant amount of 2-hydroxyterephthalic was formed with respect to irradiation time, as indicated by the high intensity, when terephthalic acid was irradiated without 4-MBA, suggesting the generation of $OH^{\bullet}$ via oxidation of H_2O. However, when irradiation was performed in the presence of 4-MBA, the PL intensity was significantly attenuated revealing the predominant oxidation of alcohol over that of water. This suggested that the involvement of OH radicals in the oxidation of alcohol is less likely. Relatively, the involvement of O_2 is intricate as compared to OH radicals as O_2 can play a dual role, could either be directly incorporated to yield oxygenated product or serve as the conduction band electron acceptor, in the photocatalytic oxidation process [62].

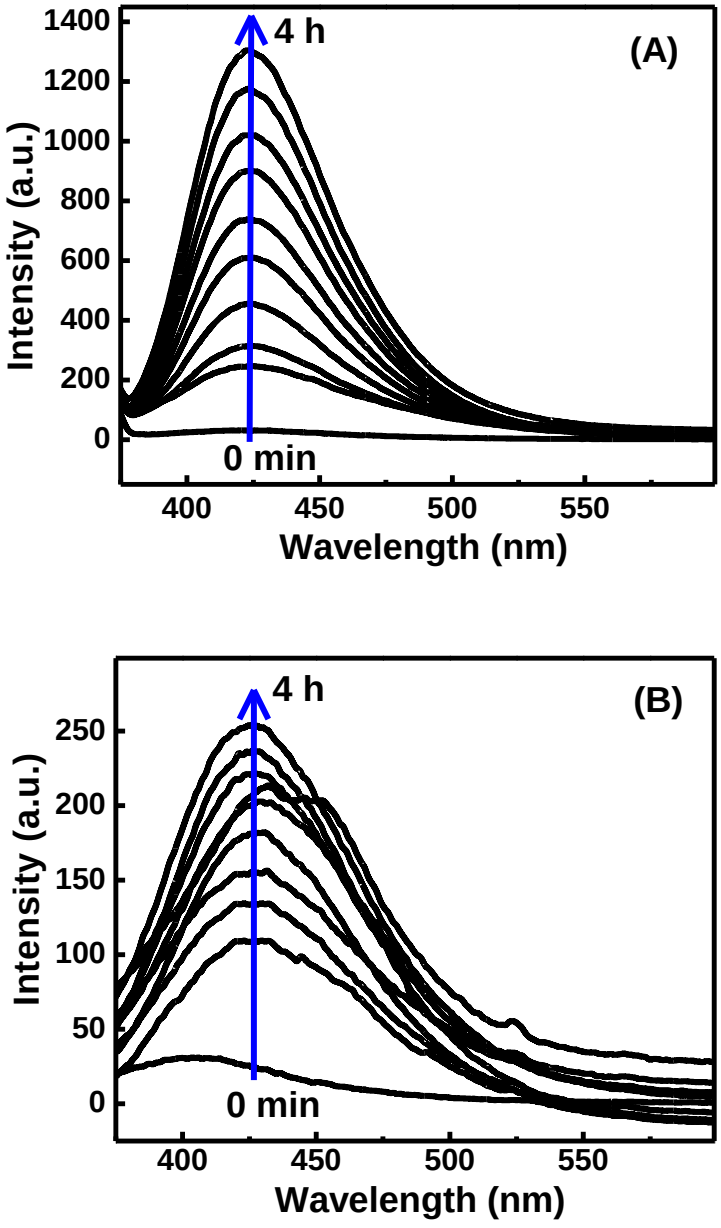

Figure 5.10 Change in fluorescence intensity of terephthalic acid as a function of irradiation time in aqueous suspensions of Pt/Bi_2WO_6: (A) in absence and (B) presence of 4-MBA.

In order to elucidate the rate determining factor and to shed light on the operative mechanism, oxidation of alcohol was studied in presence of various radical and electron scavenging entities, such as molecular O_2 and N_2, benzoquinone, ammonium persulfate ($(NH_4)_2S_2O_8$), and ammonium oxalate ($(NH_4)_2C_2O_4$), and obtained results are illustrated in fig 5.11. To determine the role of O_2, the oxidation of 4-MBA was carried out both in the absence and presence of molecular O_2, by bubbling N_2 or O_2 through photoreactor. Results, presented in fig 5.11, showed that the conversion was profoundly dependent on the ambient environment. Apparently, the oxidation in the absence of oxygen was slow (ca. 27%), indicating that O_2 played significant role in the oxidation of 4-MBA. Oxidation was also assessed under highly O_2-saturated environment, O_2 was bubbled throughout the course of the reaction, but inconsequential improvement was observed and obtained results were analogous to that of obtained only with dissolved oxygen. This indicated that the dissolved O_2 is adequate to drive the effective oxidation and the process was independent of any oxygen transport limitation. To further delve into the O_2 involvement, reactions were carried out employing $(NH_4)_2S_2O_8$ as an alternative electron acceptor in the absence of O_2 where ~45% conversion was noticed. This observation indicated that O_2 is serving as effective electron acceptor, which attenuates the recombination of exciton, during the oxidation 4-MBA. Furthermore, when benzoquinone was utilized as a trap for $O_2^{-\bullet}$, the oxidation of 4-MBA was only ~12%.

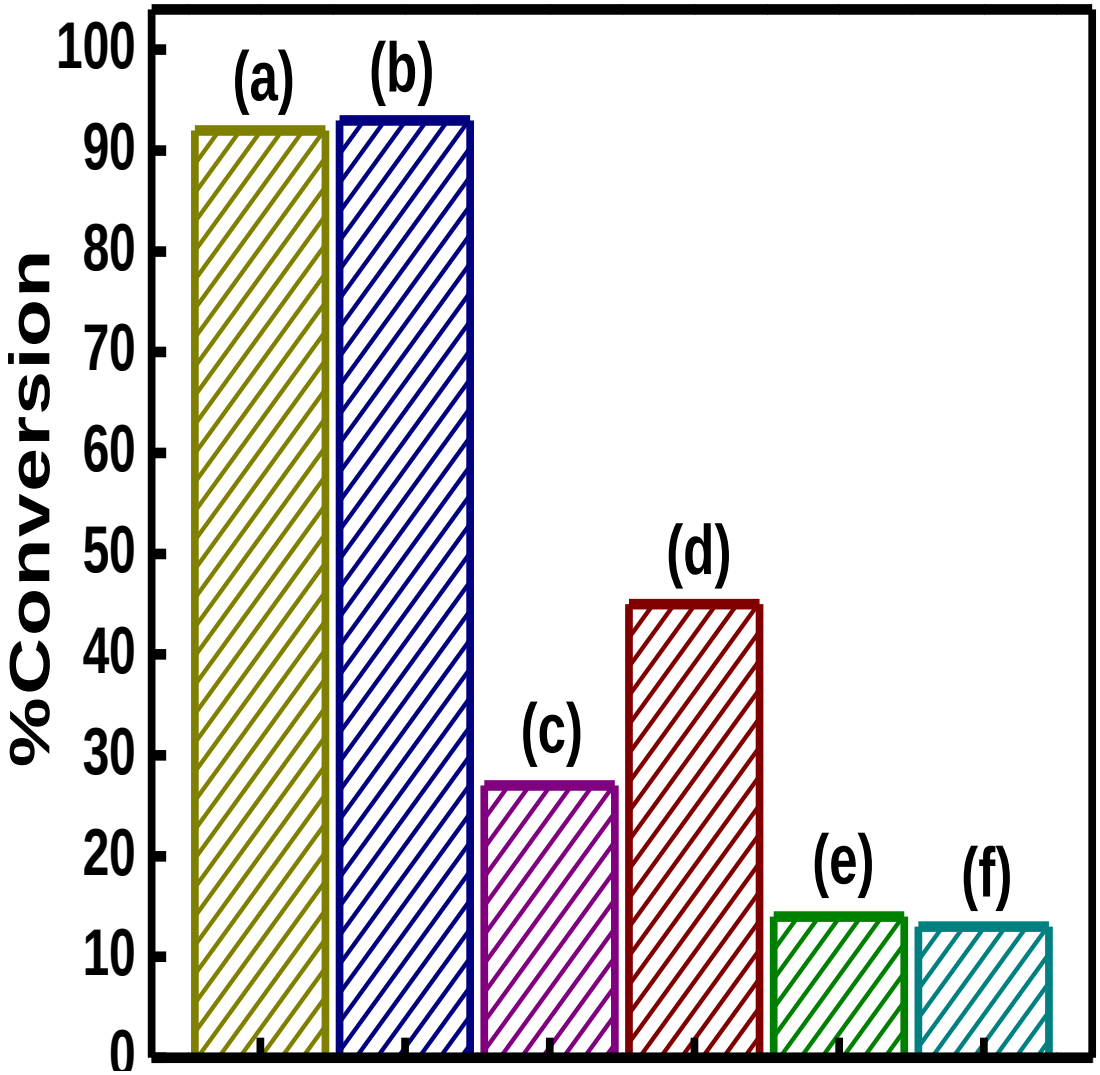

Figure 5.11 Effect of electron, hole and $O_2^{-\bullet}$ radical scavengers on the photocatalytic oxidation of 4-MBA; (a) under dissolved oxygen, (b) under bubbling of O_2, (c) in absence of O_2 or under bubbling of N_2, (d) in absence of O_2 or presence of $(NH_4)_2S_2O_8$, (e) in presence of benzoquinone, and (f) in presence of $(NH_4)_2C_2O_4$.
Experimental condition: irradiation time = 4 h, 4-MBA concentration = 0.8 mM, 0.5%Pt/Bi_2WO_6 amount = 0.5 gL^{-1}, volume (H_2O) = 130 ml.

It should be noticed that benzoquinone could be preferably oxidized under such experimental conditions and also serve as a valence band hole trap [63]. With this view, $(NH_4)_2C_2O_4$ was employed as a hole trap and extent of oxidation was investigated. Interestingly, the results obtained in presence of $(NH_4)_2C_2O_4$ were comparable to that obtained in presence of benzoquinone. This observation apparently revealed the critical involvement of valence band holes, rather than O_2, in the oxidation. Based on such findings, a plausible mechanism involving various possible pathways is presented in fig 5.12. However, it seems rational to postulate that the two-step oxidation of 4-MBA predominantly took place through valence band holes, which also appears to be a rate determining step, while O_2 primarily contributed in the improvement of photocatalytic efficiency by preventing electron-hole pair recombination. Moreover, the path (B) seems more likely as the formation of radical at the β-carbon, in case of path B, may result in the delocalization of this electron in the adjacent benzene ring, imparting additional stability and rather slow oxidation of 4-MBA.

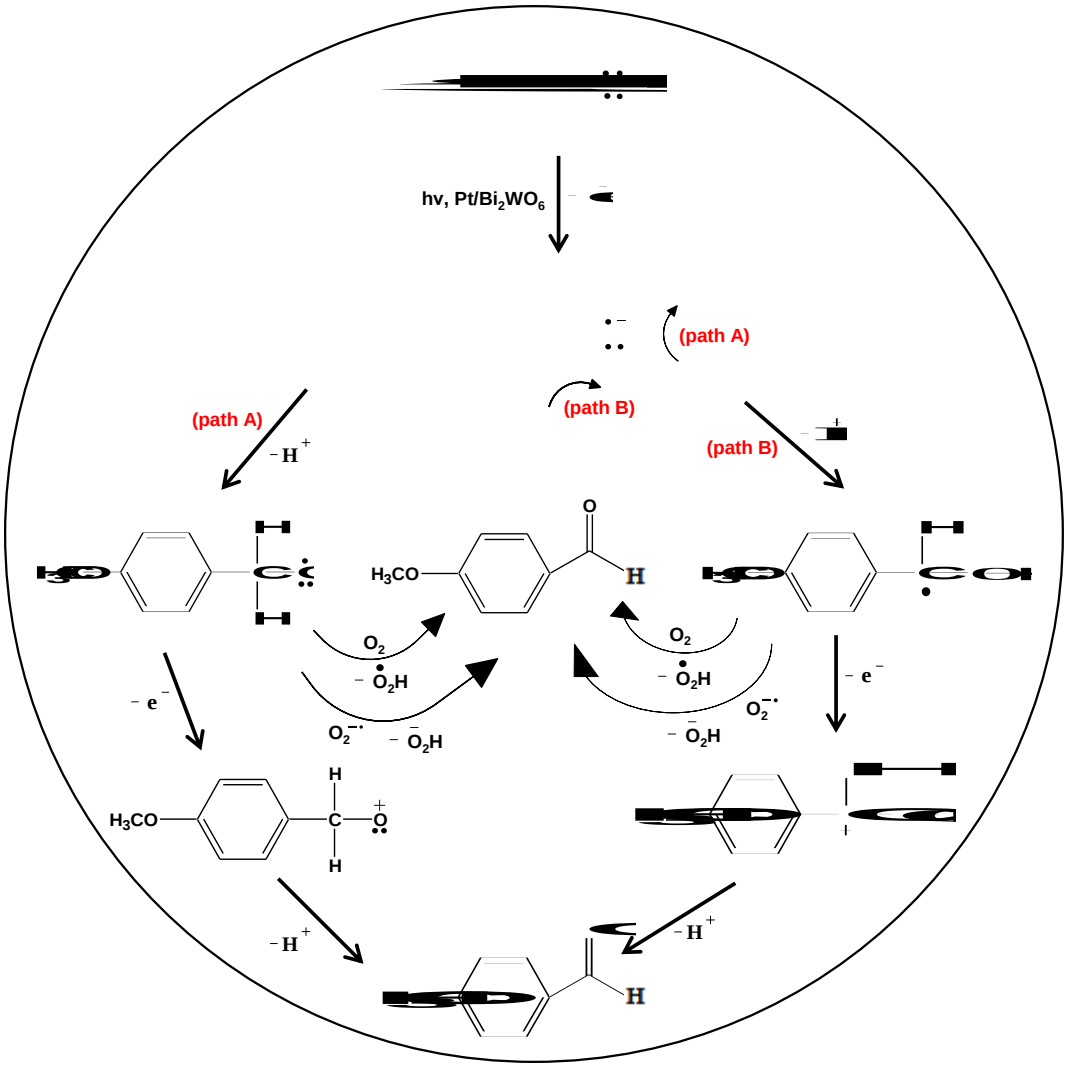

Figure 5.12 A proposed mechanism of photocatalytic oxidation of 4-MBA.

With the noted fact that noble metal supported catalysts are capable of driving oxidation of alcohols, oxidation of 4-MBA was investigated under dark in aqueous suspensions of Pt/Bi_2WO_6. Decrease in alcohol concentration and formation aldehyde, as a function of Pt amounts (0.5, 1.0, 2.0 and 5.0 wt%), deposited on nanoporous Bi_2WO_6 are shown in fig 5.13. It could be readily seen that noticeable formation of aldehyde took place even in the dark. However, change in 4-MBA concentration or formation of p-anisaldehyde was not noticeable in presence of pure Bi_2WO_6. Oxidation of alcohols on the surface of noble metals, supported or unsupported, has been discussed previously[11], and critical steps involved are presented in fig 5.14. Briefly, the reaction starts by the adsorption of alcohols onto the catalysts surface followed by the formation of metal alkoxide and metal hydride (on the neighbouring Pt atom). The adsorbed metal alkoxide undergoes β-hydride elimination process producing aldehyde, though ketones may also be produced at this stage but were not observed in this study. Finally, the adsorbed hydrogen undergoes oxidation through molecular oxygen producing water molecule and regenerating the Pt active sites for the further oxidation.

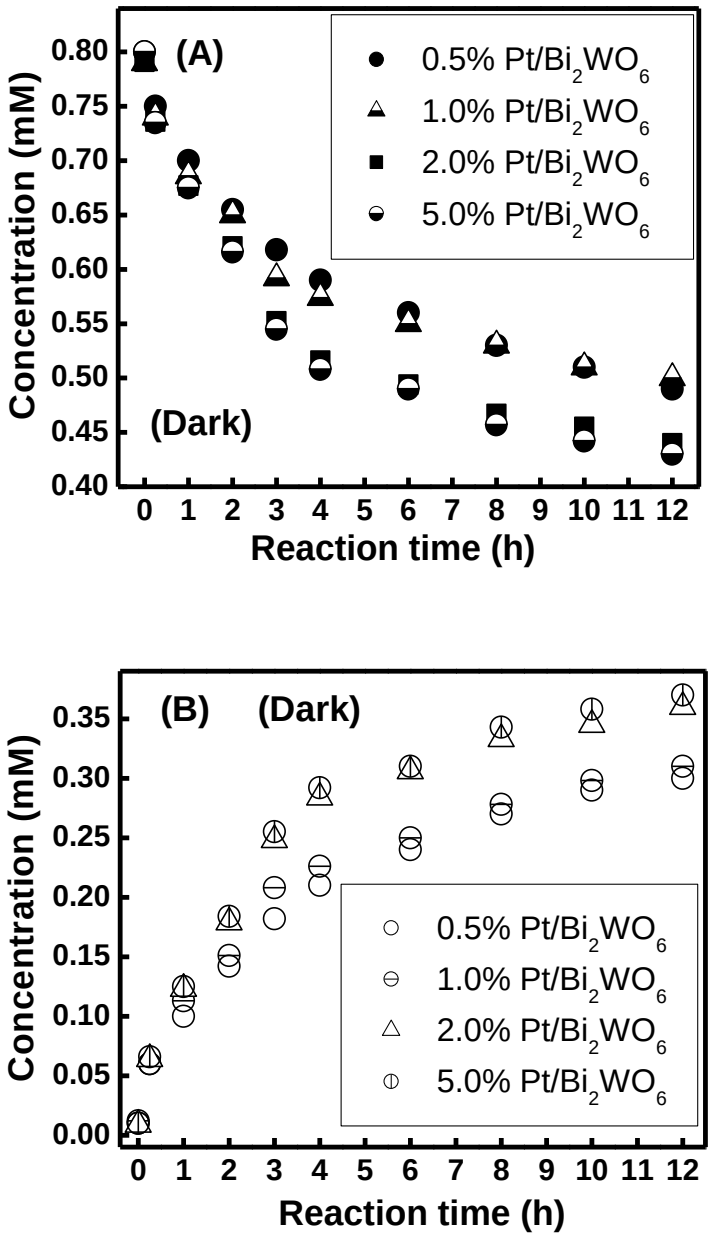

Figure 5.13 (A) change in 4-MBA concentration, and (B) formation of *p*-anisaldehyde under dark in presence of Bi_2WO_6 having various amounts of Pt.
Experimental conditions: 4-MBA concentration = 0.8 mM, photocatalyst amount = 1.0 gL^{-1}, volume (H_2O) = 130 ml.

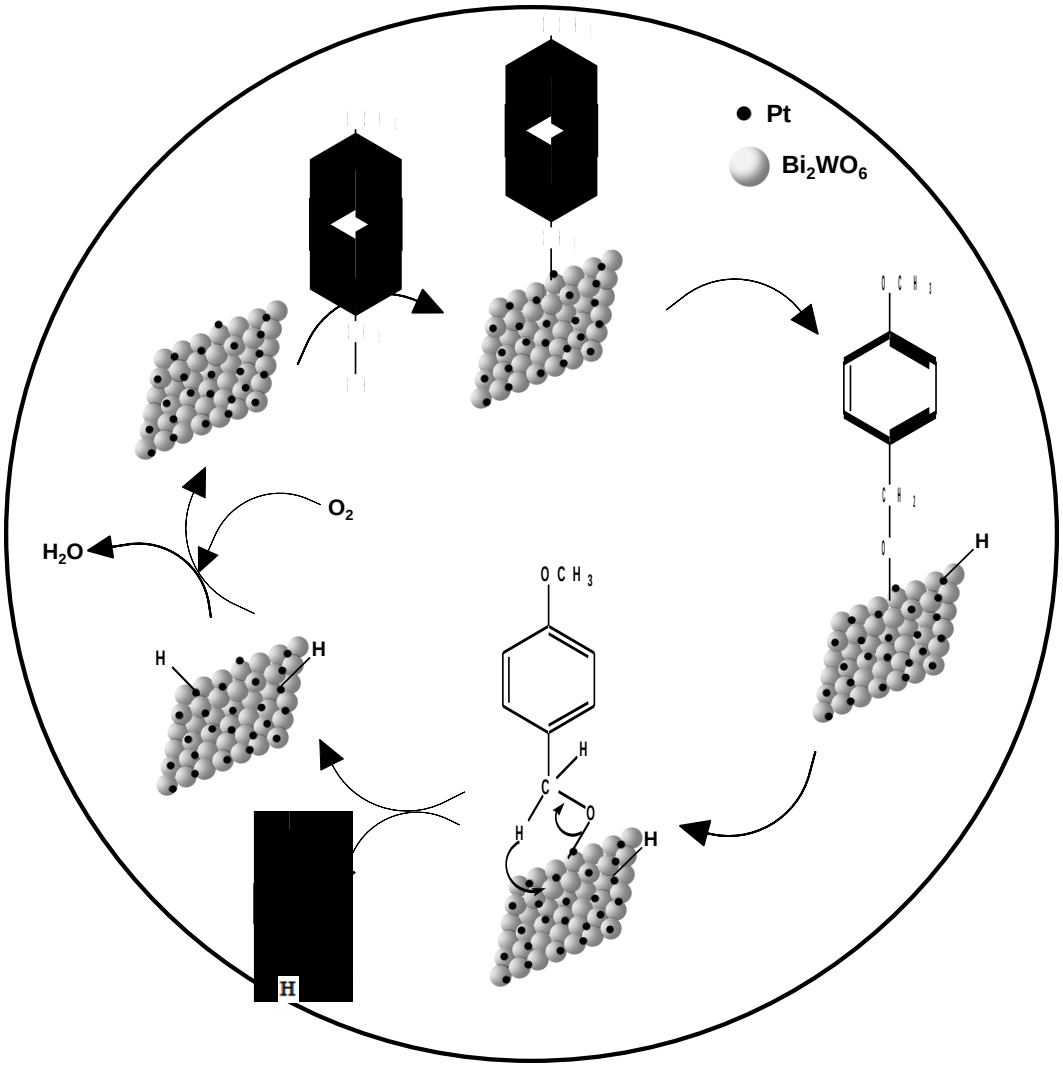

Figure 5.14 Steps for the oxidation of 4-MBA in the dark on the surface of Pt/Bi_2WO_6.

5.5 Conclusions

In summary, we have demonstrated that selective and quantitative photo-conversion of alcohols into corresponding aldehydes with high yield could be achieved with Ag_3PO_4 in water under mild conditions. Enhanced activity and selectivity are attributed to the high oxidation potential of Ag_3PO_4, passive behavior of $O_2^{-\bullet}$, and weak generation and ineffectiveness of $OH^{\bullet}$ radicals. Mechanistic observations may be anticipated to offer impetus to identify or custom-tailor other potential photocatalysts for selective photocatalytic oxidations. Although oxidation of few selected alcohols only were demonstrated, Ag_3PO_4 is likely to be active for a variety of other essential oxidation reactions. Also it was evidenced that highly efficient, chemoselective and quantitative conversion of aromatic alcohols into their corresponding aldehydes (mole-to-mole conversion) could be achieved in presence of nanoporous hierarchical Pt/Bi_2WO_6 spheres in water under mild conditions under simulated sunlight. High efficiency of Bi_2WO_6 could be attributed to nanoporous surface and hierarchical architecture, besides Pt nanoparticles that prevented the recombination of exciton. Alcohol competed with water and predominantly oxidized minimizing the generation of $OH^{\bullet}$ resulting from water splitting. Based on this, it appears rational to envisage that the reduction site of the semiconductor photocatalysts is more pivotal to be engineered in order to obtain high chemoselective oxidation of alcohols. Furthermore, it is postulated that the valence band holes are the primary catalytic sites for the two-step oxidation of alcohols, rather than direct oxidation through molecular oxygen, under studied photocatalytic conditions. Nanocomposite Pt/Bi_2WO_6 showed considerable conversion of 4-MBA into *p*-anisaldehyde under dark, though the conversion was relatively slow.

References

[1] G. Palmisano, V. Augugliaro, Photocatalysis: a promising route for 21st century organic chemistry, Chem. Commun. 33 (2007) 3425–3437.

[2] T.P. Yoon, M. a Ischay, J. Du, Visible light photocatalysis as a greener approach to photochemical synthesis, Nat. Chem. 2 (2010) 527–532.

[3] J. Xu, Y. Wang, Y. Zhu, Nanoporous Graphitic Carbon Nitride with Enhanced Photocatalytic Performance, Langmuir. 29 (2013) 10566–10572.

[4] J.C. Lang, X. J.; Ji, H. W.; Chen, C. C.; Ma W. H.; Zhao, Selective formation of imines via aerobic photocatalytic oxidation of amines on TiO2, Angew. Chem. Int. Ed. 50 (2011) 3934.

[5] C. Wang, Z. Xie, K. DeKrafft, W. Lin, Doping metal–organic frameworks for water oxidation, carbon dioxide reduction, and organic photocatalysis, J. Am. Chem. Soc. 133 (2011) 13445–13454.

[6] H. Zhu, X. Ke, X. Yang, S. Sarina, H. Liu, Reduction of nitroaromatic compounds on supported gold nanoparticles by visible and ultraviolet light, Angew. Chem. Int. Ed. 49 (2010) 9657–9661.

[7] S. Li, U. Diebold, Reactivity of TiO2 rutile and anatase surfaces toward nitroaromatics, J. Am. Chem. Soc. 132 (2009) 64–66.

[8] Y. Ide, N. Kawamoto, Y. Bando, H. Hattori, M. Sadakane, T. Sano, Ternary modified TiO2 as a simple and efficient photocatalyst for green organic synthesis, Chem. Commun. 49 (2013) 3652–3654.

[9] S. Yurdakal, G. Palmisano, Nanostructured rutile TiO2 for selective photocatalytic oxidation of aromatic alcohols to aldehydes in water, J. Am. Chem. Soc. 130 (2008) 1568–1569.

[10] A. Maldotti, A. Molinari, R. Amadelli, Photocatalysis with organized systems for the oxofunctionalization of hydrocarbons by O2, Chem. Rev. 02 (2002) 3811−3836.

[11] G. Palmisano, E. García-López, G. Marcì, V. Loddo, S. Yurdakal, V. Augugliaro, et al., Advances in selective conversions by heterogeneous photocatalysis, Chem. Commun. 46 (2010) 7074–7089.

[12] V. Augugliaro, T. Caronna, Oxidation of Aromatic Alcohols in Irradiated Aqueous Suspensions of Commercial and Home-Prepared Rutile TiO2: A Selectivity Study, Chem. Eur. J. 14 (2008) 4640–4646.

[13] Q. Wang, M. Zhang, C. Chen, W. Ma, J. Zhao, Photocatalytic aerobic oxidation of alcohols on TiO2: the acceleration effect of a Brønsted acid, Angew. Chem. Int. Ed. 49 (2010) 7976–7979.

[14] G. Palmisano, S. Yurdakal, Photocatalytic Selective Oxidation of 4-Methoxybenzyl Alcohol to Aldehyde in Aqueous Suspension of Home-Prepared Titanium Dioxide Catalyst, Adv. Synth. Catal. 349 (2007) 964–970.

[15] M. Hundlucky, Oxidations in Organic Chemistry, Washington, DC, Am. Chem. Soc. (1990) 114–133.

[16] H. Miyamura, R. Matsubara, Y. Miyazaki, S. Kobayashi, Aerobic Oxidation of Alcohols at Room Temperature and Atmospheric Conditions Catalyzed by Reusable Gold Nanoclusters Stabilized by the Benzene Rings of Polystyrene Derivatives, Angew. Chemie. 119 (2007) 4229–4232.

[17] D.I. Enache, J.K. Edwards, P. Landon, B. Solsona-Espriu, A.F. Carley, A. a Herzing, et al., Solvent-free oxidation of primary alcohols to aldehydes using Au-Pd/TiO2 catalysts, Science (80-.). 311 (2006) 362–365.

[18] M.S. Kwon, N. Kim, C.M. Park, J.S. Lee, K.Y. Kang, J. Park, Palladium nanoparticles entrapped in aluminum hydroxide: dual catalyst for alkene hydrogenation and aerobic alcohol oxidation, Org. Lett. 7 (2005) 1077–1079.

[19] Y.M.A. Yamada, T. Arakawa, H. Hocke, Y. Uozumi, A Nanoplatinum Catalyst for Aerobic Oxidation of Alcohols in Water, Angew. Chemie. 119 (2007) 718–720.

[20] K. Mori, T. Hara, T. Mizugaki, K. Ebitani, K. Kaneda, Hydroxyapatite-supported palladium nanoclusters: a highly active heterogeneous catalyst for selective oxidation of alcohols by use of molecular oxygen, J. Am. Chem. Soc. 126 (2004) 10657–10666.

[21] J.J. Joseph W. LeFevre, Oxidizing Methoxybenzyl Alcohol to Methoxybenzaldehyde Using Phase-Transfer Catalysis, Chemical Education Resources, 1999.

[22] G. Cainelli, G. Cardillo, Chromium Oxidants in Organic Chemistry, Springer, Berlin, 1984.

[23] E.J. García-Suárez, M. Tristany, A.B. García, V. Collière, K. Philippot, Carbon-supported Ru and Pd nanoparticles: Efficient and recyclable catalysts for the aerobic oxidation of benzyl alcohol in water, Microporous Mesoporous Mater. 153 (2012) 155–162.

[24] N. Zhang, Y. Zhang, X. Pan, X. Fu, Assembly of CdS nanoparticles on the two-dimensional graphene scaffold as visible-light-driven photocatalyst for selective organic transformation under ambient conditions, J. Phys. Chem. 115 (2011) 23501–23511.

[25] N. Zhang, Y. Zhang, X. Pan, Constructing Ternary CdS–Graphene–TiO2 Hybrids on the Flatland of Graphene Oxide with Enhanced Visible-Light Photoactivity for Selective Transformation, J. Phys. Chem. 116 (2012) 18023−18031.

[26] A. Tanaka, K. Hashimoto, H. Kominami, Selective photocatalytic oxidation of aromatic alcohols to aldehydes in an aqueous suspension of gold nanoparticles supported on cerium(IV) oxide under irradiation of green light, Chem. Commun. 47 (2011) 10446–10448.

[27] A. Tanaka, Preparation of Au/CeO2 Exhibiting Strong Surface Plasmon Resonance Effective for Selective or Chemoselective Oxidation of Alcohols to Aldehydes or Ketones in Aqueous Suspensions under Irradiation by Green Light, J. Am. Chem. Soc. 134 (2012) 14526−14533.

[28] and D.W.B. Michael R. Hoffmann, Scot T. Martin, Wonyong Choi, Environmental applications of semiconductor photocatalysis, Chem. Rev. 95 (1995) 69–96.

[29] X. Xiao, J. Jiang, L. Zhang, Selective oxidation of benzyl alcohol into benzaldehyde over semiconductors under visible light: The case of Bi12O17Cl2 nanobelts, Appl. Catal. B Environ. 142-143 (2013) 487–493.

[30] D. Devilliers, Semiconductor photocatalysis: Still an active research area despite barriers to commercialization, Cent. Appl. Energy Res. 17 (2006) 1–3.

[31] C.A. Varghese, O. K.; Paulose, M.; LaTempa, T. J.; Grimes, High-rate solar photocatalytic conversion of CO2 and water vapor to hydrocarbon fuels, Nano Lett. 9 (2009) 731–737.

[32] K. Maeda, K. Teramura, D. Lu, T. Takata, N. Saito, Y. Inoue, et al., Photocatalyst releasing hydrogen from water, Nature. 440 (2006) 295.

[33] S. Furukawa, T. Shishido, K. Teramura, T. Tanaka, Photocatalytic Oxidation of Alcohols over TiO2 Covered with Nb2O5, ACS Catal. 2 (2012) 175–179.

[34] M. Addamo, V. Augugliaro, M. Bellardita, Environmentally friendly photocatalytic oxidation of aromatic alcohol to aldehyde in aqueous suspension of brookite TiO2, Catal. Letters. 126 (2008) 58–62.

[35] W. Feng, G. Wu, L. Li, N. Guan, Solvent-free selective photocatalytic oxidation of benzyl alcohol over modified TiO2, Green Chem. 13 (2011) 3265–3272.

[36] W. Zhai, S. Xue, A. Zhu, Y. Luo, Y. Tian, Plasmon-Driven Selective Oxidation of Aromatic Alcohols to Aldehydes in Water with Recyclable Pt/TiO2 Nanocomposites, Chem. Cat. Chem. 3 (2011) 127–130.

[37] http://www.civil.northwestern.edu/EHE/HTML_KAG/Kimweb/Research.html, (n.d.).

[38] M. Silva, R. Marques, Evaluation of Nb2O5 and Ag/Nb2O5 in the photocatalytic degradation of dyes from textile industries, Brazilian J. Chem. Eng. 19 (2002) 359–363.

[39] S. Chueh, F. Hsu, J. Liaw, C. Wang, Visible light-induced photocatalyst, United States Pat. (2007).

[40] Z. Yi, J. Ye, N. Kikugawa, T. Kako, S. Ouyang, H. Stuart-Williams, et al., An orthophosphate semiconductor with photooxidation properties under visible-light irradiation, Nat. Mater. 9 (2010) 559–564.

[41] Y. Bi, S. Ouyang, N. Umezawa, Facet effect of single-crystalline Ag3PO4 sub-microcrystals on photocatalytic properties, J. Am. Chem. Soc. 4 (2011) 6490–6492.

[42] M. Qamar, A. Khan, Mesoporous hierarchical bismuth tungstate as a highly efficient visible-light-driven photocatalyst, RSC Adv. 4 (2014) 9542–9542.

[43] A.F. K. Honda, Electrochemical Photolysis of Water at a Semiconductor Electrode, Nature. 238 (1972) 37–38.

[44] V. Augugliaro, H. Kisch, V. Loddo, M.J. López-Muñoz, C. Márquez-Álvarez, G. Palmisano, et al., Photocatalytic oxidation of aromatic alcohols to aldehydes in aqueous suspension of home-prepared titanium dioxide, Appl. Catal. A Gen. 349 (2008) 182–188.

[45] V. Augugliaro, T. Caronna, V. Loddo, G. Marcì, G. Palmisano, L. Palmisano, et al., Oxidation of aromatic alcohols in irradiated aqueous suspensions of commercial and home-prepared rutile TiO(2): a selectivity study, Chem. Eur. J. 14 (2008) 4640–4646.

[46] L.P. and S.Y. Vincenzo Augugliaro, Vittorio Loddo, Marıa Jose Lopez-Munoz, Carlos Marquez-Alvarez, Giovanni Palmisano, Home-prepared anatase , rutile , and brookite TiO 2 for selective photocatalytic oxidation of 4-methoxybenzyl alcohol in water : reactivity and ATR-FTIR study, Photochem. Photobiol. Sci. 8 (2009) 663–669.

[47] R. Marotta, I. Di Somma, D. Spasiano, R. Andreozzi, V. Caprio, Selective oxidation of benzyl alcohol to benzaldehyde in water by TiO2/Cu(II)/UV solar system, Chem. Eng. J. 172 (2011) 243–249.

[48] D. Tsukamoto, M. Ikeda, Y. Shiraishi, T. Hara, N. Ichikuni, S. Tanaka, et al., Selective photocatalytic oxidation of alcohols to aldehydes in water by TiO2 partially coated with WO3, Chem. Eur. J. 17 (2011) 9816–9824.

[49] S. Higashimoto, N. Kitao, N. Yoshida, T. Sakura, M. Azuma, H. Ohue, et al., Selective photocatalytic oxidation of benzyl alcohol and its derivatives into corresponding aldehydes by molecular oxygen on titanium dioxide under visible light irradiation, J. Catal. 266 (2009) 279–285.

[50] X. Yu, Y. Huo, J. Yang, S. Chang, Y. Ma, W. Huang, Reduced graphene oxide supported Au nanoparticles as an efficient catalyst for aerobic oxidation of benzyl alcohol, Appl. Surf. Sci. 280 (2013) 450–455.

[51] C.M. a. Parlett, L.J. Durndell, K. Wilson, D.W. Bruce, N.S. Hondow, A.F. Lee, Selective oxidation of allylic alcohols over highly ordered Pd/meso-Al2O3 catalysts, Catal. Commun. 44 (2014) 40–45.

[52] D.I. Enache, J.K. Edwards, P. Landon, B. Solsona-Espriu, A.F. Carley, A. a Herzing, et al., Solvent-free oxidation of primary alcohols to aldehydes using Au-Pd/TiO2 catalysts, Science (80-.). 311 (2006) 362–365.

[53] E.J. García-Suárez, M. Tristany, A.B. García, V. Collière, K. Philippot, Carbon-supported Ru and Pd nanoparticles: Efficient and recyclable catalysts for the aerobic oxidation of benzyl alcohol in water, Microporous Mesoporous Mater. 153 (2012) 155–162.

[54] H. Sun, Q. Hua, F. Guo, Z. Wang, W. Huang, Selective Aerobic Oxidation of Alcohols by Using Manganese Oxide Nanoparticles as an Efficient Heterogeneous Catalyst, Adv. Synth. Catal. 354 (2012) 569–573.

[55] H. Wang, W. Fan, Y. He, J. Wang, J.N. Kondo, T. Tatsumi, Selective oxidation of alcohols to aldehydes / ketones over copper oxide-supported gold catalysts, J. Catal. 299 (2013) 10–19.

[56] A. V. Biradar, M.K. Dongare, S.B. Umbarkar, Selective oxidation of aromatic primary alcohols to aldehydes using molybdenum acetylide oxo-peroxo complex as catalyst, Tetrahedron Lett. 50 (2009) 2885–2888.

[57] K. Imamura, H. Tsukahara, K. Hamamichi, N. Seto, K. Hashimoto, H. Kominami, Simultaneous production of aromatic aldehydes and dihydrogen by photocatalytic dehydrogenation of liquid alcohols over metal-loaded titanium (IV) oxide under oxidant- and solvent-free conditions, Appl. Catal. A Gen. 450 (2013) 28–33.

[58] K. Ishibashi, A. Fujishima, T. Watanabe, K. Hashimoto, Detection of active oxidative species in TiO2 photocatalysis using the fluorescence technique, Electrochem. Commun. 2 (2000) 207–210.

[59] U. Siemon, D. Bahnemann, J.J. Testa, D. Rodríguez, M.I. Litter, N. Bruno, Heterogeneous photocatalytic reactions comparing TiO2 and Pt/TiO2, J. Photochem. Photobiol. A Chem. 148 (2002) 247–255.

[60] R.M.W. and B.L. Grung, R. M. Warner and B. L. Grung, Transistors: Fundamentals for the Integrated-Circuit Engineer, John Wiley & Sons, New York, 1983.

[61] B. Sun, A. V. Vorontsov, P.G. Smirniotis, Role of Platinum Deposited on TiO 2 in Phenol Photocatalytic Oxidation, Langmuir. 19 (2003) 3151–3156.

[62] X. Lang, X. Chen, J. Zhao, Heterogeneous visible light photocatalysis for selective organic transformations, Chem. Soc. Rev. 43 (2014) 473–486.

[63] R. Beranek, B. Neumann, S. Sakthivel, M. Janczarek, T. Dittrich, H. Tributsch, et al., Exploring the electronic structure of nitrogen-modified TiO2 photocatalysts through photocurrent and surface photovoltage studies, Chem. Phys. 339 (2007) 11–19.

Vitae

Name	: Rami Bahaeldin Abdelrahman Elsayed
Nationality	: Sudanese
Email	: ramony-13@hotmail.com
Mobile Phone	:+966.541076609
Address	: KFUPM, Dhahran, Saudi Arabia.
Academic Background	: B.Sc. in Chemistry, Sudan university of science and technology

Career history:

January 2012-May 2014	: Research assistant at KFUPM, Saudi Arabia
February 2011 - January 2012	: English teacher at IDPs community center, Yemen
August 2010 - February 2011	: Science teacher at Cambridge int. school, Yemen
December 2009 - August 2010	: Teaching assistant at Sudan university of science and technology, Sudan

Training and Certifications:

1 February 2013- 31 July 2013	: Preparation of water sample and heavy metal analysis, KFUPM - RI center of environment and water
30 October 2010-23 January 2011	: English courses, Seeds institute – Yemen
4 January 2010-3 March 2010	: Quality Control and processing of Soda Water and Mineral Water, Sudan